

South Dakota State University  
**Open PRAIRIE: Open Public Research Access Institutional  
Repository and Information Exchange**

---

Theses and Dissertations

---

2017

# Response Surface Methodology and Its Application in Optimizing the Efficiency of Organic Solar Cells

Rajab Suliman  
*South Dakota State University*

Follow this and additional works at: <http://openprairie.sdstate.edu/etd>

 Part of the [Statistics and Probability Commons](#)

---

## Recommended Citation

Suliman, Rajab, "Response Surface Methodology and Its Application in Optimizing the Efficiency of Organic Solar Cells" (2017).  
*Theses and Dissertations*. 1734.  
<http://openprairie.sdstate.edu/etd/1734>

This Dissertation - Open Access is brought to you for free and open access by Open PRAIRIE: Open Public Research Access Institutional Repository and Information Exchange. It has been accepted for inclusion in Theses and Dissertations by an authorized administrator of Open PRAIRIE: Open Public Research Access Institutional Repository and Information Exchange. For more information, please contact [michael.biondo@sdstate.edu](mailto:michael.biondo@sdstate.edu).

RESPONSE SURFACE METHODOLOGY AND ITS APPLICATION IN  
OPTIMIZING THE EFFICIENCY OF ORGANIC SOLAR CELLS

BY

RAJAB SULIMAN

A dissertation submitted in partial fulfillment of the requirements for the

Doctor of Philosophy

Major in Computational Science and Statistics


South Dakota State University

2017

RESPONSE SURFACE METHODOLOGY AND ITS APPLICATION IN  
OPTIMIZING THE EFFICIENCY OF ORGANIC SOLAR CELLS

RAJAB SULIMAN


This dissertation is approved as a creditable and independent investigation by a candidate for Doctor of Philosophy in Computational Science and Statistics degree and is acceptable for meeting the dissertation requirements for this degree. Acceptance of this does not imply that the conclusions reached by the candidate are necessarily the conclusions of the major department.

 Genfechis Djira, Ph.D.  
Dissertation Advisor

Date

Kurt Cogswell, Ph.D.  
Head, Department of Mathematics & Statistics

Date

 Dean, Graduate School

Date

## ACKNOWLEDGEMENTS

I would like to express my sincere gratitude to my advisor Dr. Gemechis D. Djira for accepting me as his advisee since November 2016. He has helped me to successfully bring my Ph.D. study to completion. In particular, he has helped me to develop simultaneous inferences for stationary points in quadratic response models. I also worked with Dr. Yunpeng Pan for three years. I appreciate his guidance and support. I could not have imagined successfully completing of my Ph.D. study without their continuous support, motivation, patience, and enthusiasm, especially through difficult times, to achieve my long-sought goal. Dr. Pan also facilitated our collaboration with the Department of Electrical Engineering and Computer Science. In this regard, I would also like to express my sincere thanks to Dr. Qiquan Qiao and Mr. Abu Farzan Mitul from Electrical Engineering and Computer Science Department for their assistance in generating the data we used for the organic solar cell experiment. They have provided an excellent environment that will foster to carry on my future independent research.

I would also gratefully acknowledge Dr. Kurt Cogswell, Head of the Mathematics and Statistics Department, and Dr. Donald Vestal, graduate program coordinator in the Department of Mathematics and Statistics, for their support. I am also grateful to all of my Ph.D. advisory committee members including Dr. Gary Hatfield and Thomas Roe from the Department of Mathematics and Statistics, and my graduate school representative Dr. Jane Mort from the College of Pharmacy. They provided me with constructive comments which greatly improved the quality of my dissertation.

My especially thanks goes to the Ministry of Higher Education, Libya, for sponsoring my Ph.D. study abroad through Libyan North American Scholarship Program (LNASP). My research is also partially benefitted by the NSF CAREER (ECCS-0950731) , and NASA EPSCoR (NNX13AD31A) grants used for the organic solar cell experiment. I also sincerely acknowledge all faculty members in the Department of Statistics at Misurata University for their encouragement. I am also indebted to Dr. Yasmina Faqih, and Dr. Hussain Kaiba who was a great mentor. I want to thank him post hum for his support.

Last but not least, my sincere thanks to my family, especially to my mother, wife, brothers, and son, for their love, sacrifices, and encouragement that helped me to complete my research. Finally, I must say that in the journey of my life I am indebted to so many of my family members, friends, and well-wishers who have provided invaluable advice during uncertain and challenging times and helped me to keep my dream alive. I wish I could thank every individual person, but nevertheless, they are always in my heart.

## TABLE OF CONTENTS

LIST OF FIGURES .....	ix
LIST OF TABLES .....	xii
ABSTRACT .....	xiv
GENERAL INTRODUCTION.....	1
INTRODUCTION TO RESPONSE SURFACE METHODOLOGY .....	3
2.1 Introduction.....	3
2.2 Overview and stages for RSM application .....	3
2.3 Screening experiment.....	6
2.4 Empirical model building .....	6
2.5 Encoding of input variable levels .....	12
2.6 First-order model .....	12
2.6.1 Two-level factorial designs.....	12
2.6.2 Two-level fractional factorial designs .....	13
2.7 Blocking in response surface designs .....	14
2.8 Steepest ascent .....	16
2.9 A second-order experimental design .....	21
2.9.1 Full $3^K$ factorial designs.....	21
2.9.2 Box–Behnken designs (BBD).....	22
2.9.3 The central composite design (CCD).....	23

2.9.4 Doehlert design .....	25
2.10 Lack-of-fit test .....	27
2.11 Variance dispersion graph.....	29
2.12 The Common design properties .....	32
2.12.1 Orthogonality .....	32
2.12.2 Rotatability.....	32
2.12.2.1 Design moment matrix.....	33
2.12.2.2 Rotatable conditions for first-order design .....	35
2.12.2.3 Rotatability conditions for a second-order design .....	36
2.12.2.4 Rotatability of the CCD .....	37
2.13 Uniform precision .....	38
<b>MODELING OF ORGANIC SOLAR CELL USING RESPONSE SURFACE</b>	
<b>METHODOLOGY .....</b>	<b>39</b>
3.1 Introduction and background .....	40
3.1 Materials, device fabrication and characterization .....	44
3.1.1 Materials .....	44
3.1.2 Single-junction device fabrication .....	45
3.1.3 Current density – voltage (J-V) characterization .....	45
3.2 Experimental design.....	46
3.3 Result and discussion.....	48

3.3.1. Model fitting for first order design .....	48
3.3.2 Moment matrix and rotatability conditions.....	51
3.4. Augmenting further to fit a quadratic response surface.....	52
3.5. Device structure .....	57
3.6. Residual analysis for fitted quadratic model.....	59
<b>SIMULTANEOUS INFERENCE FOR THE LOCATION OF A STATIONARY POINT</b>	
.....	62
4.1 Location of a stationary point .....	62
4.2 Confidence region for the location of a stationary point .....	66
4.2.1 Box and Hunter .....	67
4.2.2 Asymptotic confidence region for stationary point .....	69
4.3 Simultaneous confidence intervals for the coordinate of a stationary point.....	72
4.3.1 Bonferroni adjustment .....	74
4.3.2 Multiplicity adjustment based on equi-coordinate critical point .....	75
4.3.3 Bootstrap confidence intervals.....	76
4.4 Simulation study .....	77
4.5 Assessing the solar cell data using the bootstrap technique .....	80
4.6 Rising ridge in quadratic surfaces.....	83
4.6.1 Canonical analysis and confidence intervals for eigenvalues.....	84
4.6.2 The double linear regression method.....	85



COMBINATORIAL OPTIMATIZATION FOR DESIGN POINTS .....	94
5.1 Metaheuristics .....	94
5.2 Properties .....	96
5.3 Generalized and conditional inverse .....	98
5.3.1 Generalized inverse.....	98
5.4 The relative error with respect to the quadratic fitted model.....	101
RECENT DEVELOPMENT OF RESPONSE SURFACE METHODOLOGY .....	113
6.1 Multivariate response optimization.....	113
6.2 Robust parameter design.....	115
6.2.1 Taguchi’s approach.....	116
6.3 Generalized linear models.....	117
6.3.1 Local optimum designs .....	118
6.3.2 Sequential designs.....	118
6.3.3 Robust design technique .....	118
DISCUSSION AND CONCLUSION .....	120
7.1 Discussion and conclusions .....	120
7.2 Future research.....	122
APPENDIX A.....	131
APPENDIX B .....	135
APPENDIX C .....	156

## LIST OF FIGURES

Figure 2.1. Flow chart of RSM.....	5
Figure 2.2. Full $3^2$ factorial design ( $k = 2$ ).....	7
Figure 2.3.(a) The expected efficiency ( $y$ ) as a function of $x_1$ and $x_3$ and (b) A contour plot.....	9
Figure 2.4. Response along the path of the steepest ascent.....	18
Figure 2.5. The three-level factorial design of (a) two factors and (b) three factors and (c) Box–Behnken design of three factors.....	23
Figure 2.6. CCD (a) two factors with $\alpha = 2$ and (b) three factors with $\alpha = 1.68$ .....	25
Figure 2.7. Doelhart design (a) two factors (b) three factors originated by the two-plane.....	26
8	
Figure 2.8. VDG with three factor, five center point with $\alpha = 1.68$ and $\alpha = 1.732$ .....	30
Figure 2.9. VDG with $k = 3$ , $\alpha = 1.68$ and $\alpha = \sqrt{2}$ (one to five center point).....	30
Figure 3.1. Full $2^3$ factorial design with geometric view.....	48
Figure 3.2. Variance function plots for a cube design: (a) Profile plot and (b) Contour plot.....	49
Figure 3.3. Variance function plot for quadratic model: (a) Profile plot (b) Contour plot.....	53
Figure 3.4. Contoure plot of the efficiency.....	57

Figure 3.5. Response surface plot for solar cell efficiency.....	58
Figure 3.6. Device layout of PDPP3T-PCBM single junction polymer solar cell.....	59
Figure 3.7. J-V Characteristic curves of (a) cube, (b) foldover, and (c) star functions....	59
Figure 3.8. The residual analysis for fitted quadratic model.....	61
Figure 3.9. The studentized and studentized residuals.....	62
Figure 4.1. The surface and contour plots of the true regression function, $\beta_{12} = 0$ .....	78
Figure 4.2. The surface and contour plots of the true regression function, $\beta_{12} = 1$ .....	79
Figure 4.3. A bivariate kernel density, $\beta_1 = 0$ , $\beta_2 = 0$ , and $\beta_{12} = 0$ .....	80
Figure 4.4. Bivariate kernel density estimate, estimated stationary point when $\beta_1 = 0.4$ , $\beta_2 = 1.6$ , $\beta_{12} = 0$ .....	80
Figure 4.5. Bivariate kernel density estimate, estimated stationary point when $\beta_1 = 0.4$ , $\beta_2 = 1.6$ , $\beta_{12} = 1$ .....	81
Figure 4.6. Bootstrap estimate for best combination of organic solar cell.....	82
Figure 4.7. Stationary point of organic solar cell, the design region is shown in red box.	83
Figure 4.8. 90% Confidence regions and simultaneous confidence intervals.....	84
Figure 4.9. 95% Confidence regions and simultaneous confidence intervals.....	84
Figure 4.10. The individual approximate CI for the eigenvalues.....	92
Figure 4.11. The individual approximate 95% Bonferroni CI for the eigenvalues.....	94
Figure 5.1. The dynamic of default design points.....	101

Figure 5.2. The histogram of current solutions according to the relative error.....	107
Figure 5.3. The current solution corresponding to the relative error.....	107
Figure 5.4. The dynamic of default design points with respect to the second-order model.....	112
Figure 5.5. The candidate solution with the relative error.....	112

## LIST OF TABLES

Table 2.1. ANOVA for the first-order model.....	19
Table 2.2. Steepest ascent experiment.....	19
Table 2.3. Data for quadratic model.....	20
Table 2.4. ANOVA for quadratic model.....	21
Table 2.5. Design matrix for three-level factorial design with two factors.....	22
Table 2.6. Design matrix for Box–Behnken design with three factors.....	23
Table 2.7. Design matrix for central composite design with three factors.....	25
Table 2.8. Doehlert matrices (a) with two variables, and (b) with three variables.....	26
Table 2.9. ANOVA table for lack-of-fit test.....	28
Table 3.1. Design matrix of the CCD and the corresponding experimental results.....	47
Table 3.2. The three factors and the levels utilized in the CCD.....	47
Table 3.3. The design matrix of 23 factorial design.....	48
Table 3.4. The significance of the first-order effects according to the cube design.....	50
Table 3.5. ANOVA table for lack-of-fit test.....	56
Table 3.6. Observed values, Predicted values, Residuals, and other diagnostics.....	60
Table 4.1. Estimates of the coverage probability (nominal: $1-\alpha = 0.95$ ).....	79
Table 4.2. The estimated second-order regression model.....	91

Table 4.3. The approximate 95% confidence interval for estimated eigenvalues.....	92
Table 4.4. The approximate 95% Bonferroni confidence interval for estimated eigenvalues.....	93
Table 5.1. The first permutation matrix (swap) generated within the blocks.....	103
Table 5.2. The last permutation matrix (swap) generated within the locks.....	104
Table 5.3. The relative error according to the 276 permutation matrices.....	106
Table 5.4. The candidate trial solution (swap 44) with respect to the second-order model.....	108
Table 5.5. The candidate trial solution (swap 183) with respect to the second-order model.....	109
Table 5.6. The candidate trial solution (swap 184) with respect to the second-order model.....	110
Table 5.7. The relative error according to each swap with their iteration.....	111

## ABSTRACT

RESPONSE SURFACE METHODOLOGY AND ITS APPLICATION IN  
OPTIMIZING THE EFFICIENCY OF ORGANIC SOLAR CELLS

RAJAB SULIMAN

2017

Response surface methodology (RSM) is a ubiquitous optimization approach used in a wide variety of scientific research studies. The philosophy behind a response surface method is to sequentially run relatively simple experiments or models in order to optimize a response variable of interest. In other words, we run a small number of experiments sequentially that can provide a large amount of information upon augmentation. In this dissertation, the RSM technique is utilized in order to find the optimum fabrication condition of a polymer solar cell that maximizes the cell efficiency. The optimal device performance was achieved using 10.25 mg/ml polymer concentration, 0.42 polymer-fullerene ratio, and 1624 rpm of active layer spinning speed. The cell efficiency at the optimum stationary point was found to be 5.23% for the Poly(diketopyrrolopyrrole-terthiophene) (PDPP3T)/PC<sub>60</sub>BM solar cells. Secondly, we explored methods for constructing a confidence region for the stationary point in RSM. In particular, we developed methods for constructing simultaneous confidence intervals for the coordinates of a stationary point in a quadratic response surface model. The methods include Bonferroni adjustment, a plug-in approach based on the asymptotic distribution of maximum likelihood estimators, and bootstrapping. The simultaneous coverage probabilities of the proposed methods are assessed via simulation. The coverage

probabilities for the Bonferroni and plug-in approaches are pretty close to the nominal levels of 0.95 for large sample sizes. The metaheuristic method is also considered in order to search for an alternative solution to the design matrix that may be near to the optimal solution. Finally, we explored recent developments in RSM including generalized linear models and the case of multivariate response variables.



## CHAPTER 1

### GENERAL INTRODUCTION

It is important to any system to increase performance in order to increase the yield at low cost. One technique used for such a purpose is the so-called optimization.

Response surface methodology (RSM) is the most common optimization technique and it has been employed in many fields such as exploring chemical and biochemical processes. This technique is used to fit an empirical model to the experimental data. Usually, we consider several potential input variables that influence the system performance. Toward this aim, the lower order polynomial models are used in order to explore the system under study, and therefore, to describe an experimental design until the conditions is optimized. This dissertation focuses on various topics in RSM research. The specific objectives are:

- i. Use RSM to find the optimum conditions that will optimize cell efficiency of organic solar cell.
- ii. Develop methods for constructing simultaneous confidence intervals for the location of a stationary point.
- iii. Utilize a metaheuristic approach in order to find an alternative optimum order of the design points.
- iv. Explore recent developments in RSM research.

In order to achieve these objectives, the dissertation is organized as follows.

In Chapter 2, general introduction to RSM and various RSM designs and their properties will be explored. In Chapter 3, organic solar cell data is analyzed using response surface methodology in order to optimize cell efficiency. These data have been

collected with the help of the Department of Electrical Engineering and Computer Science (EECS), South Dakota State University. The RSM technique will allow us to find the combination of input variables that will optimize a response variable of interest. In Chapter 4, methods for simultaneous inference concerning a stationary point of a quadratic response surface model are discussed. Three methods for constructing simultaneous confidence intervals for the coordinates of a stationary point are developed. The coverage probabilities of these methods, namely, Bonferroni simultaneous confidence intervals, plug-in method (based on an equi-coordinate critical point of a multivariate normal distribution), and the bootstrap technique are assessed using simulation. Chapter 5 presents a metaheuristic search method popular in Operations Research. By this approach, one searches for an alternative order in the default design matrix associated with RSM. This approach consists of a random search and swapping within three blocks (*cube*, *foldover*, and *star*) to find an alternative solution. Chapter 6 deals with recent and advanced RSM topics such as generalized linear models (e.g., when the dependent variable is a count or binary in nature) and multivariate RSM with regard to robustness. Finally, Chapter 7 is devoted to discussions, conclusions, and some future research.

## CHAPTER 2

### INTRODUCTION TO RESPONSE SURFACE METHODOLOGY

#### **2.1 Introduction**

An essential part of any business is improving the performance of its processes and increasing the yields of the systems without increasing the associated costs. This process is referred to as optimization. A specific variable change in the general application can be determined under optimum conditions while holding the other variables at a constant level. This is often referred to as a one variable technique. One main disadvantage of using this technique is that it will not contain the interaction effects between the variables and, additionally, it will not fully describe the effects of the variables on the procedure. In order to solve these problems, optimization studies can be achieved using the technique of response surface methodology (RSM).

The RSM process is a group of statistical and mathematical methods used in developing, and optimizing process, in which a response surface of interest is effected by several variables. RSM is a powerful technique which has important applications in the design of an experiment, the development and design of a new product, and in the optimization of existing products and process designs. It defines the effects of the important factors, alone or in combination with the involved processes [1].

#### **2.2 Overview and stages for RSM application**

Several different methodologies for the response surface process were first introduced in the 1950s by Box and others [2, 3]. In fact, the term “response surface” comes from a graphical perspective created using a mathematical model. RSM is

commonly used in chemometrics, food science, and biochemistry since that time.

Response surface models are techniques that are based on fitting an experimental model to the experimental data obtained in regard to an experimental design [3].

Most applications of RSM for optimization involve of the following several stages: First, a screening factor is run to reduce the number of factors (independent) variables to a relative few, so the procedure will be more efficient and require smaller number of runs or tests. Secondly, determination is made on current levels of the major effect factors resulting in a value for the response that is close to the optimum region. If the current levels of the factors are not consistent with optimum performance, then the experimenter must adjust the process variables that will lead the process toward the optimum level. Thirdly, researchers carry out the chosen experimental design according to the selected experimental matrix. Next, mathematical/statistical models of the experimental design data are developed by fitting linear or quadratic polynomial functions. The fitness of the models then needs to be evaluated. Lastly, the stationary points (optimum values) are obtained for the variables [3]. These stages are summarized in the flowchart provided in Figure 2.1.

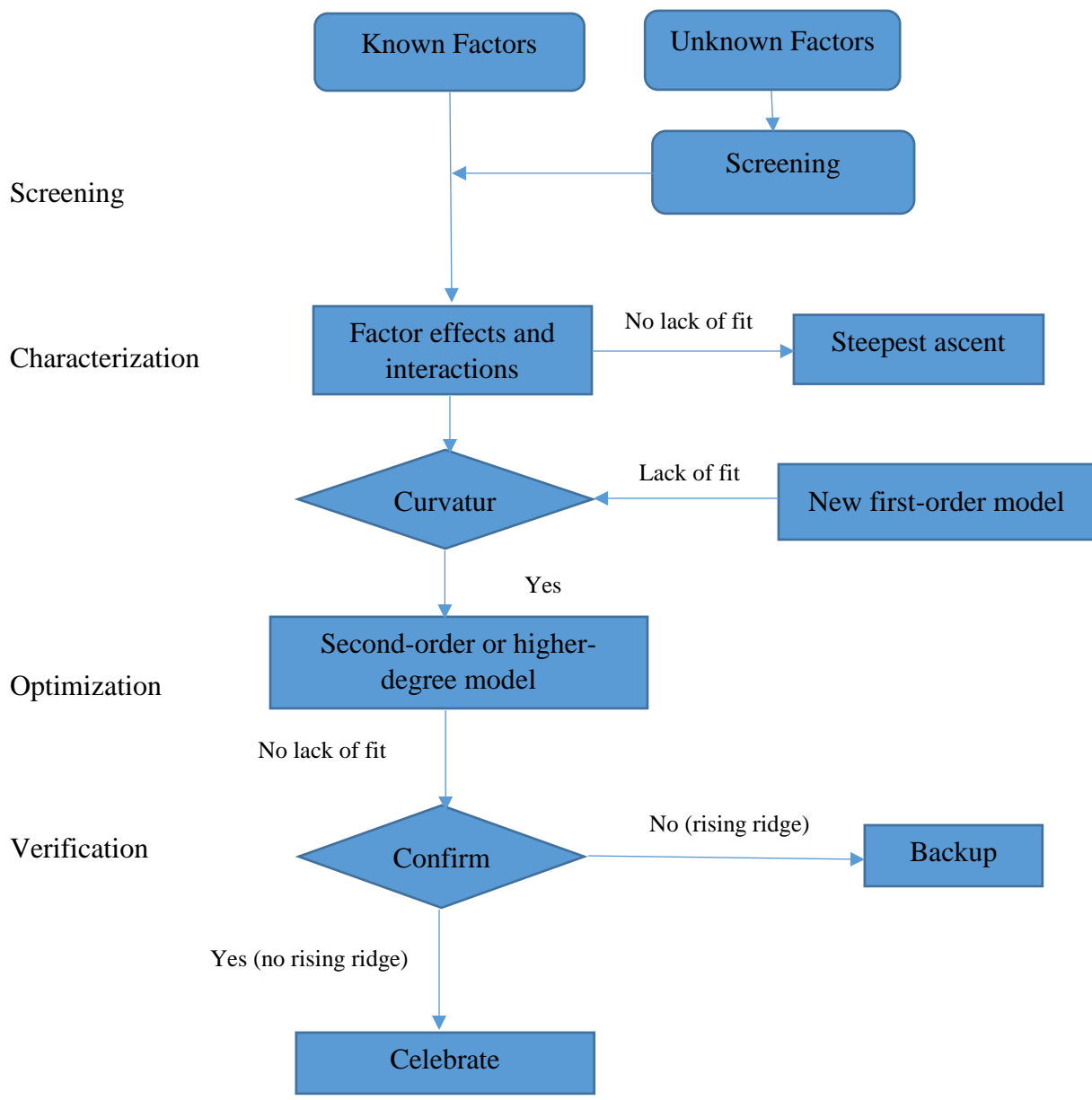


Figure 2.1. Flow chart of RSM.

### **2.3 Screening experiment**

The vast majority of applications of RSM have a sequential nature, with the process being affected by numerous variables. It is necessary to choose control variables that have main effects because it is not possible to identify the effects of all potential control variables. Instead, the process of factorial design may be utilized for this purpose. After identifying the important variables, the direction in which developments lie can be identified, and the levels of the factors are then determined. Determination of these settings is important because the achievement of process optimization directly relates to these settings; wrongly chosen levels result in an ineffective optimization. When the process nears its optimum, an accurate approximation of the true response surface is needed, so the experimenter requires a model that describes the response within a reasonably small area nearby the optimal region. Due to the true response surface typically exhibiting a curvature near the optimum region, a higher degree model will be used, such as a quadratic model. When an proper model has been found, this model may be investigated to find the optimal conditions for the system [3].

### **2.4 Empirical model building**

In most RSM analysis, the relationship among the response surface and the independent variables is unknown. Thus, a first stage in RSM is to find an appropriate approximation for the true efficient relationship between the response variable and a set of independent variables. Many researchers choose response surface design over other designs, with the central composite design being most popular. Several properties are considered when the selection of response surface designs is performed, according to Myers and Montgomery (1995).

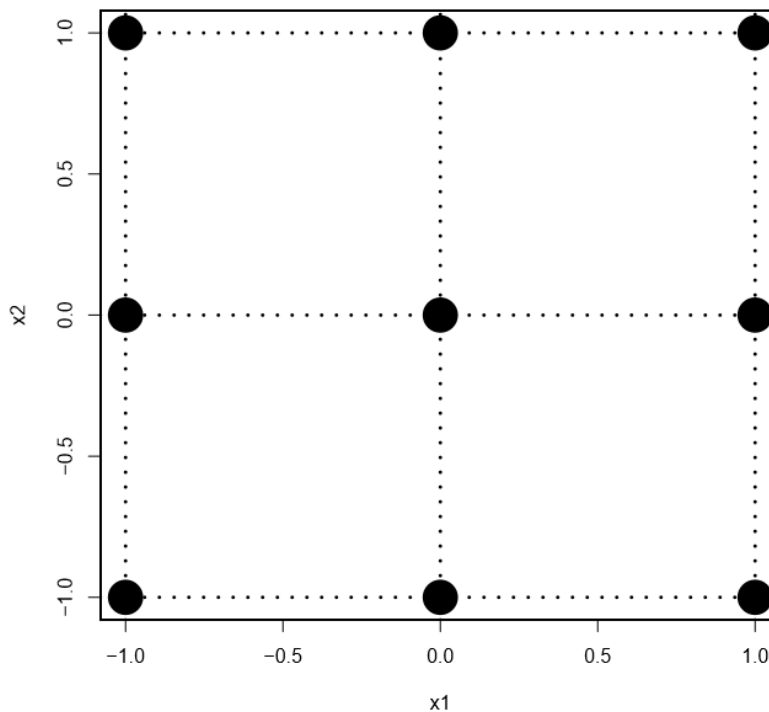


Figure 2.2. Full  $3^2$  factorial design ( $k = 2$ ).

The response surface designs produce a good fit of the model to the data, provide sufficient information to test for lack of fit, and offer an estimate of the pure experiments error. The design allows the experiment to be done in blocks, making it cost efficient. It also uses linear, quadratic, or polynomial functions to describe the effects of control variables on the outcome variable of interest. RSM also has the property of providing a good distribution (the scale prediction variance (SPV) through the design space should be reasonably constant) of  $Var[\hat{y}(X)]/\sigma^2$  throughout the design space; it does not require a high number of design runs and requires few levels of the independent variables. Some computer packages such R package, Design-Expert and JMP are available which provide optimal designs using specific measures and independent variables from the user [4]. Each design is unique with respect to its choice of experimental runs, as well as the

number of design points and blocks. When design collection, the model is defined, and coefficients of the model are estimated.

Typically at the beginning, a low-degree polynomial in some area of the independent variables is used [4, 5]. For its application, consider the relationship between the response and the associated independent variables denoted by  $x_1, x_2, \dots, x_k$ .

Generally, such a relationship is unknown, but can be approximated using a low-degree polynomial of the form

$$Y = \boldsymbol{\beta}^\top f(\mathbf{x}) + \varepsilon \quad (2.1)$$

where  $\mathbf{x} = (x_1, x_2, \dots, x_k)^\top$ ,  $f(\mathbf{x})$  is a multivariable vector function of  $p$  components that consists of power terms and cross-power terms of  $x_1, x_2, \dots, x_k$  up to a certain degree  $d (\geq 1)$ ,  $\boldsymbol{\beta}$  is a  $p$ -dimensional vector containing the regression coefficients, and  $\varepsilon$  is a random error assumed to have a zero mean and homoscedastic variance. Under these assumptions, model (2.1) provides an appropriate representation of the response. Moreover, the  $\boldsymbol{\beta}^\top f(\mathbf{x})$  term is the mean response  $\mu(\mathbf{x})$ , i.e., the expectation of response variable  $Y$ .

Specifically, approximating the relationship among the response variable and the input variables by a first-degree polynomial gives rise to the first-order model:

$$Y = \beta_0 + \sum_{i=1}^k \beta_i x_i + \varepsilon \quad (2.2)$$

As a result, the responses should not exhibit any curvature. To assess curvature, a higher-degree model will be used. A two level factorial designs are utilized to estimate the linear terms, but they fail with additional terms, such as quadratic terms. As a result, a central run in two level factorial designs can be employed for assessing curvature.



Usually, a response surface is represented graphically. For instance, suppose that an organic solar cell data, we wish to find the settings of polymer concentration ( $x_1$ ), polymer-fullerene ratio ( $x_2$ ) and active layer spinning speed ( $x_3$ ) on the cell efficiency ( $y$ ) [6]. This can be seen in Figure 2.3 (a), where  $y$  is plotted versus the levels of  $x_1$  and  $x_3$ . To help visualize the figure of a response surface, the contour of the response surface is

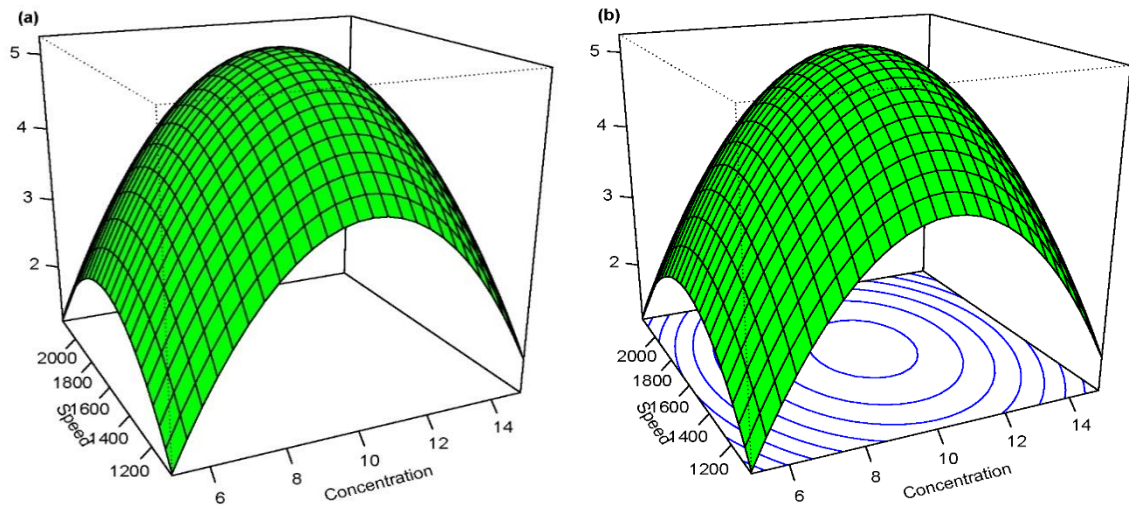


Figure 2.3. (a) The expected efficiency ( $y$ ) as a function of  $x_1$  and  $x_3$  and (b) the contour plot.

often plotted as shown in Figure 2.3 (b). The contour graph of constant response surface is shown in the  $x_1$  and  $x_3$  plane. Each contour relates to a specific height of the response surface.

The next level of the polynomial model should have an additional terms which perform the interaction between the different experimental factors. Therefore, a model for a second-degree interaction is given

$$Y = \beta_0 + \sum_{i=1}^k \beta_i x_i + \sum_{i=1}^k \sum_{j=1, i < j}^k \beta_{ij} x_i x_j + \varepsilon \quad (2.3)$$

where  $\beta_{ij}$  represents the coefficients of the interaction parameters. In order to determine a critical point (maximum, minimum, or saddle), it is necessary for the polynomial function to contain quadratic terms according to the following model

$$Y = \beta_0 + \sum_{i=1}^k \beta_i x_i + \sum_{i=1}^k \sum_{\substack{j=1 \\ i < j}}^k \beta_{ij} x_i x_j + \sum_{i=1}^k \beta_{ii} x_i^2 + \varepsilon \quad (2.4)$$

where  $\beta_{ii}$  denotes the coefficients of the quadratic terms.

To estimate the parameters in Equation (2.4), the experimental design has to assure that all process variables are preformed using at least three-factor levels.

In each run of the experiment, the response  $Y$  is measured for the specified settings of the input variables. The experimental settings constitute the so-called response surface design. This can be represented by a design matrix, denoted by  $\mathbf{D}$ , of dimension  $n \times k$ :

$$\mathbf{D} = \begin{bmatrix} x_{11} & x_{12} & \cdots & x_{1k} \\ x_{21} & x_{22} & \cdots & x_{2k} \\ & & \vdots & \\ x_{n1} & x_{n2} & \cdots & x_{nk} \end{bmatrix} \quad (2.5)$$

where  $x_{ui}$  denote the  $u$ -th design setting of the  $i$ th input variable  $\mathbf{x}_i$  ( $i = 1, 2, \dots, k; u = 1, 2, \dots, n$ ). Each row of  $\mathbf{D}$  is referred to as a design point in a  $k$ -dimensional space. Let  $y_u$  denote the response value obtained as a result of applying the  $k$ -th setting of  $\mathbf{x}$ , namely,  $\mathbf{x}_u = (x_{u1}, x_{u2}, \dots, x_{uk})^\top$  for ( $u = 1, 2, \dots, n$ ) From Equation (2.1), we have

$$\mathbf{y}_u = \beta^\top f(\mathbf{x}_u) + \varepsilon_u, u = 1, 2, \dots, n$$

where  $\varepsilon_u$  denotes the random error from the  $u$ -th experimental run. Model (2.4) can be expressed in matrix notation as follows

$$\mathbf{Y} = \mathbf{X}\boldsymbol{\beta} + \boldsymbol{\varepsilon} \quad (2.6)$$

where  $\mathbf{y} = (y_1, y_2, \dots, y_n)^\top$ ,  $\mathbf{X}$  is the matrix of dimension  $n \times p$  whose  $k$ -th row is  $f^\top(\mathbf{x}_k)$ , and  $\boldsymbol{\varepsilon} = (\varepsilon_1, \varepsilon_2, \dots, \varepsilon_n)^\top$ . Note that the first column of  $\mathbf{X}$  is the column of ones  $\mathbf{1}_n$ .

The error  $\boldsymbol{\varepsilon}$  has a zero mean and a variance-covariance matrix given by  $\sigma^2$ . The ordinary least-square estimator of  $\boldsymbol{\beta}$  is

$$\widehat{\boldsymbol{\beta}} = (\mathbf{X}^\top \mathbf{X})^{-1} \mathbf{X}^\top \mathbf{y} \quad (2.7)$$

The variance-covariance matrix of  $\widehat{\boldsymbol{\beta}}$  is given by

$$\begin{aligned} \text{Var}(\widehat{\boldsymbol{\beta}}) &= (\mathbf{X}^\top \mathbf{X})^{-1} \mathbf{X}^\top (\sigma^2 \mathbf{I}_n) \mathbf{X} (\mathbf{X}^\top \mathbf{X})^{-1} \\ &= \sigma^2 (\mathbf{X}^\top \mathbf{X})^{-1} \end{aligned} \quad (2.8)$$

Using  $\widehat{\boldsymbol{\beta}}$ , an estimate,  $\hat{\mu}(\mathbf{x}_u)$ , of the predicted response at  $\mathbf{x}_u$  is

$$\hat{\mu}(\mathbf{x}_u) = \widehat{\boldsymbol{\beta}}^\top f(\mathbf{x}_u), \quad u = 1, 2, \dots, n$$

The quantity  $\widehat{\boldsymbol{\beta}}^\top f(\mathbf{x}_u)$  also gives the predicted response,  $\hat{y}(\mathbf{x}_u)$  at the  $u$ -th design point ( $u = 1, 2, \dots, n$ ). In general, at any point  $\mathbf{x}$  in an experimental space, denoted by  $R$ , the predicted response  $\hat{y}(\mathbf{x})$  is

$$\hat{y}(\mathbf{x}) = \widehat{\boldsymbol{\beta}}^\top f(\mathbf{x}), \quad \mathbf{x} \in R. \quad (2.9)$$

Since  $\widehat{\boldsymbol{\beta}}$  is an unbiased estimator of  $\boldsymbol{\beta}$ ,  $\hat{y}(\mathbf{x})$  is also an unbiased estimator of  $\boldsymbol{\beta}^\top f(\mathbf{x})$ , which is the mean response at  $\mathbf{x} \in R$ . Using Equation (2.9), the prediction variance of  $\hat{y}(\mathbf{x})$  is

$$\text{Var}[\hat{y}(\mathbf{x})] = \sigma^2 f^\top(\mathbf{x}) (\mathbf{X}^\top \mathbf{X})^{-1} f(\mathbf{x}). \quad (2.10)$$

By choosing the proper design, the size of the prediction variance is based on the design matrix  $\mathbf{X}$ . This facilitates determination of the optimal response quantities to obtain the optimal value of  $\hat{y}(\mathbf{x})$  over the design region  $R$ . Moreover, it is important that the prediction variance is as small as possible.

## 2.5 Encoding of input variable levels

The encoding of the input variable levels is based on transforming each studied real value into coordinates inside a scale with dimensionless values. These transformed values must satisfy the condition of being proportional in their localization in the experimental space. When the original units are used, we can find different numerical results as compared to the coded unit analysis, and often these results will be difficult to interpret [4]. Encoding is a simple linear transformation of the actual measurement scale [5]. If the “High” value is  $x_h$  and the “Low” value is  $x_l$  (in the actual scale), then the scaling takes any actual  $x$  value and converts it to  $(x - a)/b$ , where  $a = (x_h + x_l)/2$  and  $b = (x_h - x_l)/2$ . Note that  $-1 \leq (x - a)/b \leq +1$ . One can easily convert the coded values to the original scales.

## 2.6 First-order model

For a first-degree design, the most common approach is a two-level factorial design ( $2^k$  factorial designs where  $k$  the number of variables).

### 2.6.1 Two-level factorial designs

When it is necessary to investigate the joint effect of several variables on a response, factorial designs are widely used, especially in experiments involving more than one factor. However, the general factorial design in several special cases is important; this is due to their wide use in research work. In a two-level factorial design, each factor is

measured at two levels, with encoded values, -1, +1, that regarding to the low and high levels, respectively, of each factor. Through this design, all possible combinations of such levels of the  $k$  factors are considered and evaluated. The row of the design matrix  $D$  represents a combination of 1s and -1s that describe a specific treatment design runs. In such cases, the number,  $n$ , of design runs is equal to  $2^k$ , providing all possible combinations without replication [7].

### 2.6.2 Two-level fractional factorial designs

As the number of variables in a two-level factorial design increases, the number of design runs for a complete replication of the design rapidly increases.

In this section, we focus on a significant class of designs called fractional factorial designs. Throughout, we assume that: (i) the variables are fixed, (ii) the designs are completely randomized, and (iii) assumptions of normality are satisfied. The  $2^{k-1}$  design is principally helpful in the early phases of experimental work when a large number of factors are likely to be studied. Through it, we are provided with the minimum number of runs with which  $k$  variables can be preformed in a complete factorial design. Therefore, these designs are commonly used in variable screening experiments. Since there are only two-levels for each variable, we consider that the response is approximately linear over the region of the factor levels chosen. As is the case with many factor-screening experiments, when the process or the system is in the beginning stages of testing, this is found to be a reasonable assumption [4].

The method of fractional factorial designs frequently results in excessive economy and effectiveness in experimentation, especially if the runs of the experiment are sequential in nature. For instance, suppose that the experimenters are investigating

$k = 3$  with all total possible runs ( $2^3 = 8$  runs) plus 8 center point repetitions. The preferred method is to run a  $2^{3-1}$  fractional design (4 runs) with 4 repetitions at the center of each half-fraction and then analyze the results. The information obtained from this process is used to make decisions on a set of the design runs to perform next.

Whenever it becomes necessary to solve ambiguity, we are able to run the alternate fraction and the entire number of design runs in a central composite design ( $n = 2^k + 2k + n_0 = 24$  runs), where  $n_0$  is the center point [3].

For example, the corresponding  $2^3$  design matrix is as follows:

$$D = \begin{bmatrix} -1 & -1 & -1 \\ 1 & -1 & -1 \\ -1 & 1 & -1 \\ 1 & 1 & -1 \\ -1 & -1 & 1 \\ 1 & -1 & 1 \\ -1 & 1 & 1 \\ 1 & 1 & 1 \end{bmatrix}$$

where the columns are the factor levels and the rows represent all possible combinations of the three factors ( $k = 3$ ).

## 2.7 Blocking in response surface designs

When response surface designs are used, it is required to consider blocking in order to exclude noise variables. For example, problems may occur when a second-degree design is collected sequentially from a first-degree design. Extensive time may elapse among the fitting of the first-degree design and the running of the additional experiments required in order to build quadratic design. In fact, check conditions may change throughout this time, more requiring blocking. A response surface design, which blocks orthogonally, the block effect will not effect the parameter estimates of the model.

In other words, if a  $2^k$  or  $2^{k-p}$  design is used as a first-degree response surface design, the center points should be allocated equally among the blocks [4].

For a second-order design to block orthogonally, two conditions must be fulfilled. If there are  $n_b$  design runs in the  $b$ th block, then these conditions are as follows:

Each block for a first-degree must be orthogonal design; that is,

$$\sum_{u=1}^{n_b} x_{iu}x_{ju} = 0 \quad i \neq j = 0, 1, \dots, k \quad \text{for all blocks.}$$

where  $x_{iu}$  and  $x_{ju}$  are the levels of  $i$ th and  $j$ th variables in the  $u$ th point of the experiment with  $x_{0u} = 1$  for all  $u$ .

The portion of the total sum of squares for each factor donated by every block must be equal to the fraction of the entire runs that occur in the block, as seen in the following:

$$\frac{\sum_{u=1}^{n_b} x_{iu}^2}{\sum_{u=1}^N x_{iu}^2} = \frac{n_b}{N} \quad i = 1, 2, \dots, k \quad \text{for all blocks}$$

where  $N$  is the number of total runs in the design.

As an example of a central composite design with  $k = 2$  factors and  $N = 12$  runs, and star point  $\alpha$ , the levels of  $x_1$  and  $x_2$  for this design in the design matrix are:

$$D = \left[ \begin{array}{cc} \left. \begin{array}{l} -1 \quad -1 \\ 1 \quad -1 \\ -1 \quad 1 \\ 1 \quad 1 \\ 0 \quad 0 \\ 0 \quad 0 \end{array} \right\} & \text{Block 1} \\ \left. \begin{array}{l} \alpha \quad 0 \\ -\alpha \quad 0 \\ 0 \quad \alpha \\ 0 \quad -\alpha \\ 0 \quad 0 \\ 0 \quad 0 \end{array} \right\} & \text{block 2} \end{array} \right]$$

Note that the design is organized into two blocks with the first block containing the factorial portion of the design with two center runs, and the second block containing the additional points with center runs.

## 2.8 Steepest ascent

More often than not, the initial estimate of the optimal conditions will be far away from the original optimum. In such situations, the aim of the experimenter is to change to the optimum as rapidly as possible by running a simple and economically effective experimental process [4]. When the results are far from the optimum region, we usually assume that a linear model is an appropriate approximation of the true response surface in a small region of the  $x$ 's. This method, known as the steepest ascent, is a technique developed to move sequentially to optimize the response. We use the fitted first-order model which given by

$$\hat{y} = \hat{\beta}_0 + \sum_{i=1}^k \hat{\beta}_i x_i$$

The contours of  $\hat{y}$ , is a series of parallel lines. The direction of steepest ascent is the direction in which a process increases most rapidly, a direction which is typical for the fitted response surface. More often than not, the path of steepest ascent is taken, as it is the line through the center of the space of interest and the results show normally improving values of the response surface. As such, we see that the steps along the path are proportional to the regression coefficients. The actual step size is determined by the experimenter based on process knowledge or other practical considerations [4].

Experiments are conducted along the path of steepest ascent until an increase in response is no longer observed. At this point, a new first-degree model may be more



appropriate, a new path of steepest ascent is determined, and the procedure continues. Eventually, the experimenter will reach a result that is near the optimum; this is usually indicated by the lack of fit of a first-order model. At this time, additional experiments are accompanied in order to estimate optimum more precisely.

Before exploring the method of steepest ascent, one must first investigate the adequacy of the first-order model. The  $2^2$  design with center points helps the experimenter to obtain an estimate of error, check for interactions in the model, and determine the existence of any quadratic effects (curvature).

It is easy to provide a general process that help in determining the coordinates of a design point on the path of steepest ascent. Assume the point  $x_1 = x_2 = \dots = x_k = 0$  is the base or origin point. Next, we choose a step size in one of the process variables, such as  $\Delta x_i$ . Usually, the variable is selected based on accumulated data, or is the one with the largest absolute regression coefficient  $|\hat{\beta}_i|$ . The step size in the other variables is

$$\Delta x_i = \frac{\hat{\beta}_i}{\hat{\beta}_j/\Delta x_j} \quad i = 1, 2, \dots, k \quad i \neq j \quad (2.11)$$

Then convert of  $\Delta x_i$  from coded variables to natural variables. The experimenter computes the design points along this path by observing the outcome (yields) at these design points using formula (2.11), until a change in response is noted, For example, Figure 2.4 show the change point. Although the mathematical computations are based on the coded variables, the actual variables must be used in running the experiments. For example, a chemical engineering is wished to determine the operating conditions that maximize the yield of the process. Two independent variables affect the process response: reaction time and reaction temperature [4]. The experimental region for fitting

the linear model should be (30, 40) minutes of reaction time and (150, 160) Fahrenheit.

The experimental design is shown in Table 2.1.

The fitted first-order model in coded variables:

$$\hat{y} = 40.44 + 0.775 x_1 + 0.325 x_2$$

The adequacy of the linear model should be studied before the steepest ascent procedure.

The  $2^2$  design with center points allows us to check for interaction and quadratic effects (curvature).

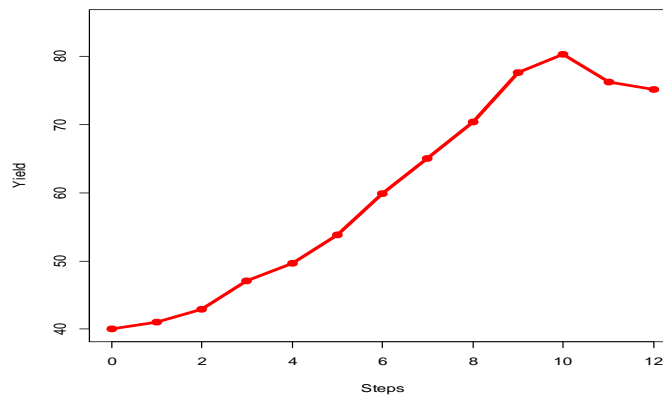


Figure 2.4. Response along the path of the steepest ascent.

Table 2.1. ANOVA for the first-order model.

Sources	Sum of square	DF	Mean square	P-Value
Regression	2.825	2	1.4125	
Residual	0.1772	6	0.0295	
Interaction	0.0025	1	0.0025	0.8215
Curvature	0.0027	1	0.0027	0.8142
Total	3.0022	8		

Table 2.2. Steepest ascent experiment.

Steps	Coded values		Original values		Response
	$x_1$	$x_2$	Reaction time ( $\xi_1$ )	Reaction temperature ( $\xi_2$ )	
Origin	0	0	35	155	-
$\Delta$	1	0.42	5	2	-
Origin + $\Delta$	1	0.42	40	157	41.0
Origin + 2 $\Delta$	2	0.84	45	159	42.9
Origin + 3 $\Delta$	3	1.26	50	161	47.1
Origin + 4 $\Delta$	4	1.68	55	163	49.7
Origin + 5 $\Delta$	5	2.10	60	165	53.8
Origin + 6 $\Delta$	6	2.52	65	167	59.9
Origin + 7 $\Delta$	7	2.94	70	169	65.0
Origin + 8 $\Delta$	8	3.36	75	171	70.4
Origin + 9 $\Delta$	9	3.78	80	173	77.6
Origin + 10 $\Delta$	10	4.20	85	175	80.3
Origin + 11 $\Delta$	11	4.62	90	179	76.2
Origin + 12 $\Delta$	12	5.04	95	181	75.1

From the ANOVA Table, there is no exhibit of the curvature, and the interaction is not significant, whereas the F-test is significant of overall regression.

The path of steepest ascent to move away from the design center toward the optimum region, the experimenter would move 0.775 units of  $x_1$  direction for every 0.325 units of  $x_2$  direction. The path of steepest ascent will pass through the design center ( $x_1 = 0$ ,  $x_2 = 0$ ) with slope 0.325/0.775. Based on the relationship between  $x_1$  and  $\xi_1$ , the experimenter decided to utilize 5 minutes of reaction time as step size. The step size is based on the largest regression coefficient of  $x_1$ . In coded values,  $\Delta x_1 = 1$ . Therefore, the step size of temperature will be

$$\Delta x_2 = \frac{\hat{\beta}_2}{\hat{\beta}_1/\Delta x_1} = \frac{0.325}{(0.775/1)} = 0.42.$$

To convert the coded step size to original units, we use the relationships

$$\Delta x_1 = \frac{\Delta \xi_1}{5} \text{ and } \Delta x_2 = \frac{\Delta \xi_2}{5}$$

which results in

$$\Delta \xi_1 = \Delta x_1(5) = 1(5) = 5 \text{ min}$$

and

$$\Delta \xi_2 = \Delta x_2(5) = 0.42(5) = 2^\circ F.$$

Furthermore, Figure 2.4 exhibits all the steps beyond the tenth point when the response starts to decrease. Therefore, another first-degree model will be fitted around the new region.

Table 2.3. Data for quadratic model.

Original values		Coded values		Response
Reaction time	Reaction temperature	$x_1$	$x_2$	
80	170	-1	-1	76.5
80	180	-1	1	77.0
90	170	1	-1	78.0
90	180	1	1	79.5
85	175	0	0	79.9
85	175	0	0	80.3
85	175	0	0	80.0
85	175	0	0	79.7
85	175	0	0	79.8

The fitted first-order model in coded values for the data in Table 2.3 is

$$\hat{y} = 78.97 + 1.00 x_1 + 0.50 x_2$$

From the ANOVA Table, the interaction and curvature checks show that the linear model is not an appropriate approximation. The curvature of the true response surface indicates that we are near to the optimum. At this point, augmenting more design points to fit

higher degree model, such as the quadratic model in order to obtain the optimum conditions [4].

Table 2.4. ANOVA for quadratic model.

Sources	Sum of square	DF	Mean square	P-Value
Regression	5.00	2		
Residual	11.1200	6		
Interaction	0.2500	1	0.2500	0.0955
Curvature	10.6580	1	10.6580	0.0001
Total	16.12	8		

## 2.9 A second-order experimental design

### 2.9.1 Full $3^k$ factorial designs

A full  $3^k$  factorial design is a design matrix with very limited application in RSM when the number of variables is greater than two. This is due to the large number of experiments required for such a design (calculated by expression  $N=3^k$ , where  $N$  is a total experiment run, and  $k$  is the number of variables). Therefore, its efficiency is lost when modeling quadratic functions. Because of this, full three-level factorial designs for more than two factors require more experimental runs than are commonly accommodated in practice. Designs containing a smaller number of design points, such as the Box–Behnken, central composite, and Doehlert designs are more frequently used [4]. For two variables, the efficiency can be compared with designs such as central composite [8].

Table 2.5. Design matrix for three-level factorial design with two factors

$x_1$	$x_2$
-1	-1
-1	0
-1	1
0	-1
0	0
0	1
1	-1
1	0
1	1

Figures 2.5 (a) and (b) show the representation of the three-level factorial designs for the optimization of two and three variables, respectively. Table 2.5 presents the experimental matrix for the optimization of two variables using this design.

### 2.9.2 Box–Behnken designs (BBD)

Box and Behnken [9] suggested a means to select design points from the three-level factorial arrangement, while also allowing for the efficient estimation of the linear and quadratic terms of the model. In this way, the designs are more efficient, as well as more economical than their corresponding  $3^k$  designs, mainly for a high number of factors. Figure 2.5(c) presents the BBD for three-factor optimization with 13 experimental points. In comparison with the original  $3^3$  design with 27 experiments is shown in Figure 2.5(b), this design is noted as being both more economical and more efficient. Table 2.6 presents the coded values of this design for three factors. In its application, it is much smaller than the central composite design. However, the disadvantages of BBD are that it provides a poor quality of prediction over the entire design region and it also requires that variable levels not be outside the region of the variables in the factorial analysis [5].

Table 2.6. Design matrix for Box–Behnken design with three factors.

$x_1$	$x_2$	$x_3$
-1	-1	0
1	-1	0
-1	1	0
1	1	0
-1	0	-1
1	0	-1
-1	0	1
1	0	1
0	-1	-1
0	1	-1
0	-1	1
0	1	1
0	0	0

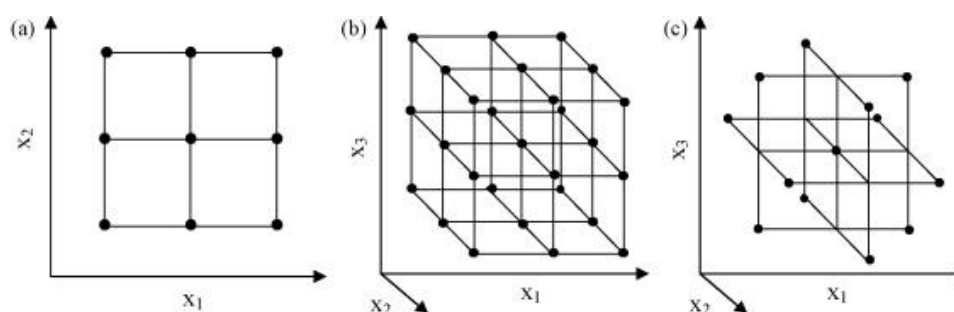


Figure 2.5. The three-level factorial design of (a) two factors and (b) three factors and (c) Box–Behnken design of three factors.

### 2.9.3 The central composite design (CCD)

The Box-Wilson Central Composite Design, commonly called a Central Composite Design (CCD), is the most popular of all second-order designs. This design consists of the following parts: i) a complete (or a fractional of)  $2^k$  factorial design whose factors' settings are coded as (Low = -1, High = 1); this is called the factorial portion; ii) an additional design, star points, which provides justification for selecting the distance of the star points from the center; the CCD always contains twice as many star points as there are factors in the design ( $2k$ ); iii)  $n_0$  central point. Thus, the total number of design

points in a CCD is  $n = 2^k + 2k + n_0$ . A CCD is obtained by augmenting the first-order design of a  $2^k$  factorial with additional experimental runs, the  $2k$  axial points, and the  $n_0$  center-point replications. This design is consistent with the sequential nature of a response surface investigation. The analysis starts with a first-order design and a fitted first-degree model, followed by the addition of design points to fit a higher second-degree model. The first-order design in the preliminary phase gives initial information about the response system and assesses the importance of the factors in a given experiment. The additional experimental runs are performed for the purpose of obtaining more information. This information helps to determine the optimum operating conditions of the independent variables by using the second-degree model. In the CCD, the values of  $\alpha$  and  $n_0$ , are chosen for their desirable properties, where  $\alpha$  is the axial point and  $n_0$  the number of center point replicates. For instance, to ensure that a CCD has a rotatable, orthogonal, and uniform precision property, all three factors are studied at five levels  $(-\alpha, -1, 0, +1, +\alpha)$ , as will be discussed in section 2.13. The orthogonality of a second-order design is achieved when the quadratic model is expressed in terms of orthogonal polynomials. The value of  $n_0$  can be determined for a rotatable CCD to have either the additional orthogonality property or the uniform precision property. For further details, we refer to Khuri and Cornell [7, 10].



Table 2.7. Design matrix for central composite design with three factors.

	$x_1$	$x_2$	$x_3$
Design point	-1	-1	-1
	1	-1	-1
	-1	1	-1
	1	1	-1
	-1	-1	1
	1	-1	1
	-1	1	1
	1	1	1
Star point	$-\alpha$	0	0
	$\alpha$	0	0
	0	$-\alpha$	0
	0	$\alpha$	0
Central point	0	0	$-\alpha$
	0	0	$\alpha$
	0	0	0
	0	0	0

This design has orthogonal, rotatable, and uniform precision property.

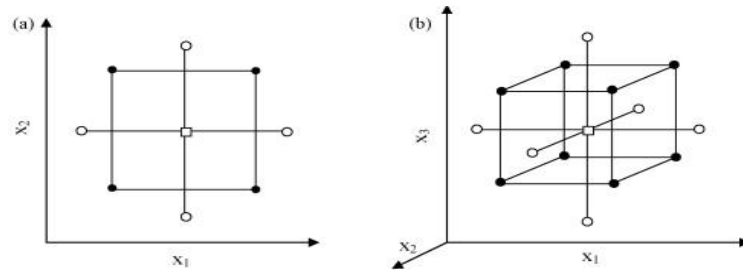


Figure 2.6. CCD (a) two factors with  $\alpha = \sqrt{2}$  and (b) three factors with  $\alpha = 1.68$ .

### 2.9.4 Doehlert design

Doehlert developed an equation such that when a simplex optimization with two variables comes to the point where it encircles the optimum, a hexagon is formed. The Doehlert designs allow for the calculation of a response surface through a minimum of experimentation. An additional attractive feature of this design is that a neighboring domain can be easily explored through the addition of a few experiments [5, 11]. The

design matrices for Doehlert designs with two and three factors are given in Tables 2.8. (a), and (b), respectively.

Table 2.8. Doehlert matrices (a) with two variables, and (b) with three variables.

(a)		(b)		
$X_1$	$X_2$	$X_1$	$X_2$	$X_3$
0	0	0	0	0
1	0	0	-1	0
0.5	0.866	1	0	0
-1	0	0	1	0
-0.5	-0.866	-1	0	0
0.5	-0.866	-0.5	-0.5	0.707
-0.5	0.866	0.5	-0.5	0.707
		0.5	0.5	0.707
		-0.5	0.5	0.707
		-0.5	-0.5	-0.707
		0.5	-0.5	-0.707
		0.5	0.5	-0.707
		-0.5	0.5	-0.707

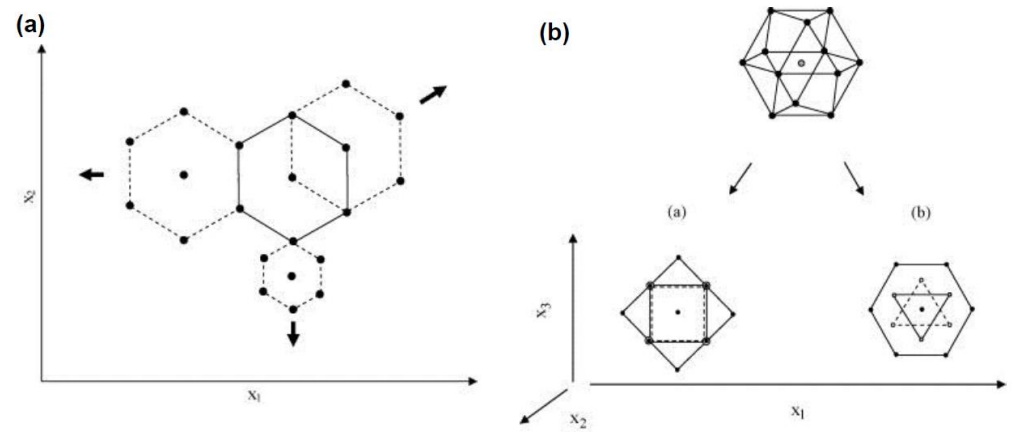


Figure 2.7. Doehlert design (a) two factors (b) three factors originated by the two-plane.

The second-order model is commonly used in response surface methodology for several reasons. Firstly, the quadratic model is very flexible, in that it will often work efficiently as an estimation of the true response surface. Secondly, the method of least

squares can be used in order to estimate the parameters (the  $\beta$ 's) in the second-degree model. Finally, there is significant practical experience showing that quadratic models work well in explaining real response surface problems [3].

### 2.10 Lack-of-fit test

In RSM application, usually the experimenters are fitting the regression model to data from the experimental design. Frequently, it is useful to have two or more replicates on the response at the same levels of the independent variables. This allows us to test for lack-of-fit of the regression model. Assume that there are  $n_i$  observations of the response at the  $i$ th settings of independent variable  $x_i, i = 1, 2, \dots, m$ . Let  $y_{ij}$  denote the  $j$ th observation on the response at  $x_i, i = 1, 2, \dots, m$  and  $j = 1, 2, \dots, n_i$ . Moreover,  $n = \sum_{i=1}^m n_i$ . Thus, the residual sum of square can be partitioned into two component,

$$SS_E = SS_{PE} + SS_{LOF},$$

$$\sum_i^m \sum_j^{n_i} (y_{ij} - \hat{y}_i)^2 = \sum_i^m \sum_j^{n_i} (y_{ij} - \bar{y}_i)^2 + \sum_i^m \sum_j^{n_i} (\bar{y}_i - \hat{y}_i)^2$$

where  $SS_{PE}$  is the sum of square of pure error,  $SS_{LOF}$  is the sum of square associated with lack-of-fit, and  $\bar{y}_i$  is the average of the  $n_i$  observations at  $x_i$ .

Analysis of variance (ANOVA) is a useful way to evaluate the performance of a fitted regression model. ANOVA is based on the idea of partitioning the total variation in the dependent variable into various components. The ANOVA table for lack-of-fit test is shown in Table 2.9. The mean square is an estimate of population variance; it is obtained by dividing the sum of squares by the corresponding number of degrees of freedom. The F-value compares the mean square with the residual mean square. The corresponding p-

value ( $\text{Prob} > F$ ) is the probability of obtaining an Fvalue equal to or more extreme than what we observed in our sample assuming the null hypothesis is true (there is no significant difference of factor effects).

Table 2.9. ANOVA table for lack-of-fit test.

Variance source	Sum of the square	df	Mean square
Regression	$SS_{reg} = \sum_i^m \sum_j^{n_i} (\hat{y}_i - \bar{y})^2$	$p - 1$	$MS_{reg} = \frac{SS_{reg}}{p - 1}$
Residuals	$SS_{res} = \sum_i^m \sum_j^{n_i} (y_{ij} - \hat{y}_i)^2$	$n - p$	$MS_{res} = \frac{SS_{res}}{n - p}$
Lack of fit	$SS_{lof} = \sum_i^m \sum_j^{n_i} (\bar{y}_i - \hat{y}_i)^2$	$m - p$	$MS_{lof} = \frac{SS_{lof}}{m - p}$
Pure error	$SS_{pure} = \sum_i^m \sum_j^{n_i} (y_{ij} - \bar{y}_i)^2$	$n - m$	$MS_{pure} = \frac{SS_{pure}}{n - m}$
Total	$SS_{total} = \sum_i^m \sum_j^{n_i} (y_{ij} - \bar{y})^2$	$n - 1$	

where  $n_i$  is number of observations;  $m$  the total number of factor levels in the design;  $p$  is the model parameters;  $\hat{y}_i$  the estimated value by the model at level  $i$ ;  $\bar{y}$  overall mean;  $y_{ij}$  repetitions performed at each individual levels; and  $\bar{y}_i$  the mean of replicates at the same set of experimental combinations. There are different F-tests for testing the linear, interactions, quadratic effects, and lack-of-fit, we want to select the model that have insignificant lack-of-fit.

## 2.11 Variance dispersion graph

A variance dispersion graph (VDG) is a graph capable of displaying the minimum, maximum, and average prediction variances for a specific design and response model versus the distance between the design point and the center of the design space. The distance, or radius, usually differs from zero (the design center) in that in a spherical design, the radius is the distance to the farthest point from the center. Normally, one plots the scaled prediction variance (SPV) as

$$N V[\hat{y}(\mathbf{x})]/\sigma^2 = N \mathbf{x}^T (\mathbf{X}^T \mathbf{X})^{-1} \mathbf{x} \quad (2.12)$$

Note that the SPV is the prediction variance in Equation (2.12) multiplied by the number of design runs ( $N$ ) and divided by the error variance  $\sigma^2$ . Dividing by  $\sigma^2$  makes the quantity scale-free and multiplying by  $N$  often helps to facilitate the comparison of designs of different sizes.

Figure 2.8.(a) is a VDG for the rotatable CCD with  $k = 3$  variables and five center runs. Since the design is rotatable, the minimum, maximum, and average SPV are identical for all points that are equidistant from the center of the design. As a result, there is only one line on the VDG. Next, observe how the graph displays the behavior of the SPV over the design space, with nearly constant variance out to a radius, and then it increases steadily from there to the boundary of the design. Figure 2.8.(b) is a VDG for a spherical CCD with  $k = 3$  variables and five center runs. Notice that there is little to no difference between the three lines for minimum, maximum, and average SPV; we can therefore conclude that any practical differences between the two types of central composite designs (the rotatable and spherical) versions of this design are minimal. Figures 2.9 (a) and (b) are the VDGs for a rotatable CCD with  $k = 3$  variables and  $\alpha =$

1.68,  $\sqrt{2}$ . In this VDG, the number of center points in the design varies from  $n_0 = 1$  to  $n_0 = 5$ . The VDG clearly shows us that a design with too few center points will have an unstable distribution of prediction variance; the prediction variance quickly stabilizes, however, with increasing values of  $n_0$ . The use of either four or five center runs will give reasonably stable prediction variance over the design space. These recommendations are based on VDG studies on the effects of changing the number of center points in the response surface design [4].

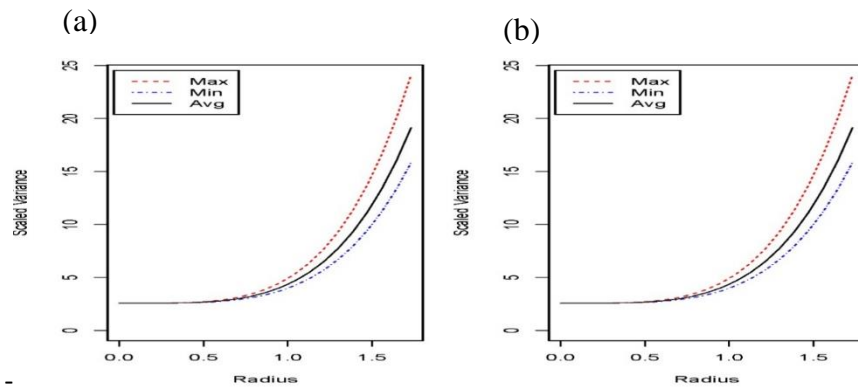


Figure 2.8. VDG with three factor, five center point with  $\alpha = 1.68$  and  $\alpha = 1.732$ .

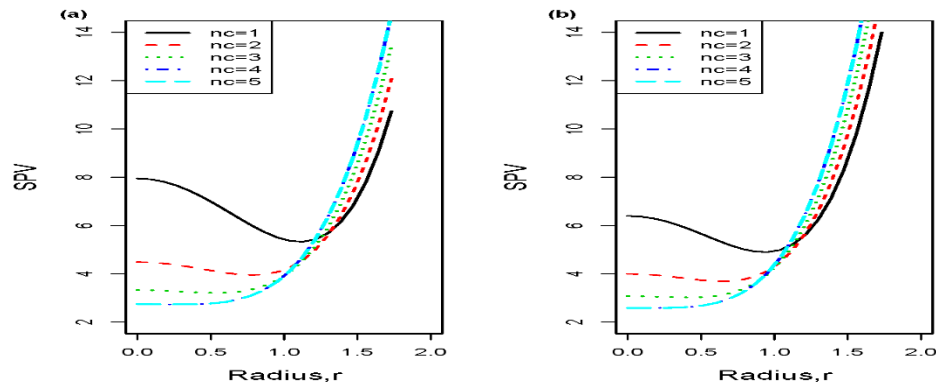


Figure 2.9. VDG with  $k = 3$  and  $\alpha = 1.68$  with  $\alpha = \sqrt{2}$  (note to five center point).

An additional benefit of using center points can be found when a factorial experiment is performed for an ongoing process [4]. Consider using the current operating

conditions (or recipe) as the center point in the design; this is done to assure the operating personnel that at least some of the runs in the experiment are going to be performed under familiar conditions. As such, the results obtained are not likely to be worse than those typically obtained. When the center point in a factorial experiment corresponds to a real-life process, the experimenter can use the observed responses at the center point to note whether anything unusual occurred during the experiment. That is, the responses of the center point should be very similar, if not identical, to any responses observed historically in the routine process. Often times, operating personnel will keep a control chart for monitoring process performance [3]. When they do so, the center point responses can be plotted directly on the control chart to check the behavior of the process within the experiment. Consider running the replicates at the center in nonrandom order, run one or two center points at or close to the beginning of the experiment, one or two near the center, and one or two near the end. By spreading the center points out over the course of the experiment, the experimenter obtains a rough check on the stability of the process. For instance, if a trend appears during the performance of the experiment, plotting the center point responses against the time order may reveal this.

In other cases, experiments must be performed in situations where there is little or no previous information regarding variability in the process. In such cases, running two or three center points in the design will be helpful for the first few runs. These runs provide a preliminary estimate of variance. If the magnitude of the variability appears to be reasonable, then additional runs can be done. On the other hand, if variability is larger than anticipated, no further runs should be done. It is then prudent to determine why the variability is so large before performing additional experiments. Usually, center points

are applied when the design variables are quantitative. However, there will sometimes be one or more qualitative or categorical factors among several quantitative ones. Center points can still be utilized in these cases. For example, consider an experiment with two quantitative variables, each variable at two levels, and a single qualitative variable, also with two levels. In such a case, the central points should be located on the opposing faces of the cube that includes the quantitative variables. In other words, center points can be employed at the high- and low levels for treatment combinations of the qualitative variables, so long as those subspaces include only quantitative variables [4].

## **2.12 The Common design properties**

In an experimental setting, the choice of design depends on the desired properties. The classical design properties to be considered in developing an RSM include orthogonality, rotatability, and uniform precision property.

### **2.12.1 Orthogonality**

A design is said to be orthogonal if the matrix  $\mathbf{X}^T \mathbf{X}$  is diagonal, where  $\mathbf{X}$  is the design matrix. This approach causes the elements of  $\hat{\boldsymbol{\beta}}$  to be independent because the off-diagonal elements of the variance-covariance matrix  $Var(\hat{\boldsymbol{\beta}})$  in Equation (2.8) will be zero. Assuming normal distribution for error vector  $\boldsymbol{\varepsilon} \sim N(\mathbf{0}, \sigma^2 \mathbf{I}_n)$  in Equation (2.6), the OLS estimates of the regression coefficients will be stochastically independent and normally distributed. This makes statistical inference of the unknown parameters in the model easier [7].

### **2.12.2 Rotatability**

The concept of rotatability was first introduced by Box and Hunter (1957) and has since become an important design criterion. A design matrix is said to be rotatable if the



prediction variance in Equation (2.10) is constant at all points with equal distance from the center of the design, which, by a proper coding of the input variables, can be chosen as the point of origin of the  $k$ -dimensional coordinates system. Thus, if the design is rotatable,  $Var[\hat{y}(\mathbf{x})]$  is constant at all points that fall on the surface of a hyper-sphere centered at the origin. This property makes the prediction of variance constant under any rotation of the coordinate axes. In addition, if optimization of  $\hat{y}(\mathbf{x})$  is desired on concentric hyperspheres, as in the application of ridge analysis, it would be desirable for the design to be rotatable. Comparing the values of  $\hat{y}(\mathbf{x})$  on a given hypersphere becomes easier since such values have constant variance. Box and Hunter [12] reported the necessary and sufficient conditions for an experimental design to be rotatable. A recent development by Khuri [10] measured rotatability as a function of the moments of the design under consideration. In applying this property to compare two or more second-order designs, rotatability may be ‘sacrificed’ to satisfy some other desirable design properties [7, 13, 14].

### **2.12.2.1 Design moment matrix**

Many properties found in experimental designs are associated with the manner in which the design points are distributed throughout the space of experimentation. Specifically, the distribution of design points in the region has a profound effect on the distribution of the scaled prediction variance  $N Var[\hat{y}(\mathbf{x})]/\sigma^2$ . The distribution of design points is quantified by its design moments. The term moments has the same conceptual meaning as sample moments. In the case of RSM, the moments reflect important geometric properties in the design, which are a function of the model being fit (linear or quadratic model) [3].

Recall that

$$\text{Var}[\hat{\mathbf{y}}(\mathbf{x})] = \sigma^2 \mathbf{x}^{(m)T} (\mathbf{X}^T \mathbf{X})^{-1} \mathbf{x}^{(m)} \quad (2.13)$$

is the prediction variance and,

$$N \text{V}[\hat{\mathbf{y}}(\mathbf{x})]/\sigma^2 = N \mathbf{x}^{(m)T} (\mathbf{X}^T \mathbf{X})^{-1} \mathbf{x}^{(m)} \quad (2.14)$$

is the scaled prediction variance and  $\mathbf{x}^{(m)}$  is a function of the location in the design variables at which one predicts. Indeed, the  $m$  in  $\mathbf{x}^{(m)}$  denotes to the model. In case of first-degree model, we have

$$\mathbf{x}^{(1)T} = [1, x_1, x_2, \dots, x_k]$$

For a  $k = 2$  the model contains  $x_1, x_2$  with the interaction terms, we have

$$\mathbf{x}^{(1)T} = [1, x_1, x_2, x_1 x_2]$$

Important moments can be derived from the moment matrix  $\mathbf{M}$  given by

$$\mathbf{M} = \frac{1}{N} \mathbf{X}^T \mathbf{X}$$

Design moments are important in characterizing the variance properties of the experimental design, which is a function of the order of the model. For example, in the case of a two-level factorial design, the moments throughout order two are important, since the design matrix contains moments with order two. Given a model matrix

$$\mathbf{X} = \begin{bmatrix} 1 & x_{11} & x_{12} & \dots & x_{1k} \\ 1 & x_{21} & x_{22} & \dots & x_{2k} \\ \vdots & \vdots & \vdots & \dots & \vdots \\ 1 & x_{n1} & x_{n2} & \dots & x_{nk} \end{bmatrix}$$

where each of the  $x_{ij}$  entries are  $\pm 1$ , according to the design moments:

$$[i] = \frac{1}{N} \sum_{u=1}^N x_{iu}, \quad i = 1, \dots, k$$

$$[ii] = \frac{1}{N} \sum_{u=1}^N x_{iu}^2, \quad i = 1, \dots, k$$

$$[ij] = \frac{1}{N} \sum_{u=1}^N x_{iu}x_{ju}, \quad i, j = 1, \dots, k ; i \neq j$$

Therefore, for a first-order model design

$$\frac{\mathbf{X}^T \mathbf{X}}{N} = \begin{bmatrix} 1 & [1] & [2] & [3] & \dots & [k] \\ & [11] & [12] & [13] & \dots & [1k] \\ & & [22] & [23] & \dots & [2k] \\ & & & \ddots & \dots & \vdots \\ & & & & & [kk] \end{bmatrix}$$

For an orthogonal first-degree design

$$\frac{\mathbf{X}^T \mathbf{X}}{N} = \begin{bmatrix} 1 & 0 & 0 & 0 & \dots & 0 \\ & [11] & 0 & 0 & \dots & 0 \\ & & [22] & 0 & \dots & 0 \\ & & & \ddots & \dots & \vdots \\ & & & & & [kk] \end{bmatrix}$$

An odd moment is any moment with at least one design factor that has an odd power. For instance,  $[i]$ ;  $[ij]$ ;  $[ijj]$ ;  $[iii]$  are the odd moments. The remaining moments are called even moments.

### 2.12.2.2 Rotatable conditions for first-order design

A first-order design is rotatable if and only if all odd moments are zero and all even second-degree moments are equal. In other words,  $[i] = 0$ ,  $[ij] = 0$ , and  $[ii] = c_2$ , where the magnitude of  $c_2$  is determined by the scaling of the design factors.

For a quadratic model, the design matrix will contain columns for the intercept, linear terms, quadratic terms, and interaction terms. Then, in addition to the first-degree model moments, the important design moments for the quadratic model are:

$$\begin{aligned}
[iii] &= \frac{1}{N} \sum_{u=1}^N x_{iu}^3 \\
[iij] &= \frac{1}{N} \sum_{u=1}^N x_{iu}^2 x_{iu}, \quad [ijk] = \frac{1}{N} \sum_{u=1}^N x_{iu} x_{ju} x_{ku} \\
[iiii] &= \frac{1}{N} \sum_{u=1}^N x_{iu}^4 \\
[iiij] &= \frac{1}{N} \sum_{u=1}^N x_{iu}^4, \quad [iijj] = \frac{1}{N} \sum_{u=1}^N x_{iu}^2 x_{ju}^2 \\
[iijk] &= \frac{1}{N} \sum_{u=1}^N x_{iu}^2 x_{ju} x_{ku}, \quad [iikl] = \frac{1}{N} \sum_{u=1}^N x_{iu} x_{ju} x_{ku} x_{lu}
\end{aligned}$$

For instance, when  $k = 3$  then

$$\mathbf{X} = \begin{bmatrix} 1 & x_{11} & x_{21} & x_{31} & x_{11}^2 & x_{31}^2 & x_{11}x_{21} & x_{11}x_{31} & x_{21}x_{31} \\ 1 & x_{12} & x_{22} & x_{32} & x_{12}^2 & x_{32}^2 & x_{12}x_{22} & x_{12}x_{32} & x_{22}x_{32} \\ \vdots & \vdots & \vdots & \vdots & \vdots & \vdots & \vdots & \vdots & \vdots \\ 1 & x_{1N} & x_{2N} & x_{3N} & x_{1N}^2 & x_{3N}^2 & x_{1N}x_{2N} & x_{1N}x_{3N} & x_{2N}x_{3N} \end{bmatrix}$$

The following is the necessary form of  $\frac{\mathbf{X}^T \mathbf{X}}{N}$  of a rotatable  $k$ -variable second-order design:

$$\frac{\mathbf{X}^T \mathbf{X}}{N} = \begin{bmatrix} 1 & \mathbf{0}_{1 \times k} & \mathbf{0}_{1 \times k^*} & c_2 \mathbf{J}_k^T \\ \mathbf{0}_{k \times 1} & c_2 \mathbf{I}_k & \mathbf{0}_{k \times k^*} & \mathbf{0}_{k \times k} \\ \mathbf{0}_{k^* \times 1} & \mathbf{0}_{k^* \times k} & c_4 \mathbf{I}_{k^*} & \mathbf{0}_{k^* \times k} \\ c_2 \mathbf{J}_k & \mathbf{0}_{k \times k} & \mathbf{0}_{k \times k^*} & c_4 (2\mathbf{I}_k + \mathbf{J}_k^T \mathbf{J}_k) \end{bmatrix}$$

where  $\mathbf{I}_k$  is the identity matrix of dimension  $k \times k$  and  $\mathbf{J}_k$  is vector of ones of dimension  $k$ .

### 2.12.2.3 Rotatability conditions for a second-order design

For all  $i$  and  $j$ , where  $i \neq j$  a second-order design is rotatable if all odd moments are zero, and

$$[ii] = \frac{1}{N} \sum_{u=1}^N x_{iu}^2 = c_2, \quad i = 1, \dots, k$$

$$[iii] = \frac{1}{N} \sum_{u=1}^N x_{iu}^4 = 3c_4$$

$$[ijj] = \frac{1}{N} \sum_{u=1}^N x_{iu}^2 x_{ju}^2 = c_4$$

The magnitudes of  $c_2$  and  $c_4$  are determined by the scaling of the design factors, and all other moments containing order four are zero. In order to avoid singularity in the related regression investigation, the proportion of  $c_4/c_2^2$  need over  $k/(k + 2)$ , nevertheless, this is can be archived by running more center points. The relationship in  $[ijj]$  among the two kinds of fourth-order moments (the pure fourth moment must be three times as big as the mixed-fourth moment) will be useful to achieve rotatability for CCDs [12].

Recall that the conditions  $[iii]$  and  $[ijj]$  can be combined into a single condition as follows:

$$\frac{[iii]}{[ijj]} = 3 ; \quad i \neq j$$

For additional details, see Montgomery, Myers, and Anderson-Cook [3].

#### 2.12.2.4 Rotatability of the CCD

For any central composite design (CCD), all odd moments are equal to zero due to orthogonality property between the  $x_i$ ,  $x_i^2$ , and  $x_i x_j$  columns. Nonorthogonality exists among the column of ones and the  $x_i^2$  columns and between the  $x_i^2$  and  $x_j^2$  columns ( $i \neq j$ ). Therefore, to have a rotatable CCD, the choice of  $\alpha$  must be appropriate so that  $\mathbf{X}^T \mathbf{X}/N$  satisfies the rotatability condition  $[iii]/[ijj] = 3$ ; and  $i \neq j$  where  $[iii]$  and  $[ijj]$  are the moments according to the products between the  $x_i^2$  columns. Furthermore,

for any CCD,  $[iiii] = F + 2\alpha^4$  and  $[ijjj] = F$  where  $F$  is the number of factorial design points. Thus, to determine rotatability:

$$\frac{[iiii]}{[ijjj]} = \frac{F + 2\alpha^4}{F} = 3 ; i \neq j$$

Solving this fraction for  $\alpha$  yields  $\alpha = \sqrt[4]{F}$ . For a CCD to be rotatable,  $\alpha = \sqrt[4]{F} = (F)^{\frac{1}{4}}$ .

If  $\alpha = \sqrt{k}$  is used, then at least one center point is required to run the CCD. Otherwise,  $(\mathbf{X}^T \mathbf{X})^{-1}$  does not exist, and therefore,  $Var[\hat{y}(\mathbf{x})]$ , does not exist [3].

### 2.13 Uniform precision

A rotatable design is said to have an additional uniform precision property if  $Var[\hat{y}(\mathbf{x})]$  at the origin is equal to its value at a distance of one from the origin. Box and Hunter [12] introduced this property to provide an approximate uniform distribution of the prediction variance inside a hypersphere of radius one. This may result in stability of the prediction variance in the locality of the design center [7, 12].

In the next chapter, RSM is employed in order to find the optimum device performance of organic polymer solar cells using three factors.

CHAPTER 3  
MODELING OF ORGANIC SOLAR CELL USING RESPONSE SURFACE  
METHODOLOGY

Suliman, Rajab, Abu Farzan Mitul, Lal Mohammad, Gemechis D. Djira, Yunpeng Pan, and Qiquan Qiao. "Modeling of the organic solar cell using response surface methodology." *Results in Physics* (2017).

**Abstract**

Polymer solar cells have drawn much attention during the past few decades due to their low manufacturing cost and compatibility in flexible substrates. In solution processed organic solar cells, the optimal thickness, annealing temperature, and morphology are key components to achieving high efficiency. In this paper, we have utilized response surface methodology (RSM) to find optimal fabrication conditions for polymer solar cells. In order to optimize cell efficiency, central composite design (CCD) was performed using different parameters such as polymer concentration, polymer-fullerene ratio, and active layer spinning speed. Optimal device performance was achieved using 10.25 mg/ml polymer concentration, 0.42 polymer-fullerene ratio, and 1624 rpm of active layer spinning speed. The predicted response (the efficiency) at the optimum stationary point was found to be 5.23% for the Poly(diketopyrrolopyrrole-terthiophene) (PDPP3T)/PC<sub>60</sub>BM solar cells. Moreover, 97% of the variation in the device performance was explained by our best model. Finally, our experimental results are consistent with the CCD prediction, which proves that this is a promising and appropriate model for optimum device performance and fabrication conditions.

**Keywords:** organic photovoltaics; performance measures; response surface; experimental design; optimization

### 3.1 Introduction and background

Renewable energy sources are considered to be clean and a great benefit for the economy and the environment. Solar, winds, geothermal, hydroelectric and bio-mass are the popular renewable energy sources. The sun is a source of enormous energy, and a great deal of research has been devoted to solar energy conversion. The challenge is to harvest solar energy efficiently at a low manufacturing cost. Solar cell devices based on inorganic semiconductors have been found to harvest solar energy more efficiently to produce electricity. However, these are not economically feasible. Organic photovoltaic (OPV) materials offer a promising alternative to solving this problem due to their inherently low cost, abundant availability, and flexibility. Researchers have already made much progress in the development of low cost organic light-emitting diodes, which has opened the path for OPV research.

A solution-processed bulk-heterojunction (BHJ) polymer solar cell not only requires a simpler fabrication technique but also offers a reduced manufacturing cost. Usually, this BHJ solar cell is comprised of electron donating organic semiconductor polymers and electron-withdrawing fullerenes as active layers. This composite active layer can be coated over a large area using spray coating, inkjet-coating, and roller-casting. During the last few years, the power conversion efficiency (PCE) of polymer solar cells has improved significantly [15]. The PCE of a solar cell is largely dependent on three major factors: open circuit voltage ( $V_{oc}$ ), the short circuit current ( $J_{sc}$ ) and the fill factor (FF). The  $V_{oc}$  of a solar cell can be determined by the energy difference between the highest occupied molecular orbital (HOMO) of the donor (conjugated polymer or small molecule) and the lowest unoccupied molecular orbital (LUMO) of the



acceptor (typically a fullerene derivative). The  $J_{sc}$  can be calculated from the absorption spectrum and absorption depth of the organic donor and the transport of photogenerated carriers through the morphology of the active layer. During the past few years, researchers have worked to increase the PCE of bulk heterojunction (BHJ) organic solar cells (OSCs) over 9.2%. The active layer of high efficiency devices consists of low bandgap donor-acceptor copolymers as electron donors and fullerene-based derivatives as electron acceptors [16]. Much research is continuing in order to improve device performance since the properties of the materials have a great impact on the overall performance of solar cells [17].

The solar energy conversion in OPV devices mainly follows four major steps: 1) absorption of sunlight by the absorber and generation of excitons; 2) diffusion of the excitons to find donor-acceptor interface, 3) dissociation of the excitons and generation of charges; and 4) charge transport and charge collection. Ideally, polymers should have wide absorption spectra in order to harvest solar energy efficiently. To achieve optimized device performance, polymer concentration, the polymer-fullerene ratio in the solvent, selection of solvent, and thickness of the active layer are important. The electronic properties, crystallinity, maximum charge transport, and minimal recombination within the active layer largely depend on the fine tuning of the polymer-fullerene mixture [18]. Therefore, the polymer-fullerene mixture, polymer concentration, and active layer thickness can change the optoelectronic properties of the organic solar cells and affect device performance. Also, the individual components have some unique properties, e.g., absorption coefficient, charge carrier mobility, crystalline/amorphous structure, which also significantly influence device performance.

Here, we have used response surface methodology (RSM) to optimize organic solar cell performance to be more efficient and precise. RSM is a popular optimization tool which has already been successfully used to optimize many biological and chemical processes. All variables to be optimized are simultaneously adjusted in a systematic manner, such as maximizing cell efficiency and cell thickness while maintaining the acceptable characteristics. Beg et al. (2003) used RSM methodology to attain Optimization of alkaline protease production from bacillus mojavensis. They investigated the effects of various factors, including the casamino acids concentration, glucose concentration, inoculum age, incubation time, and agitation rate, on the response. First, they determined the effects of the independent variables on protease production in shake flask cultures using RSM, and then the optimum variables were used in a bioreactor [19]. Senanayake et al.(2002) used the RSM technique to investigate lipase that in a biochemical reaction, with the incorporation of docosahexaenoic acid (DHA) into borage oil. They studied the effects of three independent variables, namely the reaction time, the amount of enzyme, and the reaction temperature, on the yield of DHA incorporation. This study was a good model for the determination of the range of the independent variables. In the preliminary work, the effect of the independent variables on response was investigated by varying one parameter at a time while the others were held constant. The relationship between the response variable and the independent parameters was explained using a second-order model equation [20]. In another example of RSM use, the performance of pectolytic enzymes during hydrolysis of a pectic substrate under assay conditions was investigated by Panda et. al. (1999). The parameters, both physical (temperature and pH) and chemical (volume of substrate and enzyme solution) were

optimized using central composite design (CCD). In addition to using substrate and enzyme concentrations as the independent variables, the volumes of substrate and enzyme solutions were used. Use of volume as an independent parameter is disadvantageous because both substrate and enzyme concentrations vary when changing the volume of the substrate or enzyme; this causes a change in the total reaction volume [21]. Desirability function methodology was used to optimize osmotic dehydration of cantaloupe by Corzo et. al. (2004). Three responses (water loss, mass loss, and Brix increase) were affected by three independent factors (temperature, concentration, and time); these were investigated at five levels in the central composite design (CCD). This work demonstrates a significant difference from the other RSM studies which calculated an individual desired function that varied from 0 to 1 (lowest to highest) for each response. Here, for all the desirable functions, the overall desired function was defined. A high value in the overall desirability function was called the best function of the system, which was considered to be the optimum solution of the system. Three model equations were predicted using the experimental design and the observed values of the response variables [22].

Another study by Favari et al. (2004) explored the combined effects of initial xylitol supersaturation value, and cooling temperature on xylitol crystallization from synthetic solutions using the RSM technique. The  $3^2$  full-factorial design was applied to optimize the operational conditions. They fitted a second-order model to the responses, xylitol crystallization yield, and purity degree. After excluding the insignificant terms, the first-order equation for xylitol crystallization yield and a second-order equation excluding the interaction term for the purity degree (PD) were obtained. A higher PD was

considered to be the optimal condition as it enabled the achievement of total purity of the crystals (approx.) and a cooling temperature near zero [23, 24].

In this study, we have worked with three important performance determining factors of a polymer solar cell: polymer concentration, polymer- fullerene ratio in the solvent and active layer thickness. These three factors have great impact on the charge transport mechanisms within the device. Our results show that RSM can optimize overall device performance in terms of these three major factors. We have found the statistical significance in the full quadratic models ( $p\text{-value} < 9.784 \times 10^{-8}$ ) and the lack of fit was insignificant ( $p\text{-value} = 0.55$ , in the ANOVA table). Most significantly, the stationary point is close to the design center, since all three eigenvalues (-0.150, -0.668, -1.190) are negative, indicating that the stationary point is a maximum. This indicates that the best combination is around 10.34 mg/ml polymer concentration, 0.42 polymer- fullerene ratio, and 1624 rpm active layer spinning speed. This is an ideal situation for response surface methodology, and clear evidence that the current setting of the independent parameters is consistent with optimum performance.

### **3.1 Materials, device fabrication and characterization**

#### **3.1.1 Materials**

Poly(diketopyrrolopyrrole-terthiophene) (PDPP3T) was purchased from Solarmer Materials, Inc. PC<sub>60</sub>BM was ordered from Nano-C. MoO<sub>3</sub>, Zinc Acetate, Aluminum Nitrate and nonahydrate Ethanol were purchased from Sigma Aldrich. Silver was purchased from Kurt J. Lesker Company. All materials were used without further purification. AZO sol-gel was synthesized as described by Stubhan et al.[25]. For the AZO sol-gel synthesis, 2.17 gm of zinc acetate dehydrate [ $\text{Zn}(\text{CH}_3\text{COO})_2 \cdot 2\text{H}_2\text{O}$ ] and 3.8

mg of aluminum nitrate nonahydrate  $[\text{Al}(\text{NO}_3)_3 \cdot 9\text{H}_2\text{O}]$  were dissolved in 100 ml ethanol at 80 °C for 2.5 hours. Precipitation from the AZO sol-gel was removed using a 0.45  $\mu\text{m}$  PVDF filter.

### **3.1.2 Single-junction device fabrication**

ITO coated glass slides were kept in ultra-sonication for 20 minutes in detergent water. After that, the ITOs were rinsed in de-ionized water and again maintained in ultra-sonication for 20 minutes. Finally, the ITOs were ultra-sonicated in acetone and 2-propanol for another 20 minutes. The ITO substrates were then subjected to oxygen plasma cleaning for 25 minutes before spin-coating with an AZO layer. AZO was spin coated at 4500 rpm for 1 minute and then kept on a hot plate at 150 °C for ten minutes to remove residual solvent. The AZO-coated substrates were then moved to a nitrogen-filled glove box having an  $\text{O}_2$  and  $\text{H}_2\text{O}$  concentration of less than 1 ppm. The blend of PDPP3T:PCBM solution was spin-coated at different rpm for 45 seconds. Then, the sample was moved to a thermal evaporator where 10 nm of  $\text{MoO}_3$  and 80 nm of silver (Ag) were thermally evaporated in a vacuum below  $2 \times 10^{-6}$  Torr.

### **3.1.3 Current density – voltage (J-V) characterization**

An Agilent 4155C semiconductor parameter analyzer was used for the current density-voltage (J-V) characteristic measurements of the solar cell devices. A Newport xenon lamp was used as a solar simulator (AM 1.5). Before performing the characterization of solar cells, a National Renewable Energy Laboratory (NREL) calibrated silicon photo detector was used in order to calibrate the light source. The light source had an intensity of  $100 \text{ mWcm}^{-2}$ . In order to measure the external quantum

efficiency (EQE) of the devices, a xenon lamp was attached to a Newport monochromator. Light wavelength from the monochromator was varied from 350 nm to 850 nm.

### 3.2 Experimental design

A Central Composite Design (CCD) was generated in pieces, using the *cube*, *foldover*, and *star* functions to optimize the efficiency from an inverted polymer solar cell. Three independent variables, namely polymer concentration ( $x_1$ ), the polymer-fullerene ratio ( $x_2$ ), and active layer spinning speed ( $x_3$ ) were investigated at two levels with four repetitions at the central point. This involves adding quantities such as the alpha (star points) values for rotatability and orthogonal blocking to the complete  $2^3$  design. For each of the three factors studied, high (coded value: +1) and low (coded value: -1) set points have been selected according to the results obtained with polymer solar cell systems and the required experimental conditions were taken into consideration to achieve phase optimization of the efficiency (Table 3.2). All possible combinations that were performed for the central composite design are shown in Table 3.1. The analysis was based on combining the *cube* clock, *foldover*, and the *star* block. R package (programming language) was used to generate the design experiments and to fit the model and analyze the results [26, 27].

Table 3.1. Design matrix of the CCD and the corresponding experimental results.

Run	Block	X <sub>1</sub>	X <sub>2</sub>	X <sub>3</sub>	y
1	1	0	0	0	5.59
2	1	0	0	0	5.13
3	1	-1	-1	1	3.08
4	1	0	0	0	5.25
5	1	1	1	1	3.18
6	1	1	-1	-1	3.4
7	1	0	0	0	5.1
8	1	-1	1	-1	2.43
9	2	-1	-1	-1	3.17
10	2	0	0	0	4.54
11	2	0	0	0	5.14
12	2	-1	1	1	2.2
13	2	0	0	0	4.69
14	2	0	0	0	4.7
15	2	1	1	-1	3.11
16	2	1	-1	1	3.45
17	3	0	0	$\sqrt{2}$	4.14
18	3	0	0	0	5.15
19	3	$-\sqrt{2}$	0	0	2.05
20	3	0	0	$-\sqrt{2}$	3.48
21	3	0	$\sqrt{2}$	0	4.28
22	3	$\sqrt{2}$	0	0	3.51
23	3	0	0	0	5.1
24	3	0	$-\sqrt{2}$	0	5.4

Table 10.2. The three factors and the levels utilized in the CCD.

	Low level	Center level	High level
Factors(variables)	(-1)	0	(+1)
Polymer concentration (X <sub>1</sub> )	6.5	10	13.5
Polymer-fullerene ratio (X <sub>2</sub> )	0.585	0.5	0.415
Active layer spinning speed (X <sub>3</sub> )	1200	1600	2000

The eight treatment combinations as result of  $2^3$  factorial designs can be displayed as a cube, as shown in Figure 3.1. Using the “+ and -” notation as an indication of the high and low levels of each independent variable, all possible combinations of this design are listed in tabular format as described in Table 3.3. This tabular is usually called a design

matrix [3]. The numbers in the corners of the cube in Figure 3.1 represent the observed values of the efficiency associated with the eighth treatment combinations of the  $2^3$  factorial designs.

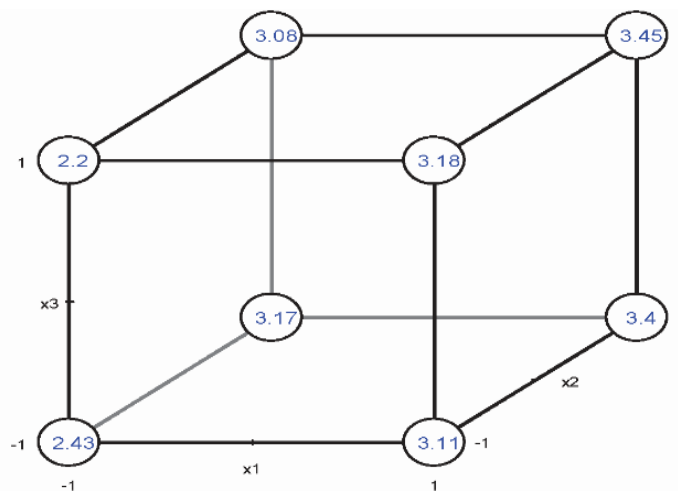


Figure 3.1. The  $2^3$  factorial design with a geometric view.

Table 3.3. The design matrix of  $2^3$  factorial design.

Run	Factor		
	X <sub>1</sub>	X <sub>2</sub>	X <sub>3</sub>
1	-	-	-
2	+	-	-
3	-	+	-
4	+	+	-
5	-	-	+
6	+	-	+
7	-	+	+
8	+	+	+

### 3.3 Result and discussion

#### 3.3.1. Model fitting for first order design

It is important to check the capability of the design before running any experiments, the variance function (*varfcn* in R package) obtained, this function is a useful tool [26] in



RSM which provides information for the system to test the variance of the predictions. This function with particular design, an appropriate model, and a different design point from the central to plot the scaled prediction variance. By looking either at a profile plot or at a contour plot, which both are shown in Figure 3.2 (a) and (b):

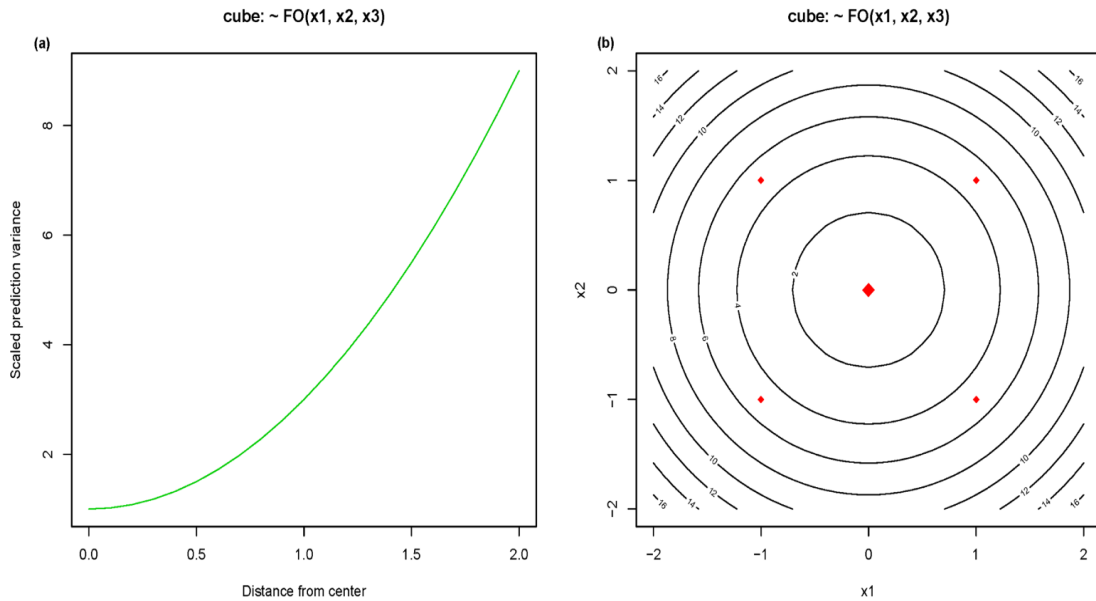


Figure 3.2. Variance function plots for a cube design (a) Profile plot and (b) Contour plot.

The variance increases, as it goes more out, and it is more suitable at the center. The contour plots of variance function for this design, which is generated using a *cube* function are circular. Hence, this design is rotatable. Then the first-degree model can be fitted. Notably, before having any data, the variance function is a helpful tool to ensure that the model can be fitted.

Table 3.4. The significance of the first-order effects according to the cube design.

	Estimate	Std. Error	<i>t</i>	p-value
(Intercept)	4.145	0.565	7.331	0.0018
X <sub>1</sub>	0.268	0.799	0.335	0.755
X <sub>2</sub>	-0.218	0.799	-0.272	0.799
X <sub>3</sub>	0.108	0.799	0.134	0.899

According to Table 3.4, none of first-order terms are statistically significant, nor they are together significant (p-value = 0.97 in the ANOVA table). Therefore there is no evidence for a specific direction. It is better to move to a better region and collect more data for more reliability.

The initial design was a half fractional factorial with additional center points generated using a *cube* function. So, more information can be obtained by doing a full factorial design for a first-order model. This was done using the *foldover* function, by switching the certain signs of some or all of the coded variables. In this paper, the first experiment was generated using  $x_3 = x_1x_2$ , so by switching  $x_1$ , then  $x_3 = -x_1x_2$ , thus the second fractional of the design [28].

Note that the other design has different design point [e.g., (6.5, 0.415, and 1200)]. For analysis, a *cube* fraction and a *foldover* design combined using a *djoin* function. Note that *djoin* creates a new blocking factor. It is important to include a block effect in the model because there were two separately randomized experiments. From the ANOVA table, the first-order terms are not significant (p-value = 0.8294), and the lack of fit test is significant (p-value < 0.0001). Response surface experimentation is different from other kinds of experiment designs, in such situation, it is essentially good to have insignificant terms, especially first-order ones. It seems that the process might be close to the optimum region.

The analysis of variance exhibits no significant main effect and there was evidence of curvature in the response surface over the region of study (p-value < 0.0001). That is, the null hypothesis  $H_0: \sum_{i=1}^3 \beta_{ii} = 0$  rejected, concluding that there was an indication of quadratic terms; that is, a linear model is not appropriate in describing the data, a polynomial of higher order must be used, such as quadratic model.

### 3.3.2 Moment matrix and rotatability conditions

Given the following design matrix  $X$  with one center point, we will check the rotatability conditions using moment matrix

$$X = \begin{bmatrix} 1 & -1 & -1 & -1 & 1 & 1 & 1 & 1 & 1 & 1 \\ 1 & -1 & 1 & -1 & -1 & 1 & -1 & 1 & 1 & 1 \\ 1 & 1 & -1 & -1 & -1 & -1 & 1 & 1 & 1 & 1 \\ 1 & 1 & 1 & -1 & 1 & -1 & -1 & 1 & 1 & 1 \\ 1 & -1 & -1 & 1 & 1 & -1 & -1 & 1 & 1 & 1 \\ 1 & -1 & 1 & 1 & -1 & -1 & 1 & 1 & 1 & 1 \\ 1 & 1 & -1 & 1 & -1 & 1 & -1 & 1 & 1 & 1 \\ 1 & 1 & 1 & 1 & 1 & 1 & 1 & 1 & 1 & 1 \\ 1 & 1.68 & 0 & 0 & 0 & 0 & 0 & 2.82 & 0 & 0 \\ 1 & -1.68 & 0 & 0 & 0 & 0 & 0 & 2.82 & 0 & 0 \\ 1 & 0 & 1.68 & 0 & 0 & 0 & 0 & 0 & 2.82 & 0 \\ 1 & 0 & -1.68 & 0 & 0 & 0 & 0 & 0 & 2.82 & 0 \\ 1 & 0 & 0 & 1.68 & 0 & 0 & 0 & 0 & 0 & 2.82 \\ 1 & 0 & 0 & -1.68 & 0 & 0 & 0 & 0 & 0 & 2.82 \\ 1 & 0 & 0 & 0 & 0 & 0 & 0 & 0 & 0 & 0 \end{bmatrix}$$

The moment matrix is  $\frac{X^T X}{N}$  and is equal to

$$\begin{bmatrix} 1 & \mathbf{0}_{1 \times k} & \mathbf{0}_{1 \times k^*} & c_2 \mathbf{J}_k^T \\ \mathbf{0}_{k \times 1} & c_2 \mathbf{I}_k & \mathbf{0}_{k \times k^*} & \mathbf{0}_{k \times k} \\ \mathbf{0}_{k^* \times 1} & \mathbf{0}_{k^* \times k} & c_4 \mathbf{I}_{k^*} & \mathbf{0}_{k^* \times k} \\ c_2 \mathbf{J}_k & \mathbf{0}_{k \times k} & \mathbf{0}_{k \times k^*} & c_4 (2\mathbf{I}_k + \mathbf{J}_k^T \mathbf{J}_k) \end{bmatrix}$$

As it can be seen, for a rotatable first-order design, all odd moments are zero, and all even quadratic moments are equal to the quantity  $c_2$  (from section 2.13.2.3).

$$[i] = 0, \quad [ij] = 0, \quad [ii] = c_2 = 13.64/15.$$

### 3.4. Augmenting further to fit a quadratic response surface

A second-order rotatable design is achieved by adding *star* points. By collecting more data these star points, the second-degree model can be fitted. The *star* function in *rsm* package runs this block for us [26, 28]. The value of parameter alpha ( $\alpha$ ) in *star* block is orthogonal to the *cube* and *foldover* blocks. The variance of the predictions, and the profile plot or a contour plot after combining the *cube* block, *foldover* fraction, and *star* block are shown in Figure 3.3 (a), and (b):

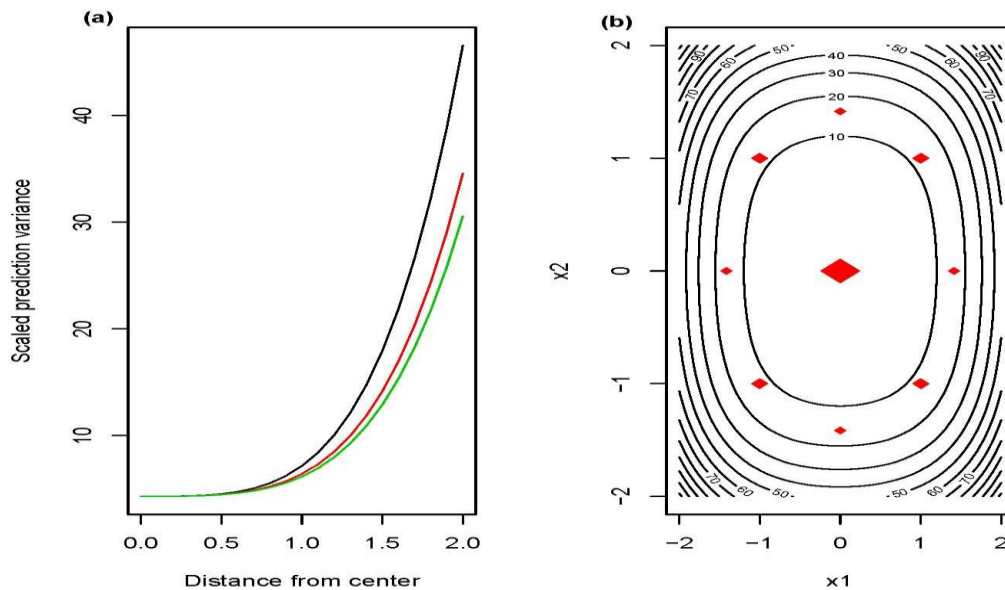


Figure 3.3. Variance function plot for quadratic model: (a) Profile plot (b) Contour plot.

The second-order is rotatable design with star points added to the complete  $2^3$  design, since it has a reasonable variance function properties. Based on augmenting this design a quadratic model can be fitted. Furthermore, based on the design matrix the conditions of block orthogonality satisfied for the quadratic model as follows:

$$D = \begin{bmatrix} 0 & 0 & 0 \\ 0 & 0 & 0 \\ -1 & -1 & 1 \\ 0 & 0 & 0 \\ 1 & 1 & 1 \\ 1 & -1 & -1 \\ 0 & 0 & 0 \\ -1 & 1 & -1 \\ \hline -1 & -1 & -1 \\ 0 & 0 & 0 \\ 0 & 0 & 0 \\ -1 & 1 & 1 \\ 0 & 0 & 0 \\ 0 & 0 & 0 \\ 1 & 1 & -1 \\ 1 & -1 & 1 \\ \hline 0 & 0 & \sqrt{2} \\ 0 & 0 & 0 \\ -\sqrt{2} & 0 & 0 \\ 0 & 0 & -\sqrt{2} \\ 0 & \sqrt{2} & 0 \\ \sqrt{2} & 0 & 0 \\ 0 & 0 & 0 \\ 0 & -\sqrt{2} & 0 \end{bmatrix} \quad \begin{array}{l} \\ \\ \textit{Cube} \\ \\ \\ \\ \\ \\ \\ \\ \\ \\ \\ \\ \\ \\ \\ \\ \\ \\ \textit{Foldover} \\ \\ \\ \\ \\ \\ \\ \\ \\ \\ \\ \\ \\ \\ \textit{Star} \end{array}$$

For cube block:

$$\sum_{u=1}^{n_b} x_{iu} x_{ju} = \sum_{u=1}^8 x_{iu} x_{ju} = 0, \quad i \neq j = 1, 2, \dots, 8.$$

This is first-order orthogonal design.

$$\frac{\sum_{u=1}^{n_b} x_{iu}^2}{\sum_{u=1}^N x_{iu}^2} = \frac{n_b}{N}$$

$$\frac{\sum_{u=1}^8 x_{iu}^2}{\sum_{u=1}^{24} x_{iu}^2} = \frac{n_b}{N}$$

The conditions of block orthogonality are satisfied, we have

$$\frac{4}{12} = \frac{8}{24}, \quad i = 1, 2, \dots, 8$$

For rotatable second-degree design all odd moments are equal to zero, and

$$[ii] = \frac{1}{N} \sum_{u=1}^N x_{iu}^2 = c_2 = \frac{13.64}{15}$$

$$[iii] = \frac{1}{N} \sum_{u=1}^N x_{iu}^4 = 3c_4 = (3) \frac{8}{15}$$

$$[ijj] = \frac{1}{N} \sum_{u=1}^N x_{iu}^2 x_{ju}^2 = c_4 = \frac{8}{15}$$

Notably, the last two conditions can be combined, that is, a CCD is rotatable since  $\mathbf{X}^T \mathbf{X} / N$  (moment matrix) satisfies the rotatability conditions.

$$\frac{[iii]}{[ijj]} = \frac{24/15}{8/15} = 3$$

In addition, for rotatability in CCD,  $[iii] = F + 2\alpha^4$  and  $[ijj] = F$

$$\frac{[iii]}{[ijj]} = \frac{F + 2\alpha^4}{F} = \frac{8 + 2(1.68^4)}{8} = 3 ; i \neq j$$

where  $F$  is the number of factorial points.

Solving for  $\alpha$  yields  $\alpha = \sqrt[4]{F}$ . Therefore,

$$\alpha = \sqrt[4]{F} = \sqrt[4]{8} = 1.682.$$

This value of  $\alpha$  will maintain the rotatability property of CCD.

The response surface was fitted using *rsm* package in R software. The model is specified using the functions FO, SO, TWI, and PQ (representing first-order, second-order, two-way interaction, and pure quadratic, respectively) as shown in 3.5.

Table 3.5. ANOVA table for lack-of-fit test.

Response	Source	Df	Sum Sq	Mean Sq	F-value	p-value
Efficiency	FO(X1,X2,X3)	3	2.784	0.928	11.968	0.00064
	TWI(X1,X2,X3)	3	0.166	0.056	0.716	0.561
	PQ(X1,X2,X3)	3	23.077	7.692	99.204	9.78E-09
	Residuals	12	0.931	0.078		
	Lack of fit	5	0.577	0.1154	2.284	0.156
	Pure error	7	0.354	0.051		

Table 3.5. Shows important quadratic terms (p-value < 0.0001) and the lack of fit is now insignificant (p-value = 0.156). The second-order response surface model involved a polymer solar cell process in which Polymer concentration, polymer-fullerene ratio, and active layer spinning speed were studied, and the response variable was the cell efficiency. The fitted model by following the same procedure in (Myers and Montgomery, 2009) is presented as

$$\hat{y} = 5.057 + 0.36 x_1 - 0.31 x_2 + 0.06 x_3 + 0.13 x_1 x_2 + 0.06 x_1 x_3 - 0.02 x_2 x_3 - 1.18 x_1^2 - 0.15 x_2^2 - 0.67 x_3^2 \quad (3.1)$$

and the contour plots of this model are shown in Figure 3.4.

The nature of the stationary point was determined using the signs of the eigenvalues. The estimated stationary point of the response surface is (0.099, -0.975, and 0.061) which is within the design space; this means there is no suggestion of a rising ridge since there is no direction of improvement out of the experimental space, and the predicted response at this stationary point is  $\hat{y}_s = 5.23$ . In the original units, the stationary points are:

$$\text{Polymer concentration} = 10 + 3.5 \times (0.099) = 10.35 \text{ mg/ml}$$

$$\text{Polymer- fullerene ratio} = 0.5 + 0.085 \times (-0.975) = 0.42$$

$$\text{Active layer spinning speed} = 1600 + 400 \times (0.06061492) = 1624 \text{ rpm}$$

This is in close agreement with the location of the optimum that would be obtained by visual inspection of Figure 3.4. Since all eigenvalues (-0.150, -0.668, -1.190) are negative, the stationary point is a maximum (as is obvious from the inspection of Figure 3.5 (a), (b), and (c)).

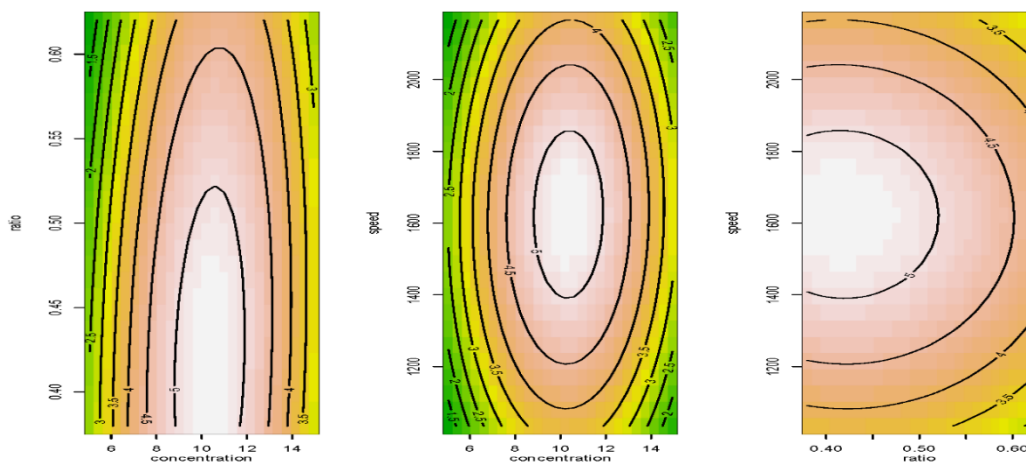


Figure 3.4. Contour plot of the efficiency.



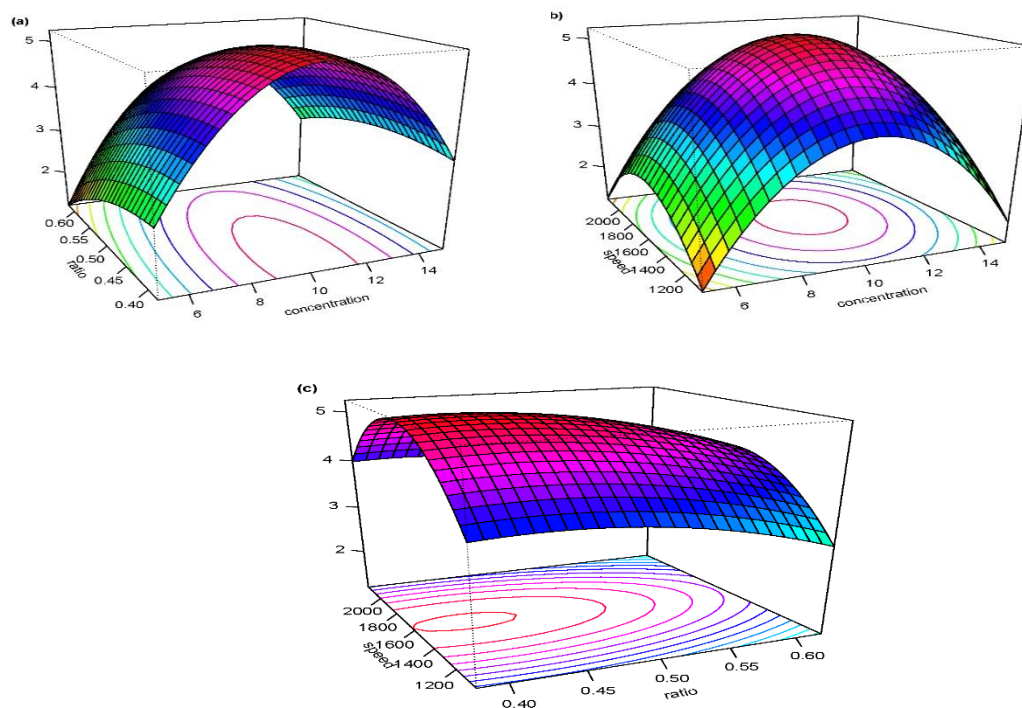


Figure 3.5. Response surface plot for solar cell efficiency.

The R codes for all analyses can be found in appendix A.

### 3.5. Device structure

Figure 3.6 shows the PDPP3T:PCBM device structure. Experimentally, it was found that the optimized device fabrication procedure is 10 mg/ml polymer concentration, 1:2 polymer-fullerene ratio and 1600 rpm of active layer spinning speed. J-V characteristic curves are shown in Figure 3.7 (a), (b), and (c). It is obvious that due to low spinning speed, the active layer turns out to be thick, which may increase absorption as well as  $J_{SC}$ . A thick active layer can also increase device resistance/ interfacial resistance, which adversely affects the FF of the overall device. In a closely intermixed donor-acceptor blend, the individual stages have a certain extend to allow for efficient transport of charges via percolated pathways towards the respective electrodes [29]. In order to

maintain efficient charge transport avoiding recombination within the device, there is always an optimum donor-acceptor ratio and polymer concentration in the solvent. The experimental results successfully coincide with the RSM methodology in device performance optimization.

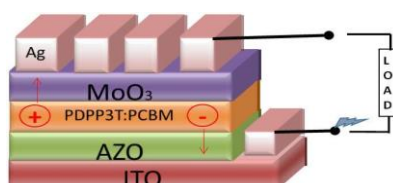


Figure 3.6. Device layout of PDPP3T-PCBM single junction polymer solar cell.

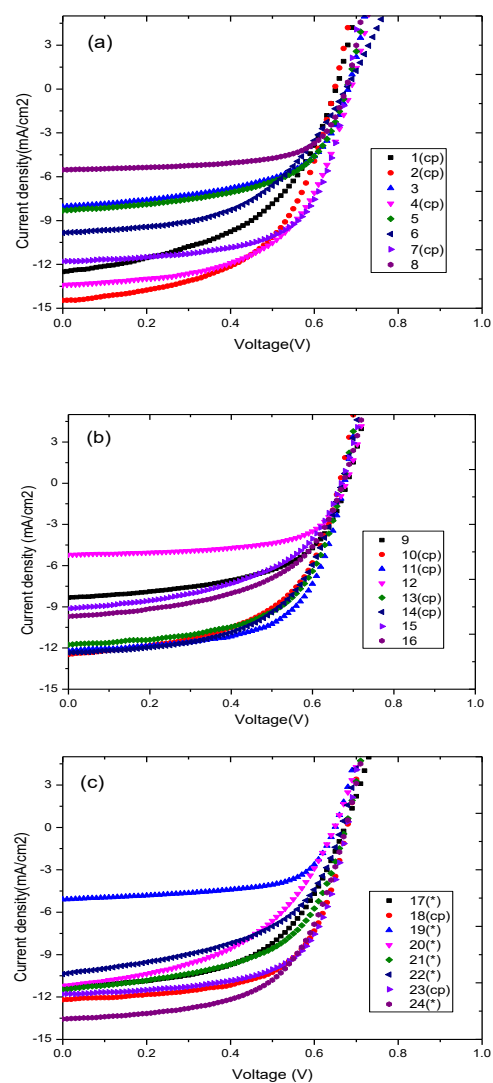


Figure 3.7. J-V Characteristic curves of (a) cube, (b) foldover, and (c) star functions.

### 3.6. Residual analysis for fitted quadratic model

A residual analysis is performed in order to validate the model assumptions. Normal Q-Q plot, Cook's distance are generated of the residuals as shown in Figure 3.8.

Table 3.6. Observed values, Predicted values, Residuals, and other diagnostics.

Observation	$y_i$	$\hat{y}_i$	$e_i$	$h_{ii}$	$D_i$
1	5.59	5.15	0.44	0.18	0.06
2	5.13	5.15	-0.02	0.18	0.00
3	3.08	3.25	-0.17	0.80	0.63
4	5.25	5.15	0.10	0.18	0.00
5	3.18	3.42	-0.24	0.80	1.30
6	3.4	3.55	-0.15	0.80	0.51
7	5.1	5.15	-0.05	0.18	0.00
8	2.43	2.34	0.09	0.80	0.17
9	3.17	2.94	0.23	0.80	1.23
10	4.54	4.88	-0.34	0.18	0.03
11	5.14	4.88	0.26	0.18	0.02
12	2.2	2.06	0.14	0.80	0.47
13	4.69	4.88	-0.19	0.18	0.01
14	4.7	4.88	-0.18	0.18	0.01
15	3.11	2.95	0.16	0.80	0.58
16	3.45	3.54	-0.09	0.80	0.19
17	4.14	3.89	0.25	0.63	0.31
18	5.15	5.14	0.01	0.18	0.00
19	2.05	2.26	-0.21	0.63	0.23
20	3.48	3.72	-0.24	0.63	0.28
21	4.28	4.39	-0.11	0.63	0.06
22	3.51	3.28	0.23	0.63	0.26
23	5.1	5.14	-0.04	0.18	0.00
24	5.4	5.28	0.12	0.63	0.07

Figure 3.8 shows the normal probability plot and the residuals versus the predicted values  $\hat{y}_i$ . None of these plots reveal any model inadequacy. Also, the hat matrix  $\mathbf{H} = \mathbf{X}(\mathbf{X}^T \mathbf{X})^{-1} \mathbf{X}^T$  is useful to identify influential observations. The average size of the diagonal elements in the hat matrix  $\mathbf{H}$  is  $p/n$ . As a guideline, if the diagonal elements of

the hat matrix  $h_{ii}$  is greater than  $2p/n$ , then the observation  $i$  is a high-leverage point. By applying this to the organic solar cell data, note that  $2p/n = 2(10)/24 = 0.83$ . Table 3.6 indicates that none of the  $h_{ii}$  exceeds 0.83, concluding that there is no leverage point in the organic solar cell data.

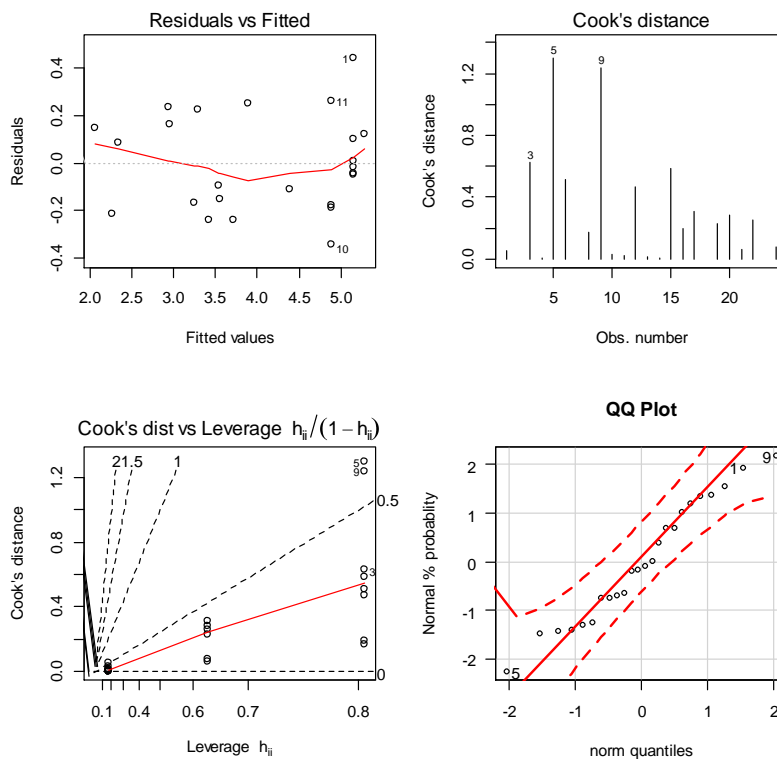


Figure 3.8. The residual analysis for fitted quadratic model.

In many surface analyses, it is preferable to work with scaled residuals, as these often provide more information than ordinary least squares residuals.

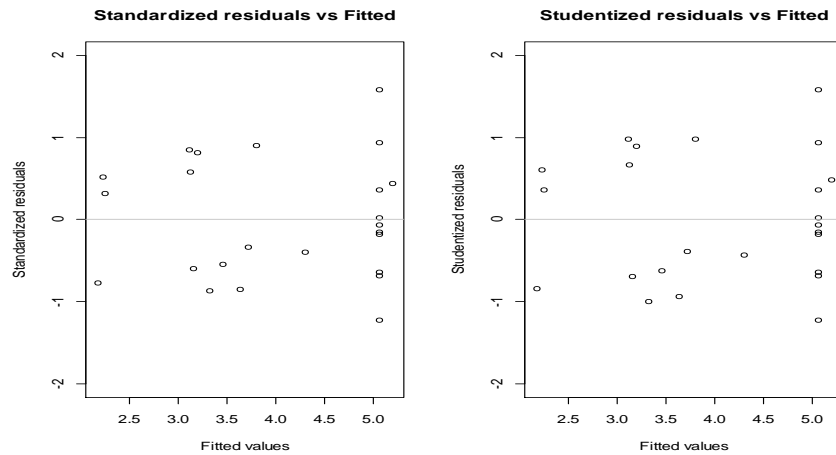


Figure 3.9. The standardized and studentized residual.

As can be seen from Figure 3.9, most of the standardized and studentized residuals lie in the interval  $(-3, 3)$ , which indicate that there are no outliers in the organic solar cell data.

In the next chapter, we will address inference for the stationary point and also perform canonical analysis to assess if there is a rising ridge.

## CHAPTER 4

## SIMULTANEOUS INFERENCE FOR THE LOCATION OF A STATIONARY POINT

In this chapter, we will develop confidence region and simultaneous confidence intervals associated with the stationary point of a quadratic response surface model. First, we focus on the confidence region and later we will propose simultaneous confidence intervals for the coordinates of a stationary point. The simultaneous coverage probability of the proposed method will be assessed via small simulation.

**4.1 Location of a stationary point**

A stationary point is a point at which the expected value of the response variable of interest is optimized. This can be the minimum or the maximum depending on the problem. A quadratic model for a response surface with  $k$  quantitative factors is given by

$$E(Y) = \beta_0 + \sum_{i=1}^k \beta_i x_i + \sum_{i=1}^k \sum_{\substack{j=1 \\ i < j}}^k \beta_{ij} x_i x_j + \sum_{i=1}^k \beta_{ii} x_i^2$$

The model in matrix notation is

$$E(Y) = \beta_0 + \mathbf{x}^T \boldsymbol{\beta} + \mathbf{x}^T \mathbf{B} \mathbf{x} \quad (4.1)$$

where  $\beta_0$ ,  $\boldsymbol{\beta}$ , and  $\mathbf{B}$  are the intercept, a vector of coefficients for the linear terms, and the matrix  $\mathbf{B}$  contains the coefficients associated with the quadratic and interaction terms, respectively. Indeed,  $\mathbf{x}^T = (x_1, x_2, \dots, x_k)$ ,  $\boldsymbol{\beta}^T = (\beta_1, \beta_2, \dots, \beta_k)$  and  $\mathbf{B}$  is a symmetric matrix of dimension  $k \times k$  given by

$$\mathbf{B} = \begin{bmatrix} \beta_{11} & \beta_{12}/2 & \dots \beta_{1k}/2 \\ \beta_{12}/2 & \beta_{22} & \dots \beta_{2k}/2 \\ \vdots & \vdots & \vdots \\ \beta_{1k}/2 & \beta_{2k}/2 & \dots \beta_{kk} \end{bmatrix} = \frac{1}{2} \begin{bmatrix} 2\beta_{11} & \beta_{12} & \dots \beta_{1k} \\ \beta_{12} & 2\beta_{22} & \dots \beta_{2k} \\ \vdots & \vdots & \vdots \\ \beta_{1k} & \beta_{2k} & \dots 2\beta_{kk} \end{bmatrix}$$

To find the stationary point, we need to derive the partial derivatives of the quadratic regression function with respect to the quantitative factors  $x_1, x_2, \dots, x_k$  and equate them to zero. This point could describe the point of minimum, the point of maximum, or a saddle point. These three cases can be determined using the sign of the eigenvalues of the matrix  $\mathbf{B}$ . Let  $\lambda_1, \lambda_2, \dots, \lambda_k$  denote the eigenvalues of the matrix  $\mathbf{B}$  determined from

$$|\mathbf{B} - \lambda \mathbf{I}| = 0.$$

- i. If all eigenvalues  $\lambda_1, \lambda_2, \dots, \lambda_k$  are negative, the stationary point is a point of maximum response.
- ii. If all the eigenvalues are positive, the stationary point is a point of minimum response.
- iii. If the eigenvalues have mixed signs, the stationary point is a saddle point.

Let us first consider quadratic models with  $k = 1, 2,$  and  $3$ .

For a quadratic model with only one factor  $x_1$ , the regression function is

$$E(Y) = \beta_0 + \beta_1 x_1 + \beta_{11} x_1^2 \text{ and}$$

$$\frac{\partial E(Y)}{\partial x_1} = \beta_1 + 2\beta_{11} x_1$$

Therefore, the stationary point is  $\frac{\partial E(Y)}{\partial x_1} = 0 \Leftrightarrow \beta_1 + 2\beta_{11} x_1 = 0 \Leftrightarrow x_s = \frac{-\beta_1}{2\beta_{11}}$

This point is of interest when  $\beta_{11} \neq 0$ .

Similarly, the stationary point in the case of two factors is as follows.

$$E(Y) = \beta_0 + \beta_1 x_1 + \beta_2 x_2 + \beta_{11} x_1^2 + \beta_{22} x_2^2 + \beta_{12} x_1 x_2$$

$$\frac{\partial E(Y)}{\partial x_1} = \beta_1 + 2\beta_{11} x_1 + \beta_{12} x_2$$

$$\frac{\partial E(Y)}{\partial x_2} = \beta_2 + 2\beta_{22} x_2 + \beta_{12} x_1$$

$$\frac{\partial E(Y)}{\partial x_1} = 0 \Leftrightarrow 2\beta_{11} x_1 + \beta_{12} x_2 = -\beta_1$$

$$\frac{\partial E(Y)}{\partial x_2} = 0 \Leftrightarrow \beta_{12} x_1 + 2\beta_{22} x_2 = -\beta_2$$

$$\Leftrightarrow \begin{bmatrix} 2\beta_{11} & \beta_{12} \\ \beta_{12} & 2\beta_{22} \end{bmatrix} \begin{bmatrix} x_1 \\ x_2 \end{bmatrix} = \begin{bmatrix} -\beta_1 \\ -\beta_2 \end{bmatrix}$$

$$\Leftrightarrow \begin{bmatrix} x_{s1} \\ x_{s2} \end{bmatrix} = \begin{bmatrix} 2\beta_{11} & \beta_{12} \\ \beta_{12} & 2\beta_{22} \end{bmatrix}^{-1} \begin{bmatrix} -\beta_1 \\ -\beta_2 \end{bmatrix}$$

$$\Leftrightarrow \begin{bmatrix} x_{s1} \\ x_{s2} \end{bmatrix} = \frac{1}{4\beta_{11}\beta_{22} - \beta_{12}^2} \begin{bmatrix} 2\beta_{22} & -\beta_{12} \\ -\beta_{12} & 2\beta_{11} \end{bmatrix} \begin{bmatrix} -\beta_1 \\ -\beta_2 \end{bmatrix}$$

Thus

$$\begin{aligned} x_{s1} &= \frac{-2\beta_{22}\beta_1}{4\beta_{11}\beta_{22} - \beta_{12}^2} + \frac{\beta_{12}\beta_2}{4\beta_{11}\beta_{22} - \beta_{12}^2} \\ &= \frac{-2\beta_{22}\beta_1 + \beta_{12}\beta_2}{4\beta_{11}\beta_{22} - \beta_{12}^2} \end{aligned}$$

And

$$x_{s2} = \frac{\beta_{12}\beta_1}{4\beta_{11}\beta_{22} - \beta_{12}^2} + \frac{2\beta_{11}\beta_2}{4\beta_{11}\beta_{22} - \beta_{12}^2}$$



$$= \frac{\beta_{12}\beta_1 + 2\beta_{11}\beta_2}{4\beta_{11}\beta_{22} - \beta_{12}^2}$$

And the location of a stationary point with three factors is

$$E(Y) = \beta_0 + \beta_1x_1 + \beta_2x_2 + \beta_2x_3 + \beta_{11}x_1^2 + \beta_{22}x_2^2 + \beta_{33}x_3^2 + \beta_{12}x_1x_2 + \beta_{13}x_1x_3 + \beta_{23}x_2x_3$$

$$\frac{\partial E(Y)}{\partial x_i} = 0, \quad i = 1, 2, 3 \Leftrightarrow$$

$$\begin{bmatrix} 2\beta_{11} & \beta_{12} & \beta_{13} \\ \beta_{12} & 2\beta_{22} & \beta_{23} \\ \beta_{13} & \beta_{23} & 2\beta_{33} \end{bmatrix} \begin{bmatrix} x_1 \\ x_2 \\ x_3 \end{bmatrix} = \begin{bmatrix} -\beta_1 \\ -\beta_2 \\ -\beta_3 \end{bmatrix}$$

$$\Leftrightarrow \begin{bmatrix} x_{s1} \\ x_{s2} \\ x_{s3} \end{bmatrix} = \begin{bmatrix} 2\beta_{11} & \beta_{12} & \beta_{13} \\ \beta_{12} & 2\beta_{22} & \beta_{23} \\ \beta_{13} & \beta_{23} & 2\beta_{33} \end{bmatrix}^{-1} \begin{bmatrix} -\beta_1 \\ -\beta_2 \\ -\beta_3 \end{bmatrix}$$

$$x_{s1} = \frac{-\beta_1(2\beta_{22}2\beta_{33} - \beta_{23}^2) + \beta_2(2\beta_{33}\beta_{12}) - \beta_{23}\beta_{13} - \beta_3(\beta_{12}\beta_{23} - 2\beta_{22}\beta_{13})}{\text{Det}(\mathbf{B})}$$

$$x_{s2} = \frac{\beta_1(\beta_{12}2\beta_{33} + \beta_{13}\beta_{22} - \beta_2(2\beta_{11}2\beta_{33} + \beta_{12}^2)) + \beta_3(2\beta_{11}\beta_{23} - \beta_{13})}{\text{Det}(\mathbf{B})}$$

$$x_{s3} = \frac{-\beta_1(\beta_{12}\beta_{23} + 2\beta_{22}\beta_{13}) + \beta_2(2\beta_{11}\beta_{23} - \beta_{12}\beta_{13}) - \beta_3(2\beta_{11}2\beta_{22} + \beta_{12}^2)}{\text{Det}(\mathbf{B})}$$

where  $\text{Det}(\mathbf{B}) = 2\beta_{11}(4\beta_{22}\beta_{33} - \beta_{23}^2) - \beta_{12}(2\beta_{12}\beta_{33} - \beta_{13}\beta_{23}) + \beta_{13}(\beta_{12}\beta_{23} - 2\beta_{13}\beta_{22})$  is the determinant of the matrix  $\mathbf{B}$ .

In general, using matrix notation, the stationary point of a quadratic model with  $k$  quantitative factors can be determined as follows.

$$E(Y) = \beta_0 + \mathbf{x}^T \boldsymbol{\beta} + \mathbf{x}^T \mathbf{B} \mathbf{x}$$

Using matrix differentiation,

$$\frac{\partial E(Y)}{\partial \mathbf{x}} = \boldsymbol{\beta} + 2\mathbf{B}\mathbf{x}$$

Equating this partial derivative to zero and solving for  $\mathbf{x}$ , the stationary point denoted by  $\mathbf{x}_s$  will be

$$\mathbf{x}_s = -\frac{1}{2}\mathbf{B}^{-1}\boldsymbol{\beta}$$

A point estimate for  $\mathbf{x}_s$  can be obtained by plugging the point estimates of the regression coefficients in  $\boldsymbol{\beta}$  and  $\mathbf{B}$  as

$$\hat{\mathbf{x}}_s = -\frac{1}{2}\hat{\mathbf{B}}^{-1}\mathbf{b}$$

where  $\mathbf{b}$  and  $\hat{\mathbf{B}}$  are the estimates of  $\boldsymbol{\beta}$  and  $\mathbf{B}$  [3]. In other words,  $\mathbf{b}^T = (b_1, b_2, \dots, b_k)$  and  $\hat{\mathbf{B}}$  is

$$\hat{\mathbf{B}} = \begin{bmatrix} b_{11} & b_{12}/2 & \dots & b_{1k}/2 \\ b_{12}/2 & b_{22} & \dots & b_{2k}/2 \\ \vdots & \vdots & \ddots & \vdots \\ b_{1k}/2 & b_{2k}/2 & \dots & b_{kk} \end{bmatrix}.$$

In the next two sections, we will discuss and develop different methods to perform simultaneous inferences for the location of a stationary point.

#### 4.2 Confidence region for the location of a stationary point

First, we will explore existing methods for establishing a confidence region for the location of a stationary point.

### 4.2.1 Box and Hunter

This useful confidence region was developed by Box and Hunter (1954) [30].

Consider the fitted quadratic response surface model. Let

$$\widehat{E}(Y) = b_0 + \sum_{i=1}^k b_i x_i + \sum_{i=1}^k \sum_{\substack{j=1 \\ i < j}}^k b_{ij} x_i x_j + \sum_{i=1}^k b_{ii} x_i^2$$

$$\widehat{E}(Y) = b_0 + \mathbf{x}^T \mathbf{b} + \mathbf{x}^T \widehat{\mathbf{B}} \mathbf{x} \quad (4.2)$$

The  $j$ th derivative  $d_j(\mathbf{x})$  of the fitted model in Equation 4.2 with respect to  $x_j$  is given by

$$d_j(\mathbf{x}) = b_j + 2\widehat{\mathbf{B}}_j^T \mathbf{x}, j = 1, 2, \dots, k.$$

where the vector  $\widehat{\mathbf{B}}_j^T$  is the  $j$ th row of the matrix  $\widehat{\mathbf{B}}$ . We denote the vector of these derivatives as a  $k$ -dimensional vector  $\mathbf{d}(\mathbf{x})$ . Note that  $\mathbf{d}(\mathbf{x})$  is a simple linear function of  $\mathbf{x}$  and the estimated regression coefficients. Now, we consider these derivatives evaluated at  $\mathbf{u}$ , where the coordinates of  $\mathbf{u}$  are the coordinates of the true stationary point of the process which are unknown. If the residuals of the quadratic response model are normally distributed as  $N(0, \sigma^2)$ , then

$$\mathbf{d}(\mathbf{u}) \sim N(\mathbf{0}, \text{Var}(\mathbf{d}(\mathbf{u})))$$

where  $\text{Var}(\mathbf{d}(\mathbf{u}))$  is the variance-covariance matrix of  $\mathbf{d}(\mathbf{u})$ . Normality holds since linear combinations of normally distributed random variables are also normally distributed. Since the partial derivatives are necessarily zero at the stationary points, we have that  $E(\mathbf{d}(\mathbf{u})) = \mathbf{0}$  [3].

Therefore,

$$\frac{\mathbf{d}^T(\mathbf{u})[\widehat{Var}(\mathbf{d}(\mathbf{u}))]^{-1}\mathbf{d}(\mathbf{u})}{k} \sim F_{k,n-p} \quad (4.3)$$

where  $Var[\mathbf{d}(\mathbf{u})]$  is a  $k \times k$  matrix that includes the error variance  $\sigma^2$  as a multiplier.

And  $F_{k,n-p}$  is an F-distribution with  $k$  and  $n - p$  degrees of freedom, where  $p$  is the number of regression coefficients in the quadratic model in Equation 4.1. For  $k$  factors,  $p = 1 + 2k + \frac{k(k-1)}{2}$ . It is also clear that  $Var[\mathbf{d}(\mathbf{u})]$  is a function of  $\mathbf{u}$ . For instance, in the case of two factors ( $k = 2$ ),

$$d_1(\mathbf{u}) = b_1 + 2(b_{11}u_1 + \frac{b_{12}}{2}u_2)$$

$$d_2(\mathbf{u}) = b_2 + 2(b_{22}u_2 + \frac{b_{12}}{2}u_1)$$

And

$$Var[\mathbf{d}(\mathbf{u})] = \begin{bmatrix} Var[d_1(\mathbf{u})] & Cov[d_1(\mathbf{u}), d_2(\mathbf{u})] \\ Cov[d_1(\mathbf{u}), d_2(\mathbf{u})] & Var[d_2(\mathbf{u})] \end{bmatrix}$$

$$d_1(\mathbf{u}) = b_1 + 2\left(b_{11}u_1 + \frac{b_{12}}{2}u_2\right)$$

$$= [0 \quad 1 \quad 0 \quad u_2 \quad 2u_1 \quad 0] \begin{bmatrix} b_0 \\ b_1 \\ b_2 \\ b_{12} \\ b_{11} \\ b_{22} \end{bmatrix}$$

$$= \mathbf{a}_1^T \hat{\boldsymbol{\theta}}$$

where  $\mathbf{a}_1^T = [0 \quad 1 \quad 0 \quad u_2 \quad 2u_1 \quad 0]$  and  $\hat{\boldsymbol{\theta}} = (\mathbf{X}^T \mathbf{X})^{-1} \mathbf{X}^T \mathbf{y}$ ,  $\mathbf{X}$  is the design matrix associated with the second degree model.

$$\begin{aligned}
\text{Var}(\mathbf{a}_1^T \hat{\boldsymbol{\theta}}) &= \mathbf{a}_1^T \text{Var}(\hat{\boldsymbol{\theta}}) \mathbf{a}_1 \\
&= \mathbf{a}_1^T \sigma^2 (\mathbf{X}^T \mathbf{X})^{-1} \mathbf{a}_1 \\
&= \sigma^2 \mathbf{a}_1^T (\mathbf{X}^T \mathbf{X})^{-1} \mathbf{a}_1
\end{aligned}$$

The elements in this matrix are computed from  $(\mathbf{X}^T \mathbf{X})^{-1} \sigma^2$ , the variance-covariance matrix for the estimated regression coefficients. To estimate  $[\widehat{\text{Var}} \mathbf{d}(\mathbf{u})]$ , we replace  $\sigma^2$  by the mean-squared error (MSE) from the ANOVA table.

Now according to (4.3) we have

$$Pr \left\{ \mathbf{d}^T(\mathbf{u}) [\widehat{\text{Var}}(\mathbf{d}(\mathbf{u}))]^{-1} \mathbf{d}(\mathbf{u}) \leq k F_{\alpha; k, n-p} \right\} = 1 - \alpha \quad (4.4)$$

where the  $\mathbf{u}$  is unknown, and all other quantities in (4.4) are known, the  $F_{\alpha; k, n-p}$  is the upper  $\alpha$ th percentile of the F-distribution with  $k, n - p$  degrees of freedom. The values of  $u_1, u_2, \dots, u_k$  that satisfy

$$\widehat{\mathbf{d}}^T(\mathbf{u}) [\widehat{\text{Var}}(\mathbf{d}(\mathbf{u}))]^{-1} \widehat{\mathbf{d}}(\mathbf{u}) \leq k F_{\alpha; k, n-p} \quad (4.5)$$

will constitute a  $100(1 - \alpha)\%$  confidence region for the true stationary point.

#### 4.2.2 Asymptotic confidence region for stationary point

Here we utilize the asymptotic distribution of an estimator for the stationary point. Under the normality of the error terms, the point estimator

$$\hat{\mathbf{x}}_s = \frac{1}{2} \hat{\mathbf{B}}^{-1} \mathbf{b}$$

derived in the previous section is also the maximum likelihood estimator. This holds due to the invariance property of maximum likelihood estimators [31]. Since maximum likelihood estimators are asymptotically normally distributed, we have

$$\hat{\mathbf{x}}_s \sim N(\mathbf{x}_s, \text{Var}(\hat{\mathbf{x}}_s)), \quad (4.6)$$

For example, for  $k = 1$ , the stationary point is a ratio of regression coefficients  $\hat{x}_s = -b_1/2b_{11}$  and,

$$\hat{x}_s \sim N\left(\frac{-\beta_1}{2\beta_{11}}, \text{Var}(\hat{x}_s)\right)$$

Using Taylor series expansion for a function of two variables [32], an approximate variance for the ratio of two random variables  $U$  and  $V$  is

$$\text{Var}\left(\frac{U}{V}\right) \approx \left(\frac{\mu_U}{\mu_V}\right)^2 \left[ \frac{\sigma_U^2}{\mu_U^2} + \frac{\sigma_V^2}{\mu_V^2} - \frac{2\text{Cov}(U,V)}{\mu_U\mu_V} \right].$$

In our case,  $U = -b_1$  and  $V = 2b_{11}$ . Therefore, the approximate variance is

$$\text{Var}\left(\frac{-b_1}{2b_{11}}\right) = 0.25 * \text{Var}\left(\frac{b_1}{b_{11}}\right) \approx 0.25 * \left(\frac{\beta_1}{\beta_{11}}\right)^2 \left[ \frac{\sigma_{b_1}^2}{\mu_{b_1}^2} + \frac{\sigma_{b_{11}}^2}{\mu_{b_{11}}^2} - \frac{2\text{Cov}(b_1, b_{11})}{\mu_{b_1} \mu_{b_{11}}} \right]$$

For  $k = 2$ ,  $\hat{\mathbf{x}}_s$  will have an asymptomatic bivariate normal distribution. Using the delta method, the variance-covariance matrix can be derived as follows:

To derive the asymptotic variance-covariance matrix for  $\hat{\mathbf{x}}_s$ , we need to derive the derivatives of  $x_{s1}$  and of  $x_{s2}$  with respect to the regression parameters in a quadratic model. For  $k = 2$ ,

$$x_{s1} = \frac{-2\beta_{22}\beta_1 + \beta_{12}\beta_2}{4\beta_{11}\beta_{22} - \beta_{12}^2}$$

$$\frac{\partial x_{s1}}{\partial \beta_0} = 0$$

$$\frac{\partial x_{s1}}{\partial \beta_1} = \frac{-2\beta_{22}}{4\beta_{11}\beta_{22} - \beta_{12}^2}$$

$$\frac{\partial x_{s1}}{\partial \beta_2} = \frac{\beta_{12}}{4\beta_{11}\beta_{22} - \beta_{12}^2}$$

$$\frac{\partial x_{s1}}{\partial \beta_{12}} = \frac{\beta_{12}^2\beta_2 - 4\beta_{22}\beta_1\beta_{12} + 4\beta_{22}\beta_2\beta_{11}}{(4\beta_{11}\beta_{22} - \beta_{12}^2)^2}$$

$$\frac{\partial x_{s1}}{\partial \beta_{11}} = \frac{-4\beta_{22}(-2\beta_{22}\beta_1 + \beta_{12}\beta_2)}{(4\beta_{11}\beta_{22} - \beta_{12}^2)^2}$$

$$\frac{\partial x_{s1}}{\partial \beta_{22}} = \frac{2\beta_1\beta_{12}^2 - 4\beta_{12}\beta_2\beta_{11}}{(4\beta_{11}\beta_{22} - \beta_{12}^2)^2}$$

The derivatives of  $x_{s2}$  with respect to the regression parameters:

$$x_{s2} = \frac{\beta_{12}\beta_1 - 2\beta_{11}\beta_2}{4\beta_{11}\beta_{22} - \beta_{12}^2}$$

$$\frac{\partial x_{s2}}{\partial \beta_0} = 0$$

$$\frac{\partial x_{s2}}{\partial \beta_1} = \frac{\beta_{12}}{4\beta_{11}\beta_{22} - \beta_{12}^2}$$

$$\frac{\partial x_{s2}}{\partial \beta_2} = \frac{-2\beta_{11}}{4\beta_{11}\beta_{22} - \beta_{12}^2}$$

$$\frac{\partial x_{s2}}{\partial \beta_{12}} = \frac{4\beta_1\beta_{11}\beta_{22} + \beta_{12}^2\beta_1 - 4\beta_{12}\beta_{11}\beta_2}{(4\beta_{11}\beta_{22} - \beta_{12}^2)^2}$$

$$\frac{\partial x_{s2}}{\partial \beta_{11}} = \frac{2\beta_{12}^2\beta_2 - 4\beta_{12}\beta_1\beta_{22}}{(4\beta_{11}\beta_{22} - \beta_{12}^2)^2}$$

$$\frac{\partial x_{s2}}{\partial \beta_{22}} = \frac{-4\beta_{11}(\beta_{12}\beta_1 - 2\beta_{11}\beta_2)}{(4\beta_{11}\beta_{22} - \beta_{12}^2)^2}$$

Let's denote the derivatives of  $x_{s1}$  and  $x_{s2}$  with respect to the six regression parameters by  $\mathbf{G}$  and  $\mathbf{H}$ , respectively. That is,  $\mathbf{G}^T = (g_1, g_2, g_3, g_4, g_5, g_6)$  and  $\mathbf{H}^T = (h_1, h_2, h_3, h_4, h_5, h_6)$ .

Then,

$$\hat{\mathbf{x}}_s \sim N\left(\begin{bmatrix} x_{s1} \\ x_{s2} \end{bmatrix}, \boldsymbol{\Sigma}_s\right)$$

where,  $\boldsymbol{\Sigma}_{\hat{\mathbf{x}}_s} = \begin{bmatrix} \mathbf{G}^T \\ \mathbf{H}^T \end{bmatrix}_{2 \times 6} \boldsymbol{\Sigma}_{6 \times 6} [\mathbf{G} \ \mathbf{H}]_{6 \times 2}$  and  $\boldsymbol{\Sigma} = \sigma^2(\mathbf{X}^T \mathbf{X})^{-1}$ .

Now using the asymptotic distribution in Equation 4.6, the set of points  $\mathbf{u} = (u_1, u_2, \dots, u_k)^T$  for which

$$(\mathbf{u} - \hat{\mathbf{x}}_s)^T \text{Var}(\hat{\mathbf{x}}_s) (\mathbf{u} - \hat{\mathbf{x}}_s) \leq kF_{\alpha, k, n-p}$$

will constitute a  $(1 - \alpha)100\%$  confidence region for  $\mathbf{x}_s$  [31].

### 4.3 Simultaneous confidence intervals for the coordinate of a stationary point

The confidence regions discussed in the previous sections are non-rectangular in shape, and this makes their interpretations difficult. In this section, we propose two methods for constructing simultaneous confidence intervals for the coordinate of a stationary point. Simultaneous confidence intervals are rectangular in shape and therefore, they are easy to interpret.

#### Case 1: One factor

In the case of one factor ( $k = 1$ ), methods for constructing confidence intervals for



$$x_s = \frac{-\beta_1}{2\beta_{11}}$$

are well developed. Note that the parameter  $x_s$  is a ratio of linear combinations of the regression coefficients. Popular methods to estimate  $x_s$  by a confidence interval include the, (i) delta method, (ii) Fieller method, (iii) bootstrap (e.g, see Dilba et al. 2006; Hare et al. 2007) [33, 34].

The delta method is based on the asymptotic distribution discussed in the previous section. A  $(1 - \alpha)100\%$  confidence interval for  $x_s$  is given by

$$\hat{x}_s \pm z_{1-\alpha/2} * SE(\hat{x}_s)$$

$$SE(\hat{x}_s) = \sqrt{\left(\frac{b_1}{b_{11}}\right)^2 \left[ \frac{s_{b_1}^2}{b_1^2} + \frac{s_{b_{11}}^2}{b_{11}^2} - \frac{2Cov(b_1, b_{11})}{b_1 b_{11}} \right]}$$

The Fieller method [35, 36] works as follows.

Suppose that  $\hat{\beta}_1, \hat{\beta}_{11}$  have a bivariate normal distribution with mean vector  $(\beta_1, \beta_{11})^T$

and the variance- covariance matrix  $\begin{bmatrix} v_{11} & v_{12} \\ v_{21} & v_{22} \end{bmatrix}$ , where  $v_{11}, v_{22}$ , and  $v_{12} = v_{21}$  denote

the variance and the covariance of  $\hat{\beta}_1$  and  $\hat{\beta}_{11}$ , respectively. Now,  $x_s = -\frac{\beta_1}{2\beta_{11}}$  implies

that  $\beta_1 + \beta_{11}x_s^2 = 0$ . Therefore,

$$b_1 + b_{11}x_s^2 \sim N(0, \sigma^2)$$

where  $\sigma^2 = (v_{11} + 2x_s v_{12} + x_s^2 v_{22})$  [35, 36].

A  $(1 - \alpha)\%$  Fieller's confidence interval is a set of  $x_s$  values that satisfy the inequality

$$\frac{(\hat{\beta}_1 + 2\hat{\beta}_{11}x_s)^2}{v_{11} + 2x_s v_{12} + x_s^2 v_{22}} < z_{\alpha/2}^2 \quad (4.7)$$

As seen in (4.7), it is quadratic function in  $x_s$ , by solving (4.7) for  $x_s$  leads to the confidence intervals as:

$$\hat{x}_s + \left(\frac{g}{1-g}\right)\left(\hat{x}_s + \frac{v_{12}}{v_{22}}\right) \pm \frac{z_{\alpha/2}}{\hat{\beta}_{11}(1-g)} \left\{ v_{11} + 2\hat{x}_s v_{12} + \hat{x}_s^2 v_{22} - g \left( v_{11} - \frac{v_{12}^2}{v_{22}} \right) \right\}^{\frac{1}{2}}$$

where  $g = z_{\alpha/2}^2 \frac{v_{22}}{\hat{\beta}_{11}^2}$ .

In general, we also refer to the *mratio*s library in the R software (Djira et al., 2012) for constructing Fieller simultaneous confidence intervals for ratios of linear combinations of the coefficients in the general linear models.

### Case 2: Two or more factors ( $k \geq 2$ )

For two or more factors, to our knowledge, there is no method available to construct simultaneous confidence intervals for the coordinates of a stationary point. We propose three methods for doing this.

#### 4.3.1 Bonferroni adjustment

The first simple, but conservative method we can use is to adjust the marginal asymptotic confidence intervals for the coordinates using Bonferroni correction. For  $k$  factors, each confidence interval will be constructed at  $1 - \alpha/(2k)$  confidence level. Therefore, a  $(1 - \alpha)$  100% Bonferroni simultaneous confidence intervals for the  $k$  coordinates is given by

$$\hat{x}_{s,j} \pm z_{1-\alpha/(2k)} * SE(\hat{x}_{s,j}), \quad j = 1, 2, \dots, k.$$

In simultaneous confidence interval estimations,  $(1 - \alpha)100\%$  is also known as the family confidence interval [37].

### 4.3.2 Multiplicity adjustment based on equi-coordinate critical point

In this section, we propose a multiplicity adjustment for the critical point based on the asymptotic distribution of the estimated stationary point. Multiplicity adjusted critical points from multivariate normal or multivariate  $t$  distribution can be calculated using the *mvtnorm* R package by Genz and Bretz (2009). Similar to the plug-in estimate for the covariance matrix in ratio estimations (Dilba et al 2006; Djira and Schaarschmidt, 2010), the asymptotic variance-covariance matrix are functions of the regression coefficients. Plug-in estimates are obtained by plugging the estimated regression coefficients in the variance-covariance.

For  $k$  factors, a two-sided equi-coordinate critical point  $c_{1-\alpha}$  from a  $k$ -variate normal or  $t$  distribution is calculated as

$$p\{|Z_j| \leq c_{1-\alpha}, j = 1, \dots, k\} = 1 - \alpha \quad (4.8)$$

In our case, an estimator for stationary point follows approximate multivariate normal distribution,  $N_k(\boldsymbol{\mu}_s, \boldsymbol{\Sigma}_s)$ ;  $\boldsymbol{\mu}_s$  is the true stationary point and  $\boldsymbol{\Sigma}_s$  is the variance-covariance matrix of the estimated stationary point. Thus, simultaneous confidence interval estimates with a given  $(1 - \alpha) 100\%$  family confidence level are determined as

$$\hat{x}_{s,j} \pm c_{1-\alpha} * SE(\hat{x}_{s,j}), j = 1, 2, \dots, k.$$

### 4.3.3 Bootstrap confidence intervals

Bootstrapping is a computer intensive technique that involves resampling of the original sample several times. The number of bootstrap samples needed depends mainly on the purpose of the inference. For estimating standard errors, about five hundred bootstrap samples might be enough. In estimating probabilities of quantiles, one may need a few thousand bootstrap samples. A simple procedure to construct approximate bootstrap confidence intervals is by setting up a  $1 - \alpha$  confidence interval using the reflection method [37]. The confidence intervals for  $x_s$  is based on the  $(\alpha/2)100$  and  $(1 - \alpha/2)100$  percentiles of the bootstrap distribution of  $x_s^*$ . These percentiles can be denoted by  $x_s^*(\alpha/2)$  and  $x_s^*(1 - \alpha/2)$ , and

$$d_1 = \hat{x}_s - x_s^*(\alpha/2)$$

$$d_2 = x_s^*(1 - \alpha/2) - \hat{x}_s$$

where  $d_1$  and  $d_2$  are the distances based on the percentiles from  $x_s$  and the estimate of  $x_s$  from the actual sample.

Then,

$$x_s^* - d_2 \leq x_s \leq x_s^* + d_1$$

an approximate  $(1 - \alpha)\%$  confidence intervals for  $x_s$ .

And a bootstrap confidence intervals using Bonferroni-type adjustment of the empirical distribution is

$$d_1 = \hat{x}_s - x_s^*(\alpha/2 * k)$$

$$d_2 = x_s^*(1 - \alpha/2 * k) - \hat{x}_s$$

$$x_s^* - d_2 \leq x_s \leq x_s^* + d_1 \quad (4.9)$$

#### 4.4 Simulation study

In this section, we perform a small simulation study to assess the coverage probabilities of the methods proposed in the previous section in the case of two factors ( $k = 2$ ). We generated the observed values of  $y$  randomly from a quadratic model with a given parameter configurations  $(\beta_0, \beta_1, \beta_2, \beta_{12}, \beta_{11}, \beta_{22})$  and the error term is assumed to follow a normal distribution,  $\varepsilon \sim N(0, 1)$ . The sample sizes are 12, 24, and 48. For  $n = 12$ , the number of center point is four and the size of design point is twice as the sample size increases. The design points are  $x_1 = (-1, 1, -1, 1, -\sqrt{2}, \sqrt{2}, 0, 0, 0, 0, 0, 0)$  and  $x_2 = (-1, 1, -1, 1, 0, 0, -\sqrt{2}, \sqrt{2}, 0, 0, 0, 0)$ . The number of simulation runs is set to  $10^4$ , and the number of bootstrap samples is 2000. The linear terms are set at different values  $\beta_1 = 0, 0.4, \beta_2 = 0, 1.6$  and the interaction term  $\beta_{12} = 0, 1$  and the coefficients of the quadratic terms are set at -1 and -2. See Figures 4.1 and 4.2 for the response surface and the associated contours for  $t$  of the scenarios considered in our simulation. The nominal simultaneous coverage probability is 0.95. The true coverage probabilities associated with the three proposed methods are estimated by simulation. See Table 4.1 for the summary of the estimates.

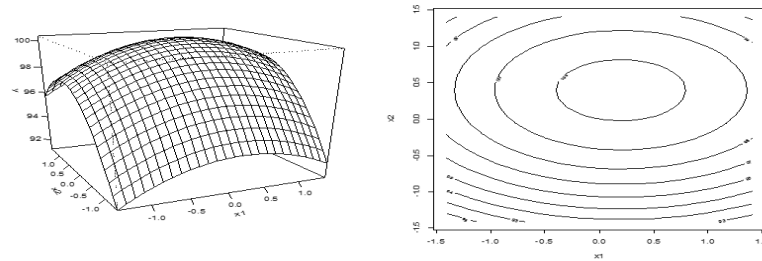


Figure 4.1. The surface and contour plots of the true regression function when  $\beta_{12} = 0$ .

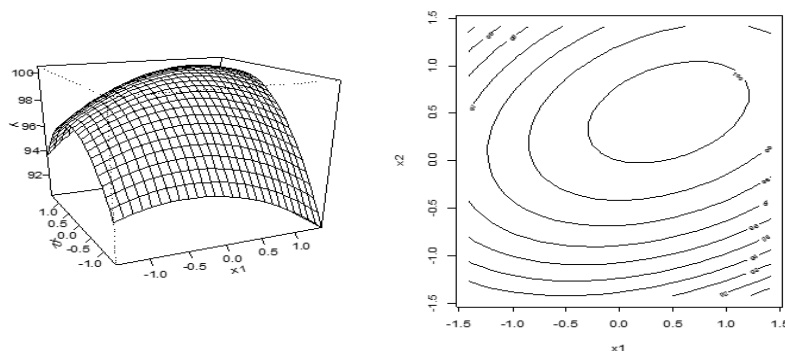


Figure 4.2. The surface and contour plots of the true regression function when  $\beta_{12} = 1$ .

Table 4.1. Estimates of the coverage probability (*nominal*:  $1 - \alpha = 0.95$ ).

$n$	Parameter settings	Stationary point	Bonferroni	Plug-in	Bootstrap
12			0.9362	0.9187	0.7645
24	$\beta_1 = 0, \beta_2 = 0,$	$\begin{bmatrix} 0 \\ 0 \end{bmatrix}$	0.9576	0.9348	0.8854
48	$\beta_{12} = 0$		0.9529	0.9524	0.9222
12			0.926	0.9239	0.7762
24	$\beta_1 = 0.4, \beta_2 =$	$\begin{bmatrix} 0.2 \\ 0.4 \end{bmatrix}$	0.9461	0.9431	0.8835
48	$1.6,$ $\beta_{12} = 0$		0.9615	0.9345	0.9245
12			0.8911	0.8876	0.8464
24	$\beta_1 = 0.4, \beta_2 =$	$\begin{bmatrix} 0.4571 \\ 0.5143 \end{bmatrix}$	0.9258	0.9218	0.9388
48	$1.6,$ $\beta_{12} = 1$		0.9334	0.9319	0.9461

In Table 4.1, the estimates of coverage probabilities for the proposed methods of constructing simultaneous confidence intervals for the location of the stationary point are displayed for various scenarios. As can be seen, the estimates of the coverage

probabilities are the largest for the Bonferroni SCI for all different sample size followed by the plug-in approach. For the Bonferroni and plug-in approaches, the estimates of the coverage probabilities with increasing the sample size are pretty close to the nominal levels of 0.95.

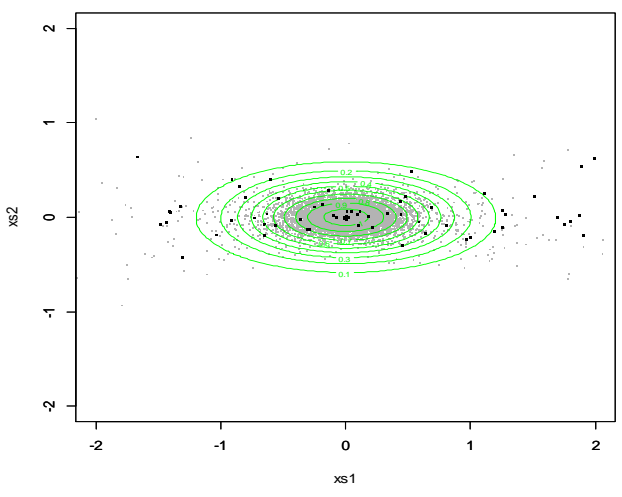


Figure 4.3. A bivariate kernel density when  $\beta_1 = 0, \beta_2 = 0, \text{ and } \beta_{12} = 0$ .

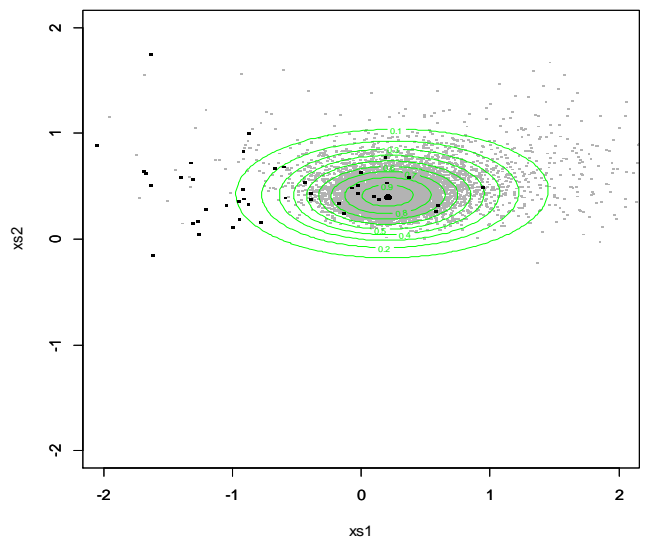


Figure 4.4. Bivariate kernel density estimate, estimated stationary point when  $\beta_1 = 0.4, \beta_{12} = 1.6, \beta_{12} = 0$ .

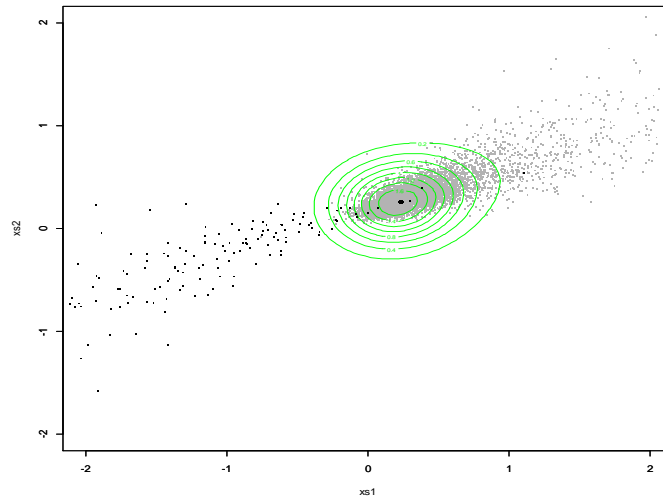


Figure 4.5. Bivariate kernel density estimate, estimated stationary point when  $\beta_1 = 0.4$ ,  $\beta_{12} = 1.6$ ,  $\beta_{12} = 1$ .

As shown in Figures 4.3, 4.4 and 4.5, the kernel density plots are effective ways to visualize the sampling distribution. Most of the estimated stationary points are located around the true stationary point of the true quadratic model. The bold black dot in the middle of the graph is the true stationary point (maximum point). Note that some the estimated stationary points are saddle point as shown by small black dots in figures. In other words, even if the true model has a maximum, the sample data may lead to a saddle point in some cases. The R codes used for the simulation are in appendix B.

#### 4.5 Assessing the solar cell data using the bootstrap technique

A simple bootstrap procedure is useful to understand how well the stationary point is estimated. We simulated a 5000 re-fits of the quadratic model, and the residuals were added back to the fitted values; then the estimated values from the fitted quadratic model were plotted along with the stationary point. The bootstrap estimates for the stationary point are shown in Figure 4.6 using three bivariate scatter plots.



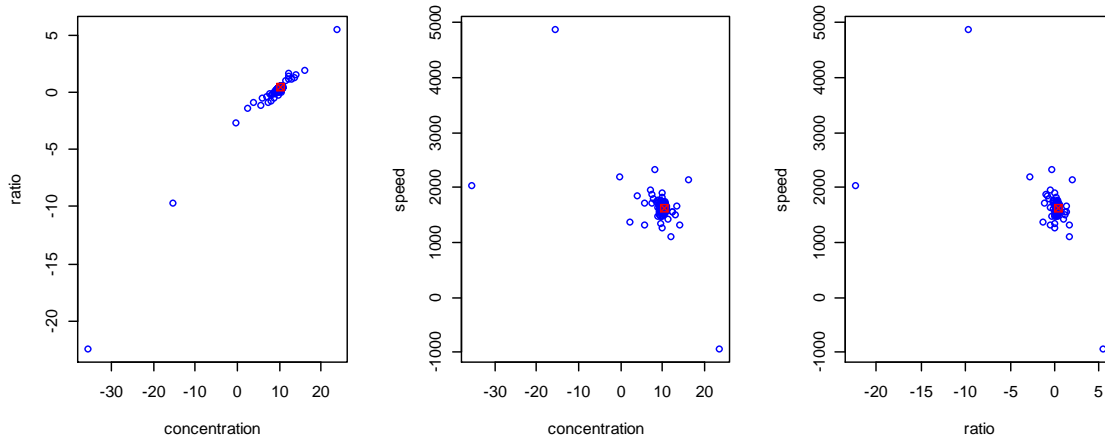


Figure 4.6. Bootstrap estimate for best combination of organic solar cell.

The estimate of the stationary point from the original sample in coded values is  $(0.099, -0.975, 0.061)$ . The dynamic of Figure 4.6 is similar to the confidence region for the best combination, in that most of the bootstrap estimates are located around the optimum combination.

The second-order model obtained (in encoded values) for the response variable (the efficiency) can be described by the following equation:

$$\hat{\eta} = 12.28 + 1.75 x_1 + 13.97 x_2 + 0.0066 x_3 + 0.45 x_1 x_2 + 0.000039 x_1 x_3 + 0.00044 x_2 x_3 - 0.097 x_1^2 - 21.40 x_2^2 - 0.0000042 x_3^2$$

The coefficient of determination for the fitted model is 97%, meaning that the fitted quadratic model explains 97% of the variation in the cell efficiency.

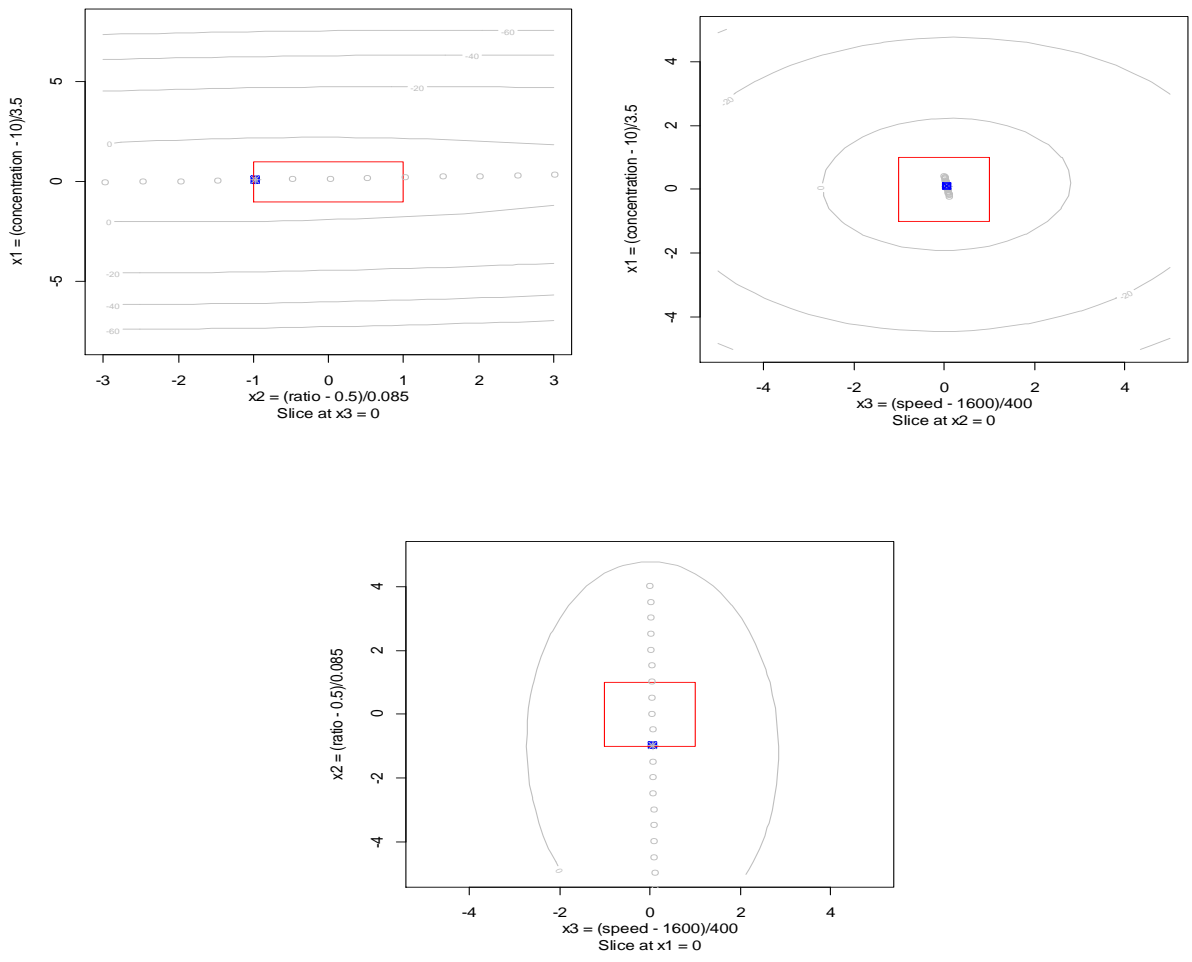


Figure 4.7. Stationary point of organic solar cell, the design region is shown in red box.

As can be seen, the estimated stationary point falls inside of the design space.

As can be seen, from the Figures 4.8 and 4.9 the simultaneous confidence intervals are more liberal than the exact and asymptomatic confidence regions.

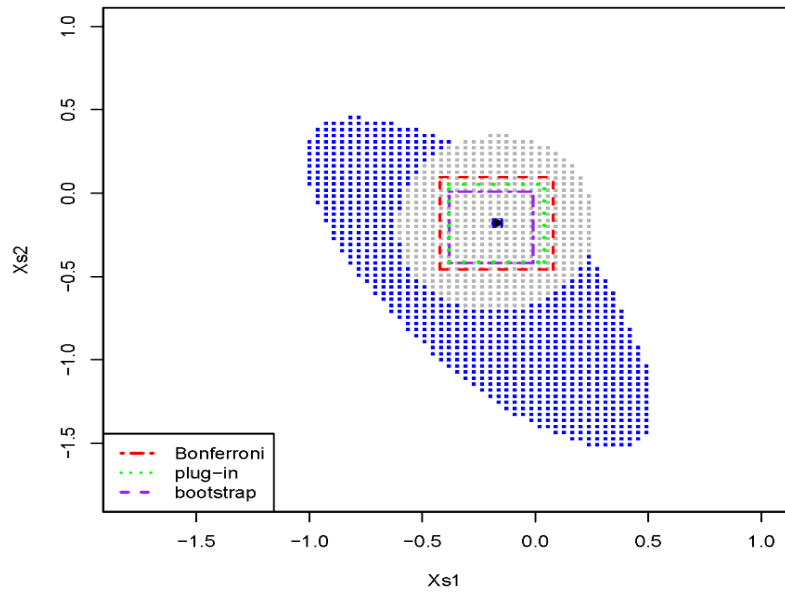


Figure 4.8. 90% Confidence regions and simultaneous confidence intervals.

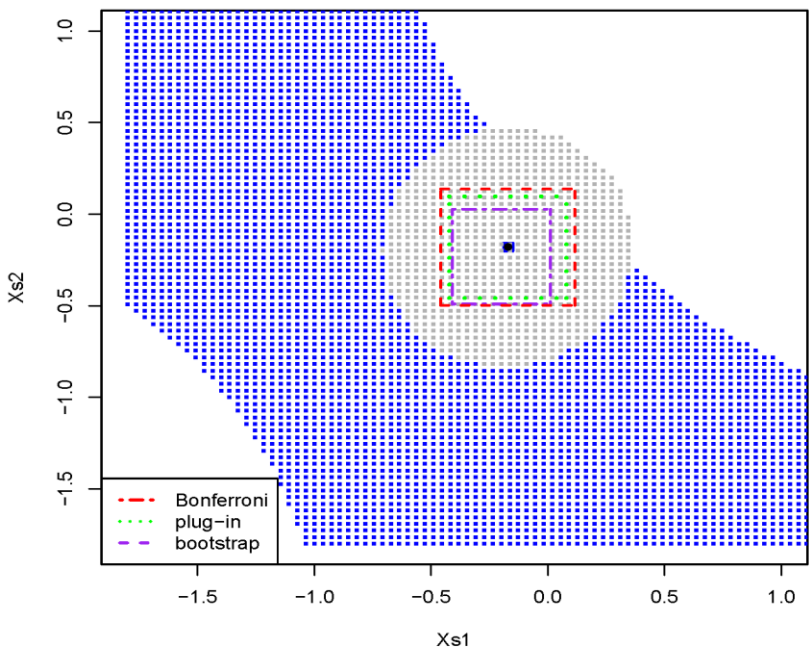


Figure 4.9. 95% Confidence regions and simultaneous confidence intervals.

### 4.6 Rising ridge in quadratic surfaces

A common technique for exploring the fitted second-order response surfaces is canonical analysis. This method allows us to identify the rising ridge behavior in response surfaces to optimize the response. However, determining whether there is a

rising ridge or a stationary ridge helps us decide whether to continue setting process variables.

#### 4.6.1 Canonical analysis and confidence intervals for eigenvalues

Canonical analysis of a quadratic response surface model states that the model in a new coordinate system is defined by new variables, denoted by  $\mathbf{z} = (z_1, z_2, \dots, z_k)$ . These a new variables are a linear combination of the actual variables, but the coordinate axes have been rotated in order to be associated with the natural directions of the fitted quadratic response surface. In other words, the new axes are parallel to the first axes of the quadratic response surface [38]. So by denoting *ith* to normalized eigenvector of  $\hat{\mathbf{B}}$  by  $\hat{\mathbf{d}}_i$ , then

$$\hat{\mathbf{D}} = [\hat{\mathbf{d}}_1, \hat{\mathbf{d}}_2, \dots, \hat{\mathbf{d}}_k]$$

A new rotation with the canonical factors  $\mathbf{z}$  can be expressed as a function of the actual factors  $\mathbf{X}$  as follows:

$$\mathbf{z} = \hat{\mathbf{D}}^T \mathbf{X}$$

Now let  $\hat{\lambda}_i$  be the corresponding eigenvalue to the  $\hat{\mathbf{d}}_i$  then the fitted surface of the coordinate rotated system is given by

$$\widehat{E(\mathbf{y})} = \hat{\beta}_0 + \mathbf{z}^T \hat{\boldsymbol{\phi}} + \mathbf{z}^T \hat{\Lambda} \mathbf{z} \quad (4.9)$$

where  $\hat{\boldsymbol{\phi}} = (\hat{\phi}_1, \hat{\phi}_2, \dots, \hat{\phi}_k)^T = \hat{\mathbf{D}}^T \hat{\boldsymbol{\beta}}$  and  $\hat{\Lambda} = \hat{\mathbf{D}}^T \hat{\mathbf{B}} \hat{\mathbf{D}} = \text{diag}(\hat{\lambda}_1, \hat{\lambda}_2, \dots, \hat{\lambda}_k)$ . Since  $\hat{\Lambda}$  is a diagonal matrix and the canonical model does not contain any of the interaction terms. Usually the magnitudes and signs of the eigenvalues of matrix  $\hat{\mathbf{B}}$ , which depends on the pure second-order terms of the canonical model, allow the researcher to visualize the shape of the surface.

### 4.6.2 The double linear regression method

The double linear regression (DLR) method is a new technique for finding the standard error for the eigenvalues  $\hat{\mathbf{B}}$  of a fitted quadratic response surface model. Based on these estimated parameters we can then compute the matrix  $\hat{\mathbf{D}}$ . The basic idea is that by rotating the actual coordinate factors  $\mathbf{X}$ , they are replaced by the new axes corresponding to the canonical axes  $\mathbf{z}$  using  $\mathbf{z} = \hat{\mathbf{D}}^T \mathbf{X}$  of the response [39]. Finally, we use the regression to refit the second-degree model using the new rotated coordinated  $\mathbf{z}$  as follows:

$$E(\hat{y}) = \hat{\beta}_0^* + \mathbf{z}^T \hat{\beta}^* + \mathbf{z}^T \hat{\mathbf{B}}^* \mathbf{z} \quad (4.10)$$

Where  $\hat{\beta}^* = (b_1^*, b_2^*, \dots, b_k^*)^T$  and

$$\hat{\mathbf{B}}^* = \frac{1}{2} \begin{bmatrix} 2b_{11}^* & b_{12}^* & \dots & b_{1k}^* \\ b_{12}^* & 2b_{22}^* & \dots & b_{2k}^* \\ \vdots & \vdots & \ddots & \vdots \\ b_{1k}^* & b_{2k}^* & \dots & 2b_{kk}^* \end{bmatrix}$$

The standard error of *ith* diagonal elements of  $\hat{\mathbf{B}}^*$  is approximately the standard error of  $\hat{\lambda}_i$ , the *ith* eigenvalue of  $\hat{\mathbf{B}}$ . Thus the estimate of the standard error for the eigenvalues is computed by any linear regression to achieve this quadratic regression model. The next section focuses on describing the DLR method step-by-step.

Consider an experiment, with one response  $y$ , and  $k$  independent variables indicated by  $\mathbf{X} = (x_1, x_2, \dots, x_k)^T$ .

Suppose there are  $n$  design runs, then, the design matrix denoted by  $\mathbf{X}_D$ , is an  $n \times k$  matrix. This matrix contains the  $(i, j)$ th element of  $\mathbf{X}_D$  which is the level of  $x_j$  in the  $i$ th observation. The full quadratic model has  $p = (k + 1)(k + 2)/2$  parameters. The steps of the DLR method is as follows:

- i. Use the ordinary least square (OLS) to fit a full quadratic model in Equation (4.1) and obtain the value of  $\hat{\beta}_0, \hat{\beta}, \dots, \hat{B}$ .
- ii. Compute the eigenvalues,  $\lambda_i, i = 1, 2, \dots, k$ , and the associated eigenvectors of  $\hat{B}$ , as well as the rotation matrix  $\hat{D}$  which is the matrix of eigenvectors from the standard canonical relationships as follows:

$\lambda_i$  is the  $i$ th eigenvalues of  $\hat{B}$ ;

$\hat{D} = [\hat{d}_1, \hat{d}_2, \dots, \hat{d}_k]$ ;  $\hat{d}_i$  are the  $i$ th normalized eigenvectors of  $\hat{B}$ .

- iii. Rotate the coordinate original vectors, so the design runs in the new coordinate system are  $\mathbf{z} = \hat{D}^T \mathbf{X} = (z_1, z_2, \dots, z_k)^T$ . This step is done for all design points by multiplying the actual design matrix by  $\hat{D}$ . The new design matrix is then

$$\mathbf{z}_D = \mathbf{X}_D \hat{D}$$

- iv. Based on the design matrix,  $\mathbf{z}_D$ , the full quadratic model in Equation (4.1) is again fitted using OLS.
- v. From step 4 the values of  $\hat{\beta}_{ij}^*$ 's will be close to zero, the  $\hat{B}_{ii}^*, i = 1, 2, \dots, k$  will be equal to,  $\hat{\lambda}_i$  and the standard error  $se(\hat{\beta}_{ii}^*)$  provided by a linear regression routine for  $b_{ii}^*$  is utilized as an approximate standard error for the  $\lambda_i$ .
- vi. The construction of the following equation yields an approximate  $100(1 - \alpha)\%$  confidence interval for  $\hat{\lambda}_i$ :

$$\hat{\lambda}_i \pm t_{1-\alpha/2, n-p} se(\hat{\beta}_{ii}^*)$$

where  $n$  is the total number of the design,  $p$  is the number of parameters, and the

$t_{1-\alpha/2, n-p}$  is  $1 - \alpha/2$  quantile of student's  $t$ -distribution with  $n-p$  degrees of freedom.

Notably, in case all the eigenvalues are to be tested individually, the Bonferroni

confidence interval replaces  $t_{1-\alpha/2, n-p}$  with  $t_{1-\alpha/2k, n-p}$ , where the  $k$  is the eigenvalues being compared to zero.

Now the computation and details of DLR will be shown. However, let us review the last steps of the quadratic regression and how the  $se(\hat{\beta}_{ii}^*)$  in step 4 is estimated. The  $Z$  is an  $n \times p$  matrix is given

$$\mathbf{Z} = [\mathbf{1}, \mathbf{z}_1, \dots, \mathbf{z}_k, \mathbf{z}_{12}, \mathbf{z}_{(k-1)k}, \mathbf{z}_{11} \dots, \mathbf{z}_{kk}]$$

In this section, we will discuss more details of steps of the DLR approach using the organic solar cell experiment.

All three steps are taken as one large trial, with the matrix  $\mathbf{X}_D$ , and the observed vector is as given below:

$$\mathbf{X}_D = [\mathbf{x}_1, \mathbf{x}_2, \mathbf{x}_3] = \begin{bmatrix} 0 & 0 & 0 \\ 0 & 0 & 0 \\ -1 & -1 & 1 \\ 0 & 0 & 0 \\ 1 & 1 & 1 \\ 1 & -1 & -1 \\ 0 & 0 & 0 \\ -1 & 1 & -1 \\ -1 & -1 & -1 \\ 0 & 0 & 0 \\ 0 & 0 & 0 \\ -1 & 1 & 1 \\ 0 & 0 & 0 \\ 0 & 0 & 0 \\ 1 & 1 & -1 \\ 1 & -1 & 1 \\ 0 & 0 & \sqrt{2} \\ 0 & 0 & 0 \\ -\sqrt{2} & 0 & 0 \\ 0 & 0 & -\sqrt{2} \\ 0 & \sqrt{2} & 0 \\ \sqrt{2} & 0 & 0 \\ 0 & 0 & 0 \\ 0 & \sqrt{2} & 0 \end{bmatrix} \quad \text{and} \quad \mathbf{y} = \begin{bmatrix} 5.59 \\ 5.13 \\ 3.08 \\ 5.25 \\ 3.18 \\ 3.4 \\ 5.1 \\ 2.43 \\ 3.17 \\ 4.54 \\ 5.14 \\ 2.2 \\ 4.69 \\ 4.7 \\ 3.11 \\ 3.45 \\ 4.14 \\ 5.15 \\ 2.05 \\ 3.48 \\ 4.28 \\ 3.51 \\ 5.1 \\ 5.4 \end{bmatrix}$$

The columns of the matrix for fitting the full quadratic model is

$$\mathbf{X} = [\mathbf{1}, \mathbf{x}_1, \mathbf{x}_2, \mathbf{x}_3, \mathbf{x}_{12}, \mathbf{x}_{13}, \mathbf{x}_{23}, \mathbf{x}_{11}, \mathbf{x}_{22}, \mathbf{x}_{33}]$$

Using OLS to fit the model, we find that:

$$\hat{\mathbf{B}} = \begin{bmatrix} -1.18 & 0.07 & 0.03 \\ 0.07 & -0.15 & -0.01 \\ 0.03 & -0.01 & -0.67 \end{bmatrix}, \quad \hat{\boldsymbol{\beta}} = \begin{bmatrix} 0.36 \\ -0.31 \\ 0.06 \end{bmatrix}, \quad \hat{b}_0 = 5.15$$

Based on these estimates, the matrix of the eigenvalues of  $\hat{\mathbf{B}}$  is  $\hat{\boldsymbol{\Lambda}} = \text{diag}(\hat{\lambda}_1, \hat{\lambda}_2, \hat{\lambda}_3) =$

$(-1.19, -0.67, -0.15)$  and their coordinate eigenvectors,  $\hat{\mathbf{D}} = [\hat{\mathbf{d}}_1, \hat{\mathbf{d}}_2, \hat{\mathbf{d}}_3]$  to be

$$\hat{\boldsymbol{\Lambda}} = \begin{bmatrix} -1.19 & 0 & 0 \\ 0 & -0.67 & 0 \\ 0 & 0 & -0.15 \end{bmatrix}$$

and

$$\hat{\mathbf{D}} = \begin{bmatrix} 0.997 & 0.054 & -0.064 \\ -0.064 & 0.008 & -0.998 \\ -0.054 & 0.999 & 0.011 \end{bmatrix}$$

The estimated stationary points are (0.099, -0.975, and 0.061) and the estimated response at this stationary point is 5.23. Since the stationary point is within the design space, in such cases,  $B$ -canonical is usually fit for model explanation, which can be written as follows:

$$E(y) = 5.23 - 1.19w_1^2 - 0.67w_2^2 - 0.15w_3^2$$

where  $\mathbf{w} = (w_1, w_2, w_3)^T = \hat{\mathbf{D}}^T(\mathbf{X} - \mathbf{X}_s)$ , the coefficients are the eigenvalues of matrix  $\hat{\mathbf{B}}$ .

Now the DLR method is employed to obtain an approximate confidence interval for the eigenvalues. The  $A$ -canonical analysis uses  $\mathbf{z} = \hat{\mathbf{D}}^T \mathbf{X}$  for each experiment in the design matrix  $\mathbf{X}_D$  by multiplying  $\mathbf{X}_D$  by  $\hat{\mathbf{D}}$ . Thus the design matrix for the quadratic model in the DLR method is given



$$\mathbf{Z}_D = \mathbf{X}_D \hat{\mathbf{D}} = [\mathbf{z}_1, \mathbf{z}_2, \mathbf{z}_3] = \begin{bmatrix} 0 & 0 & 0 \\ 0 & 0 & 0 \\ -0.986 & 0.937 & 1.073 \\ 0 & 0 & 0 \\ 0.879 & 1.060 & -1.050 \\ 1.114 & -0.952 & 0.923 \\ 0 & 0 & 0 \\ -1.007 & -1.045 & -0.945 \\ -0.879 & -1.060 & 1.050 \\ 0 & 0 & 0 \\ 0 & 0 & 0 \\ -1.114 & 0.952 & -0.923 \\ 0 & 0 & 0 \\ 0 & 0 & 0 \\ 0.986 & -0.937 & -1.073 \\ 1.007 & 1.045 & 0.945 \\ -0.076 & 1.412 & 0.016 \\ 0 & 0 & 0 \\ -1.409 & -0.077 & 0.090 \\ 0.076 & -1.412 & -0.016 \\ -0.091 & 0.011 & -1.411 \\ 1.409 & 0.077 & -0.090 \\ 0 & 0 & 0 \\ 0.091 & -0.011 & 1.411 \end{bmatrix}; \mathbf{y} = \begin{bmatrix} 5.59 \\ 5.13 \\ 3.08 \\ 5.25 \\ 3.18 \\ 3.4 \\ 5.1 \\ 2.43 \\ 3.17 \\ 4.54 \\ 5.14 \\ 2.2 \\ 4.69 \\ 4.7 \\ 3.11 \\ 3.45 \\ 4.14 \\ 5.15 \\ 2.05 \\ 3.48 \\ 4.28 \\ 3.51 \\ 5.1 \\ 5.4 \end{bmatrix}$$

Based on coordinate rotation, the new full second-order model is fitted in the new coordinate process

$$E(y) = b_0^* + b_1^* z_1 + b_2^* z_2 + b_3^* z_3 + b_{12}^* z_1 z_2 + b_{13}^* z_1 z_3 + b_{23}^* z_2 z_3 + b_{11}^* z_1^2 + b_{22}^* z_2^2 + b_{33}^* z_3^2$$

The columns of the matrix  $\mathbf{Z}_D$  of regressor for fitting the full second-order model with regression is performed element-by-element to obtain

$$\mathbf{Z} = [\mathbf{1}, \mathbf{z}_1, \mathbf{z}_2, \mathbf{z}_3, \mathbf{z}_{12}, \mathbf{z}_{13}, \mathbf{z}_{23}, \mathbf{z}_{11}, \mathbf{z}_{22}, \mathbf{z}_{33}]$$

The pure quadratic terms from the fitted regression  $b_{11}^*$ ,  $b_{22}^*$ , and  $b_{33}^*$ , are equal to the eigenvalues of  $\hat{\mathbf{B}}$  from the initial regression.

Now  $S_\lambda$  is the variance-covariance matrix for the pure quadratic coefficients obtained by the usual OLS. This  $S_\lambda$  is a  $3 \times 3$  submatrix of  $s^2(\mathbf{Z}^T \mathbf{Z})^{-1}$  where  $s^2$  is the estimated

residual variance. The square root of the diagonal elements of  $S_\lambda$  is the approximated standard error of the eigenvalues. For this data,

$$S_\lambda = \begin{bmatrix} 0.010 & -0.002 & -0.002 \\ -0.002 & 0.010 & -0.002 \\ -0.002 & -0.002 & 0.010 \end{bmatrix}$$

Using  $S_\lambda$ , provides an approximate  $100(1 - \alpha)\%$  confidence interval for  $\lambda_i$  as given by:

$$\hat{\lambda}_i \pm t_{1-\alpha/2, n-p} (\mathbf{e}_i^T S_\lambda \mathbf{e}_i)^{1/2}$$

where  $\mathbf{e}_i$  is a vector containing zeros excepting for the one in the  $i$ th position and  $t_{1-\alpha/2, n-p}$  is  $1 - \alpha/2$  quantile of student's  $t$ -distribution with  $n - p$  degree of freedom.

Note that this calculation was already found by the standard regression model. In this case,  $t_{1-\alpha/2, n-p} = t_{0.975, 14} = 2.1448$ . The estimated eigenvalues, associated standard error and the approximate 95% confidence interval are shown in Table 4.3.

Table 4.2. The estimated second-order regression model

	Estimate	Std. Error
(Intercept)	5.057	0.094
x1	0.360	0.088
x2	-0.314	0.088
x3	0.061	0.088
x1:x2	0.133	0.108
x1:x3	0.055	0.108
x2:x3	-0.015	0.108
x1^2	-1.185	0.100
x2^2	-0.155	0.100
x3^2	-0.670	0.100

Table 4.3 shows the estimation of the eigenvalues with associated an approximate standard errors calculated utilizing the DLR method and corresponding approximate 95% confidence interval for the organic solar cell.

Table 4.3. The approximate 95% confidence interval for estimated eigenvalues.

Canonical parameter	DLR regression parameter	Estimate	Standard error	Approximate 95% CI
$\hat{\lambda}_1$	$b_{11}^*$	-1.190	0.10	(-1.40, -0.97)
$\hat{\lambda}_2$	$b_{22}^*$	-0.668	0.10	(-0.88, -0.45)
$\hat{\lambda}_3$	$b_{33}^*$	-0.150	0.10	(-0.36, 0.06)

The confidence interval of the first two eigenvalues does not contain zero. Moreover, the confidence interval for  $\hat{\lambda}_3$  contains zero by a small margin as shown Figure 4.10. This is an indication that there might be rising ridge in the surface with a maximum in the third canonical axis.

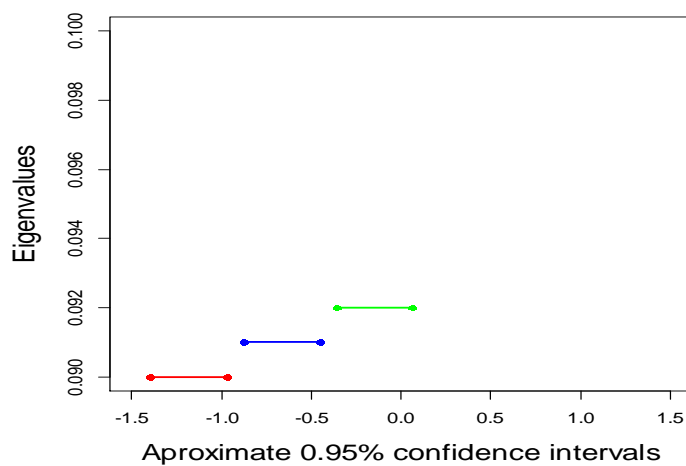


Figure 4.10. The individual approximate CI for the eigenvalues.

A Bonferroni adjustment can be used as an alternative for multiple comparisons, as follows:

$$\hat{\lambda}_i \pm t_{1-\alpha/2k, n-p} (\mathbf{e}_i^T \mathbf{S}_\lambda \mathbf{e}_i)^{1/2}$$

where  $t_{1-\alpha/2k, n-p}$  is  $1 - \alpha/2$  quantile of student's t-distribution with  $n - p$  degree of freedom. Note that this calculation was already found by the standard regression model. In this case  $t_{1-\alpha/2k, n-p} = t_{0.975, 14} = 2.6245$  when constructing Bonferroni confidence intervals.

The estimated eigenvalues with their standard error and the approximate 95% Bonferroni confidence interval are summarized in Table 4.4.

Table 4.4. The approximate 95% Bonferroni confidence interval for estimated eigenvalues.

Canonical parameter	DLR regression parameter	Estimate	Standard error	Approximate 95% CI
$\hat{\lambda}_1$	$b_{11}^*$	-1.190	0.10	(-1.45, -0.92)
$\hat{\lambda}_2$	$b_{22}^*$	-0.668	0.10	(-0.93, -0.40)
$\hat{\lambda}_3$	$b_{33}^*$	-0.150	0.10	(-0.41, 0.11)

As shown, the Bonferroni intervals for the first two eigenvalues are both negative, and for the third eigenvalue the Bonferroni confidence intervals includes zero as shown in Figure 4.11.

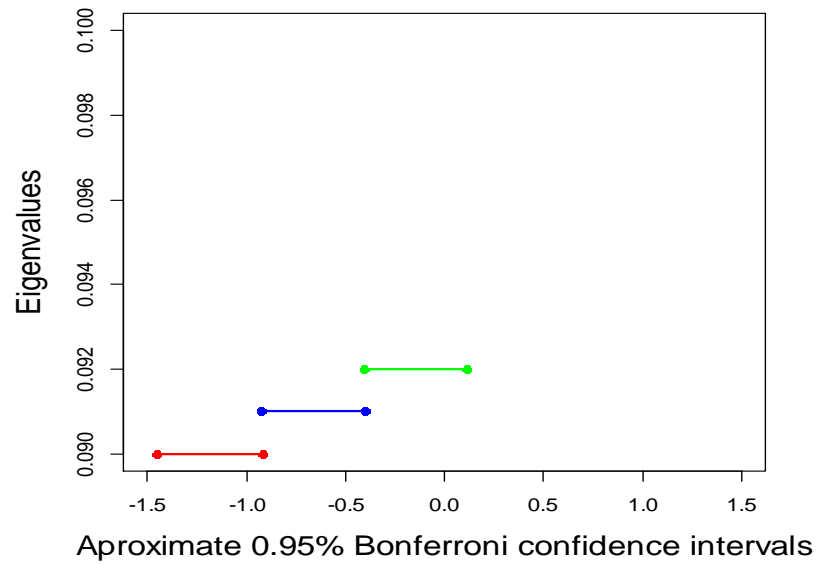


Figure 4.11. The individual approximate 95% Bonferroni CI for the eigenvalues.

In the following chapter, a metaheuristic search method is addressed in order to find an alternative solution for our design matrix that might be closer to the optimum solution.

## CHAPTER 5

### COMBINATORIAL OPTIMIZATION FOR DESIGN POINTS

Generally, combinatorial optimization problems are sufficiently complicated that it might not be possible to find the optimal solution. In such situations, heuristic methods are often used to obtain a near optimal solution. The RSM is silent about what to do with the partial experimental results obtained using CCD during the course of completing all design points. Can any useful insights be gleaned from the progressively available data in order to adapt the experimental research process in light of new and current information obtained? RSM (CCD) also does not provide guidance in regards to the order in which design points should be carried out. Is the performance of the experiments reliable by following the design points as shown in the design matrix (best performance)? Would choosing an alternative design matrix (design points) lead to any improvement?

To answer to these questions, the metaheuristic search method [40] from Operations Research can be employed to search for more optimum solution.

#### **5.1 Metaheuristics**

Metaheuristic algorithms, which are a class of approximation techniques, were developed in the 1980's. The term "heuristic" originates from the ancient Greek word "heuriskein", meaning the art of determining new strategies that can resolve problems. Also the suffix "meta" is a Greek word, meaning the upper level approach. Fred Glover (1986) first presented the term metaheuristic in the paper "Future Paths for Integer Programming and Links to Artificial Intelligence" (Talbi, 2009, p.1). Furthermore, some problems are so complicated according to the Operation Research (OR) models that it

may not be easy find the optimum solution. In such situations, it is still worthwhile to search for a feasible solution that could be reasonably close to optimal, so heuristic techniques commonly are utilized to search for such a solution.

A heuristic method is a process of searching for a reasonably good solution (not necessarily the optimal solution) for a specific problem being studied. No such evidence can guarantee the quality of the solution obtained, but a better solution that is nearly optimal can usually be obtained by a well-designed heuristic method. Additionally, the method should be sufficiently effective to deal with large-scale problems.

Heuristic approaches are frequently based on a reasonably simple idea for obtaining a better solution. These ideas need to be carefully designed to fit the particular problem of interest.

For many years, the OR team would need to start from scratch to improve a heuristic technique to fit the problem at hand, wherever a procedure for finding an optimum solution was not available. This has all improved in modern years with the development of the powerful metaheuristic method. A metaheuristic is a general solution approach that provides both a common structure and approach guidelines for developing a particular heuristic method to fit a specific kind of problem. Furthermore, the metaheuristics is one of most important techniques in the tool of OR practitioners.

Metaheuristics are applied to find answers to problems when there is very little available information and knowledge, regarding the characteristics of the optimal solution.

Sometimes we do not know how to go in finding the optimal solution in principled manner, and a brute-force exploration is out of the question because the solution space is

too large, such as in genetics research. But if we are given a candidate solution, we can verify it and evaluate its appropriateness. That is, we know a good solution when it is available.

There is no guarantee based on metaheuristics that an optimum solution can be found for many classes of problems [41]. Many metaheuristics implement some form of stochastic optimization, so that the solution found is dependent on the set of random variables generated [42]. In combinatorial optimization, by searching over a large set of reasonable solutions, metaheuristics can often find a better solutions with less computational effort than optimization processes, iterative approaches, or simple heuristics [41]. As such, they are useful methods for optimization problems [42].

The simplest strategy in some situation is a Random Search, trying random sets of solutions as long as there is time, and return the best one found. Then a small, random modification is made to it and the new version is tried. If the new version is better, the old one is thrown away, if not, the original is modified in another way. If this newest version is better, the current version is discarded; if not, the newest version is discarded and the older version is modified yet again. This process is repeated as long as exit conditions have not yet been met.

## **5.2 Properties**

The properties that characterize the most metaheuristics [41]:

- i. Metaheuristics are approaches that guide the search process.
- ii. The aim is to capably discover the search region in order to find near optimum solutions.



- iii. Metaheuristic procedures are approximate and commonly nondeterministic.
- iv. Metaheuristics are not problem specific.

As mentioned above, the metaheuristic search method is applied because the CCD does not provide guidance in regards to which design points should be used to precisely optimize the solar device performance. Furthermore, the design points of fractional factorial designs frequently result in great low-cost and effectiveness in research, especially if the runs of the experiment can be made successively. For instance, consider that the experimenters were exploring  $k = 3$  intended variables as we have in this work with a total of all possible runs ( $2^3 = 8$  runs) plus 8 center point repetitions. The preferred method is to run a  $2^{3-1}$  fractional design (4 runs) with 4 repetitions at the center of each half-fraction, and then analyze the results. The information obtained from this process is used to make a decision about the best set of points to implement next. Whenever it becomes essential to solve ambiguity, we are able to run the alternate fraction and the total number of design runs in a CCD ( $n = 2^k + 2k + n_0 = 24$  runs).

To apply the metaheuristic search method, the full factorial design was generated using a generator ( $\sim x_1 + x_2 + x_3$ ) based on the cube function and then combined to the star block to obtain all possible combinations of CCD. One hundred random samples were simulated with different orders to determine the behavior of the design points of CCD, as shown in Figure 5.1 below. The preliminary results show that the permutation is indeed important with respect to the first-order model. Moreover, in an RSM application, by using a few data points some design points are discarded due to the singularities; one of these design points is then brought back to the design and the singularities determined

using generalized inverse (g-inverse), which estimates the coefficients when the matrix is not full rank. For more details on generalized inverse, please refer to Graybill et al. [43]. This design point was added to Figure 5.2 with a bold yellow line, note the behavior of this discarded design point as compared with the 100 simulated samples and default design points (design matrix in Table 3.1). A brief overview of the generalized inverse is presented next.

### 5.3 Generalized and conditional inverse

If a matrix  $\mathbf{A}$  has an inverse, the matrix  $\mathbf{A}$  must be square and the determinant must be nonzero. The theory of linear models, which includes a large part of theoretical and applied statistics, involves the solutions of a system of linear equations

$$\mathbf{A}\mathbf{u} = \mathbf{X}$$

if  $\mathbf{A}$  is an  $n \times n$  nonsingular matrix, the solution to the system in the Equation (4) exists, is unique, is given by  $\mathbf{u} = \mathbf{A}^{-1}\mathbf{X}$ . However, there are cases where  $\mathbf{A}$  is not a square matrix or  $\mathbf{A}$  is a square matrix but is singular. In these situations, there may still be a solution to the system, and a unified theory to treat all situations is desirable. One such theory involves the use of generalized and conditional inverses of matrices.

Let  $\mathbf{A}$  be an  $m \times n$  matrix of rank  $r$ . The investigation of the matrix denoted by  $\mathbf{A}^-$  which has many of properties that the inverse of the matrix  $\mathbf{A}$  would have if the inverse existed, is in the next section.

#### 5.3.1 Generalized inverse

Let  $\mathbf{A}$  be an  $m \times n$  matrix. If a matrix denoted by  $\mathbf{A}^-$  exists that satisfies the four conditions below, it will be defined as a generalized inverse of  $\mathbf{A}$ .

- i.  $\mathbf{AA}^-$  is symmetric;
- ii.  $\mathbf{A}^- \mathbf{A}$  is symmetric;
- iii.  $\mathbf{AA}^- \mathbf{A} = \mathbf{A}$
- iv.  $\mathbf{A}^- \mathbf{AA}^- = \mathbf{A}^-$

The terminology “g-inverse” is used to denote the generalized inverse. If  $\mathbf{A}$  is nonsingular, it is clear that  $\mathbf{A}^-$  satisfies the conditions of a g-inverse. However, if  $\mathbf{A}^-$  is a square matrix and singular, or if  $\mathbf{A}$  is not a square matrix, then the problem remains as to whether a matrix  $\mathbf{A}^-$  exists that satisfies with  $\mathbf{A}^- \mathbf{AA}^- = \mathbf{A}^-$ . Finally, for each matrix  $\mathbf{A}$ , a g-inverse matrix  $\mathbf{A}^-$  exists and is unique [43].

Generalized Inverse (g-inverse) is used to solve the singularities for the discarded design point as follows:

$$\mathbf{A} = \begin{bmatrix} -1 & 1 & -1 \\ 0 & 0 & 0 \\ -1 & -1 & 1 \\ 0 & 0 & 0 \\ 0 & 0 & 0 \\ 1 & 1 & -1 \\ 0 & 0 & 0 \\ 1 & -1 & 1 \end{bmatrix}; \quad \mathbf{A}^T = \begin{bmatrix} -1 & 0 & -1 & 0 & 0 & 1 & 0 & 1 \\ 1 & 0 & -1 & 0 & 0 & 1 & 0 & -1 \\ -1 & 0 & 1 & 0 & 0 & -1 & 0 & 1 \end{bmatrix}$$

$$\mathbf{A}_1 = \mathbf{A}^T \mathbf{A} = \begin{bmatrix} 4 & 0 & 0 \\ 0 & 4 & -4 \\ 0 & -4 & 4 \end{bmatrix}$$

If the matrix  $\mathbf{A}^T \mathbf{A}$  has zero determinant, then the matrix  $\mathbf{A}^T \mathbf{A}$  is not invertible (that is, a singular matrix). A g-inverse matrix  $\mathbf{A}^-$  exists for the matrix  $\mathbf{A}^T \mathbf{A}$  that satisfies  $\mathbf{A}^- \mathbf{A}_1 \mathbf{A}^- = \mathbf{A}^-$  is given as:

$$\mathbf{A}^- = \begin{bmatrix} 0.25 & 0 & 0 \\ 0 & 0.063 & -0.063 \\ 0 & -0.063 & 0.063 \end{bmatrix}$$

$$\mathbf{A}_1 \mathbf{A}^- = \begin{bmatrix} 1 & 0 & 0 \\ 0 & 0.5 & -0.5 \\ 0 & -0.5 & 0.5 \end{bmatrix} \text{ is symmetric}$$

$$\mathbf{A}^- \mathbf{A}_1 = \begin{bmatrix} 1 & 0 & 0 \\ 0 & 0.5 & -0.5 \\ 0 & -0.5 & 0.5 \end{bmatrix} \text{ is symmetric}$$

$$\mathbf{A}_1 \mathbf{A}^- \mathbf{A}_1 = \begin{bmatrix} 4 & 0 & 0 \\ 0 & 4 & -4 \\ 0 & -4 & 4 \end{bmatrix} = \mathbf{A}^T \mathbf{A}$$

$$\mathbf{A}^- \mathbf{A}_1 \mathbf{A}^- = \begin{bmatrix} 0.25 & 0 & 0 \\ 0 & 0.063 & -0.063 \\ 0 & -0.063 & 0.063 \end{bmatrix} = \mathbf{A}^-$$

The g-inverse matrix  $\mathbf{A}^-$  exists for the

matrix  $\mathbf{A}^T \mathbf{A}_1$  and is unique.

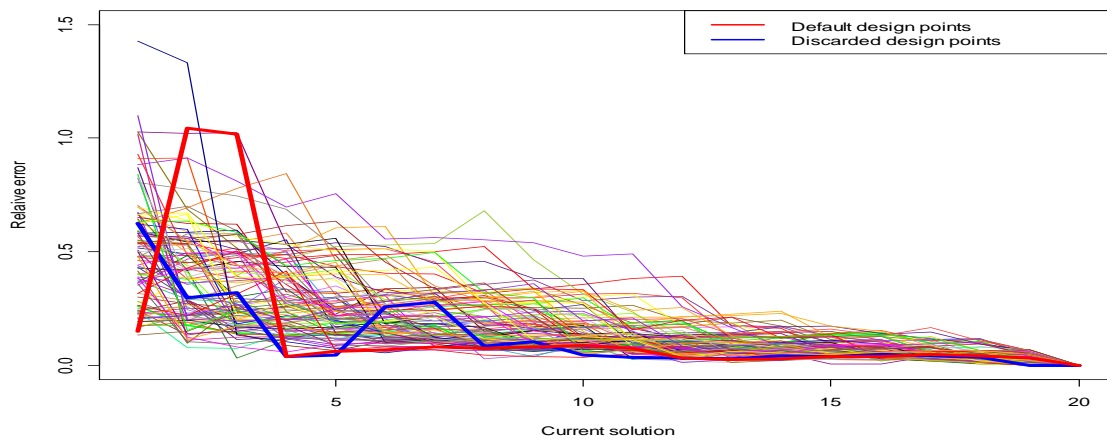


Figure 5.1. The dynamic of default design points.

As seen in Figure 5.1 the dynamic of discarded design combination during the first few runs has around 60% relative error. Furthermore, after a few experiments are added, it has around 10% of error which initially leads to the summary that those design points which have been discarded by the RSM due to singularity have an important effect in the CCD as compared to those that have been kept in the design.

#### **5.4 The relative error with respect to the quadratic fitted model**

Even if the design points are proven to be important based on random search with respect to the first-degree model, how we can systematically search with respect to the second-order model for an optimal or near-optimal design combination in CCD to be cost effective. For this purpose, a neighboring rows was based on swapping the location of two elements within the three blocks (*cube*, *foldover*, and *star* blocks) of the permutation to search for a better feasible solution which generated 276 matrices as shown in Table 5.3. In addition, the strategy is to search for a better solution for each swap with respect to the quadratic model, the relative error is obtained based on a given candidate solution (default matrix). If the new swap version has less relative error, then the old one is discarded; if it does not, then discard the newest version. Repeat this process as long as a better solution (better improvement) is obtained. The scenario is that for each permutation, a second-degree model is fitted, starting with eighteen design points, because the quadratic model requires eight design points for  $k = 3$ , four center points, and six star points (total runs  $n = 18$ ). Then the rest of the design points are added cumulatively to fit the quadratic model and the relative error computed each time.

Table 5.1. The first permutation matrix (swap) generated within the blocks.

Block	X <sub>1</sub>	X <sub>2</sub>	X <sub>3</sub>	Y	Run
1	0	0	0	5.13	2
1	0	0	0	5.59	1
1	-1	-1	1	3.08	3
1	0	0	0	5.25	4
1	1	1	1	3.18	5
1	1	-1	-1	3.4	6
1	0	0	0	5.1	7
1	-1	1	-1	2.43	8
2	-1	-1	-1	3.17	9
2	0	0	0	4.54	10
2	0	0	0	5.14	11
2	-1	1	1	2.2	12
2	0	0	0	4.69	13
2	0	0	0	4.7	14
2	1	1	-1	3.11	15
2	1	-1	1	3.45	16
3	0	0	$\sqrt{2}$	4.14	17
3	0	0	0	5.15	18
3	$-\sqrt{2}$	0	0	2.05	19
3	0	0	$-\sqrt{2}$	3.48	20
3	0	$\sqrt{2}$	0	4.28	21
3	$\sqrt{2}$	0	0	3.51	22
3	0	0	0	5.1	23
3	0	$-\sqrt{2}$	0	5.4	24

Table 5.2. The last permutation matrix (swap) generated within the blocks.

Block	X <sub>1</sub>	X <sub>2</sub>	X <sub>3</sub>	Y	Run
3	0	$-\sqrt{2}$	0	5.4	24
3	0	0	0	5.1	23
3	$\sqrt{2}$	0	0	3.51	22
3	0	$\sqrt{2}$	0	4.28	21
3	0	0	$-\sqrt{2}$	3.48	20
3	$-\sqrt{2}$	0	0	2.05	19
3	0	0	0	5.15	18
3	0	0	$\sqrt{2}$	4.14	17
2	1	-1	1	3.45	16
2	1	1	-1	3.11	15
2	0	0	0	4.7	14
2	0	0	0	4.69	13
2	-1	1	1	2.2	12
2	0	0	0	5.14	11
2	0	0	0	4.54	10
2	-1	-1	-1	3.17	9
1	-1	1	-1	2.43	8
1	0	0	0	5.1	7
1	1	-1	-1	3.4	6
1	1	1	1	3.18	5
1	0	0	0	5.25	4
1	-1	-1	1	3.08	3
1	0	0	0	5.13	2
1	0	0	0	5.59	1

Table 5.1 and Table 5.2 represent an alternative design matrix of first and last swap out of the 276 swaps.

The relative error is calculated as:

$$D = \sum_{i=1}^p d_i$$

where  $d_i$  is the Euclidean distance between the columns of matrix  $\hat{\beta}$  which is given by the Pythagorean formula:

$$d_i = d(\hat{\beta}_{ij}, \hat{\beta}_{pj}) = \sqrt{\sum_{i=1}^p (\hat{\beta}_{ij} - \hat{\beta}_{pj})^2} / \sqrt{\sum_{j=1}^m (\hat{\beta}_{pj})^2}, \quad i = 1, 2, \dots, p; j = 1, 2, \dots, m$$

and

$$\hat{\beta} = \begin{bmatrix} b_{11} & b_{21} & \dots & b_{p1} \\ b_{12} & b_{22} & \dots & b_{p2} \\ \vdots & \vdots & \ddots & \vdots \\ b_{1m} & b_{2m} & \dots & b_{pm} \end{bmatrix}$$

where  $p = 6$  which represents the number of fitted quadratic models according to the cumulative design points and  $m = 10$  is number of parameters (intercept, main effects, interaction effects, and quadratic effects of a second-order model).

For example the matrix  $\hat{\beta}$  for the design matrix in Table 5.1 is:

$$\hat{\beta} = \begin{bmatrix} 5.03 & 5.03 & 5.03 & 5.04 & 5.05 & 5.06 \\ 0.28 & 0.28 & 0.29 & 0.36 & 0.36 & 0.36 \\ -0.27 & -0.27 & -0.28 & -0.26 & -0.26 & -0.31 \\ -0.03 & 0.06 & 0.06 & 0.06 & 0.06 & 0.06 \\ 0.13 & 0.13 & 0.13 & 0.13 & 0.13 & 0.13 \\ 0.06 & 0.06 & 0.06 & 0.06 & 0.06 & 0.06 \\ -0.02 & -0.02 & -0.02 & -0.02 & -0.02 & -0.02 \\ -1.29 & -1.29 & -1.27 & -1.15 & -1.15 & -1.18 \\ -0.31 & -0.13 & -0.16 & -0.24 & -0.24 & -0.15 \\ -0.43 & -0.61 & -0.60 & -0.63 & -0.64 & -0.67 \end{bmatrix}$$

$$\text{and } d_1 = d(\hat{\beta}_{1j}, \hat{\beta}_{6j}) = \sqrt{\sum_{i=1}^6 (\hat{\beta}_{1j} - \hat{\beta}_{6j})^2} / \sqrt{\sum_{j=1}^{10} (\hat{\beta}_{6j})^2} = 0.06$$

Similarly for  $d_2 = 0.03$ ,  $d_3 = 0.03$ ,  $d_4 = 0.02$ ,  $d_5 = 0.02$ ,  $d_6 = 0$ , the relative error is given



$$D = \sum_{i=1}^6 d_i = 0.06 + 0.03 + 0.03 + 0.02 + 0.02 + 0 = 0.16$$

Also, the relative error is computed in the same manner for all permutations (swaps) as shown in Table 5.3.

Table 5.3. The relative error according to the 276 permutation matrices.

Relative Error	Permutation
0.05	3
0.06	1
0.07	11
0.08	11
0.09	4
0.1	14
0.11	13
0.12	13
0.13	8
0.14	20
0.15	7
<b>0.16</b>	<b>50</b>
0.17	1
0.18	17
0.19	8
0.2	15
0.21	3
0.22	20
0.23	5
0.24	2
0.25	3
0.26	1
0.27	3
0.29	8
0.31	2
0.32	30
0.34	1
0.38	1
0.39	1

According to Table 5.3, there are 150 an alternative a better solution of our design matrix based on the relative error that might be close to the optimum solution, a fifty of them has the same relative error of the default matrix, and the rest are worse as shown in figures 5.2 and 5.3.

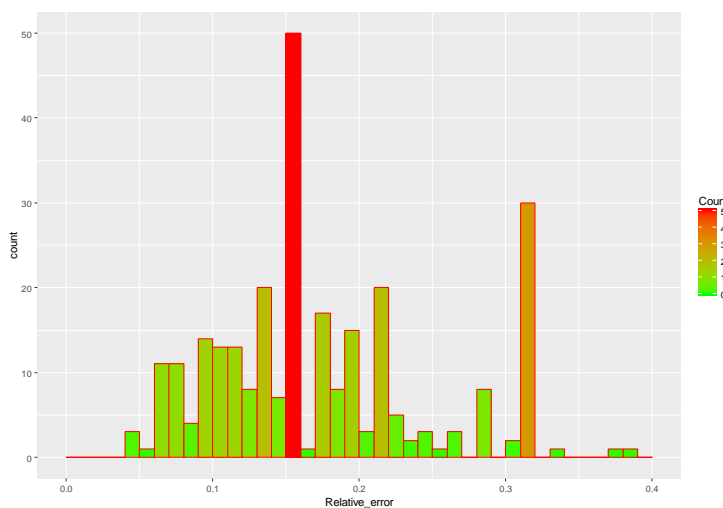


Figure 5.2. The histogram of current solutions according to the relative error.

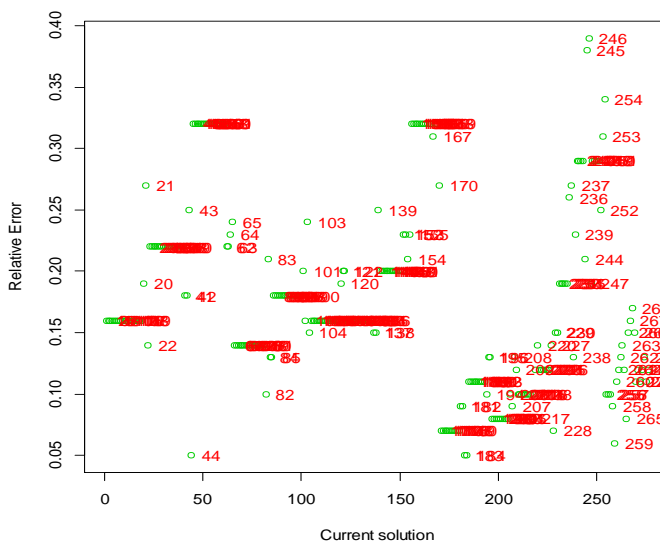


Figure 5.3. The current solution corresponding to the relative error.

Table 5.4. The candidate trial solution (swap 44) with respect to the second-order model.

Blocks	$X_1$	$X_2$	$X_3$	$y$	Run
3	0	$-\sqrt{2}$	0	5.4	24
3	$\sqrt{2}$	0	0	3.51	22
1	0	0	0	5.59	1
1	0	0	0	5.13	2
1	-1	-1	1	3.08	3
1	0	0	0	5.25	4
1	1	1	1	3.18	5
1	1	-1	-1	3.4	6
1	0	0	0	5.1	7
1	-1	1	-1	2.43	8
2	-1	-1	-1	3.17	9
2	0	0	0	4.54	10
2	0	0	0	5.14	11
2	-1	1	1	2.2	12
2	0	0	0	4.69	13
2	0	0	0	4.7	14
2	1	1	-1	3.11	15
2	1	-1	1	3.45	16
3	0	0	$\sqrt{2}$	4.14	17
3	0	0	0	5.15	18
3	$-\sqrt{2}$	0	0	2.05	19
3	0	0	$-\sqrt{2}$	3.48	20
3	0	$\sqrt{2}$	0	4.28	21
3	0	0	0	5.1	23

Table 5.5. The candidate trial solution (swap 183) with respect to the second-order model.

Block	$X_1$	$X_2$	$X_3$	$y$	Run
3	0	$-\sqrt{2}$	0	5.4	24
3	0	0	0	5.1	23
3	$\sqrt{2}$	0	0	3.51	22
3	0	$\sqrt{2}$	0	4.28	21
3	0	0	$-\sqrt{2}$	3.48	20
3	$-\sqrt{2}$	0	0	2.05	19
3	0	0	0	5.15	18
3	0	0	$\sqrt{2}$	4.14	17
2	1	-1	1	3.45	16
2	0	0	0	4.69	13
1	0	0	0	5.59	1
1	0	0	0	5.13	2
1	-1	-1	1	3.08	3
1	0	0	0	5.25	4
1	1	1	1	3.18	5
1	1	-1	-1	3.4	6
1	0	0	0	5.1	7
1	-1	1	-1	2.43	8
2	-1	-1	-1	3.17	9
2	0	0	0	4.54	10
2	0	0	0	5.14	11
2	-1	1	1	2.2	12
2	0	0	0	4.7	14
2	1	1	-1	3.11	15

Table 5.6. The candidate trial solution (swap 184) with respect to the second-order model.

Block	$X_1$	$X_2$	$X_3$	$y$	Run
3	0	$-\sqrt{2}$	0	5.4	24
3	0	0	0	5.1	23
3	$\sqrt{2}$	0	0	3.51	22
3	0	$\sqrt{2}$	0	4.28	21
3	0	0	$-\sqrt{2}$	3.48	20
3	$-\sqrt{2}$	0	0	2.05	19
3	0	0	0	5.15	18
3	0	0	$\sqrt{2}$	4.14	17
2	1	-1	1	3.45	16
2	0	0	0	4.7	14
1	0	0	0	5.59	1
1	0	0	0	5.13	2
1	-1	-1	1	3.08	3
1	0	0	0	5.25	4
1	1	1	1	3.18	5
1	1	-1	-1	3.4	6
1	0	0	0	5.1	7
1	-1	1	-1	2.43	8
2	-1	-1	-1	3.17	9
2	0	0	0	4.54	10
2	0	0	0	5.14	11
2	-1	1	1	2.2	12
2	0	0	0	4.69	13
2	1	1	-1	3.11	15

Table 5.7. The relative error according to each swap with their iteration.

Iteration	Swap	Relative Error
1	21	0.27
<b>2</b>	<b>44</b>	<b>0.05</b>
3	63	0.22
4	82	0.1
5	85	0.13
6	100	0.18
7	103	0.24
<b>8</b>	<b>119</b>	<b>0.16</b>
9	120	0.19
10	138	0.15
11	139	0.25
12	151	0.2
13	167	0.31
14	168	0.32
<b>15</b>	<b>180</b>	<b>0.07</b>
<b>16</b>	<b>183</b>	<b>0.05</b>
<b>17</b>	<b>184</b>	<b>0.05</b>
18	236	0.26
19	239	0.23
20	244	0.21
21	245	0.38
22	246	0.39
23	251	0.29
24	254	0.34
25	258	0.09
<b>26</b>	<b>259</b>	<b>0.06</b>
27	263	0.14
<b>28</b>	<b>265</b>	<b>0.08</b>
29	268	0.17
30	272	0.11
31	273	0.12

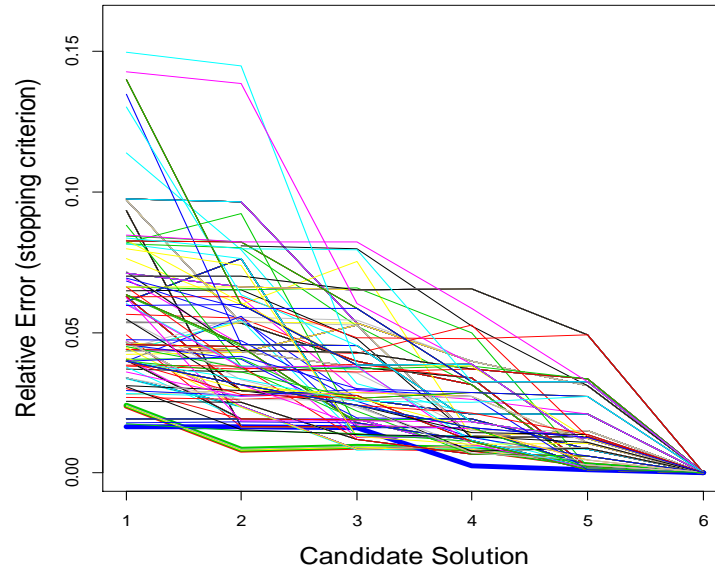


Figure 5.4. The dynamic of default design points with respect to the second-order model.

As seen from Figure 5.4 the three candidates solution that have a minimum relative error with blue, green and red bold colors are associated with swapping 44, 183, and 184.

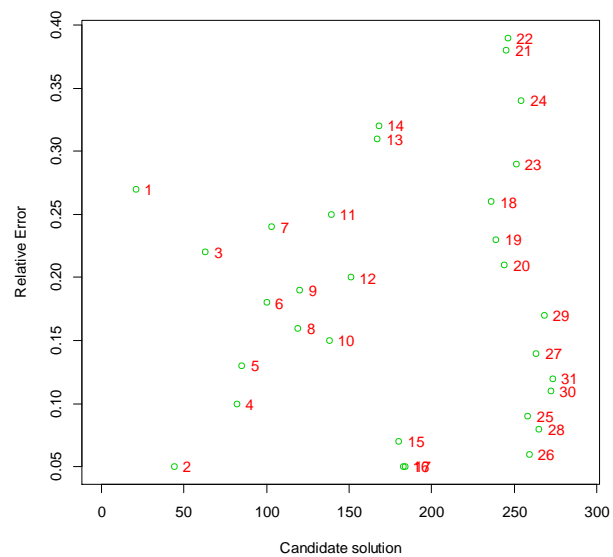


Figure 5.5. The candidate solution with the relative error.

Metaheuristics is employed in this chapter to search for a near- optimal solution. The neighboring trial move (or swap) within the three blocks (*cube*, *foldover*, and *star*) is utilized to search for the best neighborhood candidate solution. The neighborhood search moves from the current candidate solution to the best neighboring trial solution at each iteration (at each swap) by occasionally allowing a non-improving swap when an improving swap is not available. In summary, according to these the candidate solutions (permutations 44, 183, and 184) which have a minimum relative error (0.05) as it can be seen from Figure 5.5, as well as the swapping 180, 256, and 259 that have following minimum relative errors (0.06, 0.07, and 0.08), respectively. All these candidate solutions (swaps with minimum relative error) should start with the axial points (*star*) rather than the corner points with respect to the fitted quadratic model. This is reasonable because CCDs provide high quality predictions over the entire design space while requiring (*star* point) variables settings outside the region of variables in the factorial design. Notably, when it is possible to run the CCD before starting a factorial analysis, factor regions can be reduced to ensure the  $\pm\alpha$  for each encoded variable exists according to reasonable (feasible) levels. It would seem to be a good starting point to run a CCD based on the organic solar cell data, but we cannot make such a generalization based on a random dataset without theoretical justifications from mathematics and statistics or by considering various scenarios via simulations.

Finally, in last chapter, we will discuss the recent development of RSM.



## CHAPTER 6

### RECENT DEVELOPMENT OF RESPONSE SURFACE METHODOLOGY

In this chapter, we briefly explore to recent development of response surface methodology, multivariate response surface optimization, robust parameter design, and generalized linear models.

#### **6.1 Multivariate response optimization**

In most response surface designs, the problem is to find the optimum operating conditions for a single response. However, in some cases, the researchers are interested in optimizing multivariate responses simultaneously. In this case, the simplest method is a visual inspection. The surfaces can be investigated in order to find the design space that optimizes the entire responses studies [44, 45].

It has been shown to be significantly more challenging to find the operating conditions that will simultaneously optimize all responses when the optimum values for each response are located in different regions. The difficulty of this process increases if the optimum conditions become more faraway from each other and fail to overlap. In fact, it is not unusual to observe the cases where the response surfaces found do not present an optimal regarding the same design region. Thus, changes in one factor's level can improve one particular response, while also having a significant negative impact on another response. One method for resolving such problem of the optimization of multivariate responses is by using a multi-criteria methodology. This criteria is employed whenever multiple responses to be considered simultaneously. The Derringer function, also known as the desirable function [46], is the most frequently employed multi-criteria methodology in optimizing an analytical process. This method is primarily based on the

calculation of a desirable function for each response individually. Essentially, the stately properties for every response are changed into a dimensionless of individual desirable function ( $d_i$ ) scale. Based on these individual desirable functions, an analysis may introduce the conditions that each individual response must meet throughout the measured process. The scale of each desirable function lies between  $d = 0$ , for a fully undesired response, and  $d = 1$ , for a completely desirable response; anything out this rating would not be importance to the analyst. This method allows us combining the results attained for the properties that are measured through changed orders of scale. Now that we have obtained the individual desirable functions, it is possible to find the overall desirable ( $D$ ). The overall desirable function  $D$  is a weighted geometric mean of each individual desirable function ( $d_i$ ), as follows:

$$D = \sqrt[m]{d_1 d_2 \dots d_m}$$

where  $m$  represents the number of responses studied. Thus, the simultaneous optimization procedure is reduced so that we may obtain the levels of independent variables which demonstrate maximum overall desirability.

There are different types of transformation are potential to obtain the individual desirable function. As such, when ( $T$ ) the target value for the response  $y$  is to be a maximized, the individual desirable function is given

$$d = \begin{cases} 0 & ; y < L \\ \left(\frac{y-L}{T-L}\right)^s & ; L \leq y \leq T \\ 1 & ; y > T \end{cases}$$

where  $L$  is the lower accepting value to the response surface and  $s$  represents the weight. Thus, when  $s = 1$ , the desirable function is linear. In case of  $s > 1$  major significance is given to the points that is near the target value. When  $s < 1$ , it would have no importance to the analyst.

When response  $y$  is to be minimized, though, desirable function ( $d$ ) is given

$$d = \begin{cases} 1 & ; y < T \\ \left(\frac{U-y}{U-T}\right)^t & ; T \leq y \leq U \\ 0 & ; y > U \end{cases}$$

where  $U$  is the upper accepting value to the response and  $t$  represents the weight. The same principle for  $s$  is also applied to  $t$ . If the target value ( $T$ ) is filled among  $L$  and  $U$ , then, a two-sided desirable function must be utilized. This function is as follows:

$$d = \begin{cases} 0 & ; y < L \\ \left(\frac{y-L}{T-L}\right) & ; L \leq y \leq T \\ \left(\frac{U-Y}{U-T}\right)^t & ; T \leq y \leq U \\ 0 & ; y > U \end{cases}$$

As we have previously shown,  $t$  and  $s$  control the variation rate of the desirable functions.

## 6.2 Robust parameter design

Robust parameter design is a technique to produce realization events that focuses on selecting the settings of independent variables in a process. Firstly, it ensures that the average of the response variable has achieved a desirable level. Secondly, it confirms that

the variability nearby this level is minimized. This technique was developed by Genichi Taguchi.

### **6.2.1 Taguchi's approach**

Robust parameter design is a technique developed in order to improve the quality of the yield by studying the robustness of the variability that caused by the uncontrollable factors occur in the production procedure. Genichi Taguchi introduced parameter design in US during the 1980s, a several studies have been published, such as Kackar [47], Taguchi and Wu [48], Taguchi [49], Nair and shoemaker [50] as well as a textbooks authored by Khuri and Cornell, and Taguchi [51] , Phadke [52], and others. There were two types of process variables; the first are the independent variables which are under control, and the second are uncontrollable variables that in general the reason of the variations in a production system. The main purpose of studying the parameter robustness is to identify the levels of the independent variables that the response of the process is robust to the variability in the process, the variability that caused by uncontrollable variables. In order to reach such goal, Taguchi supported using the crossed arrays, a process achieved by crossing the orthogonal runs of independent variables with the noise factors.

Through this method, Taguchi was able to identify three specific goals in an experiment:

- i. The smaller, the better that will minimize the response.
- ii. The larger, the better that will maximize the response.
- iii. Achieving a specific target.

Based on the signal-to-noise ratio ( $S/N$ ), the three goals are defined as follows:

- i. The smaller is better;  $-10 \log \left[ \frac{1}{n} \sum_{i=1}^n y_i^2 \right]$ .
- ii. The larger, the better;  $-10 \log \left[ \frac{1}{n} \sum_{i=1}^n \frac{1}{y_i^2} \right]$ .
- iii. The target is achieved (the best)  $-10 \log \left( \frac{s^2}{\bar{y}^2} \right)$  where  $y_i$  is response values,  $\bar{y}$  is the sample mean and  $s^2$  is the sample variance.

All the three  $S/N$  ratios must be maximized. Taguchi method in more details were discussed by Myers and Montgomery [3], Box [53, 54], Easterling [55], Pignatiello and Ramberg [56], Nair and Pregibon[57], and Nair [58].

### 6.3 Generalized linear models

Generalized linear models (GLMs) are extensions of the general linear models (example, regression and standard ANOVA models). GLMs developed by Nelder and Wedderburn [59]. For further details, see for example McCullagh and Nelder [60], and more books by Lindsey [61], Dobson [62], McCulloch and Searle[63] and Agresti [64]. Typically, the response variable in GLMs is assumed to follow a distribution from an exponential family [60]. The mean response is modeled as

$$g(\mu) = \mathbf{X}^T \boldsymbol{\beta}$$

where  $g$  is link function (it can be logit or log),  $\mathbf{X}$  is the design matrix, and  $\boldsymbol{\beta}$  is a vector of regression coefficient, which usually estimated using MLE method. A well-designed equation is the one that has a small prediction variance or small mean square error of the prediction [65]. However, these criteria for the GLMs are dependent on the unknown parameters of the fitted model. So, a prior knowledge of these parameters is required in order to minimize the criteria [66]. We will now explore some solutions to these issues.

### 6.3.1 Local optimum designs

GLMs designs are dependent upon the unknown parameters of the fitted equation. Because of this dependency, a prior knowledge of the parameters is required in order to calculate these equations. Optimal measure, such as  $D$ -optimality or  $A$ -optimality, is called locally optimum. These designs involve optimization criteria that minimize the variance of the regression coefficients for a pre-specified model, as well as select the design runs that maximize the determinant of  $\mathbf{X}^T \mathbf{X}$  [67].

### 6.3.2 Sequential designs

This technique does not stop at the initial step, the estimates of the unknown parameters are repeated and used to obtain an additional design runs that the process will converge with respect to some optimality manner, such as,  $D$ -optimality [68-70].

### 6.3.3 Robust design technique

This method is a minimax approach that often used in order to acquire designs which are robust in relation to a weak estimation of the initial parameters. When using this technique,  $D$ -optimality and Fieller confidence intervals for the median response dose are used in order to construct optimality functions for these procedures [7, 71].

Several recent works have been published regarding GLMs, including Dror and Steinberg [72], Woods et al. [73], and Russell et al. [74]. These studies concentrated on GLMs that contains multiple independent variables, while the previous studies discussed design issues found in GLMs with solely surface response. There was not much work has been done to understand multivariate GLMs, specifically designing such models. The models using multiple responses can be investigated for each level of a group of controllable factors; they are also considered when multiple responses are sufficiently

represented by GLMs. More discussion and analysis of multiple response models for GLMs have been published by McCullagh and Nelder [60], and Fahrmeir and Tutz [75].

Some authors have studied optimal designs as a key to multivariate GLMs [76, 77]. In fact, Heise and Myers [76] studied bivariate logistic regression in the pursuit of optimal design, whereas Zocchi and Atkinson's [77] work is based on optimum designs for multinomial logistic models. More recently, Mukhopadhyay and Khuri [78] compared designs for multiple response GLMs through use of quantile dispersion graphs. The optimization issue in a GLMs application unable to improve closely to the linear models. In case of using a single response approach with GLMs, Paul and Khuri used modification of rising ridge analysis in order to optimize the response [79]. Moreover, Paul and Khuri [79] optimized the linear variables rather than optimizing the mean response. Mukhopadhyay and Khuri [80] decided to use the generalized distance approach; a technique, which was initially developed for multiple response GLMs, that optimized several linear response surface models simultaneously. They used this technique to effectively optimize a multivariate GLM situation and also studied the mean as a function of both the inner and the noise variables, while the variance was a function of the independent variables only. Engel and Huele [81] followed single response model of Myers et al. [82], assuming the existence of non-constant error variances. In their work, the variance was based on both the non-controllable factors and the residual variance. They modeled the residual variance through the use of an exponential model, in order to guarantee non negative variance estimates; a model which was formerly utilized by Box and Meter [83], Grego [84], Chan and Mak [85].

## CHAPTER 7

## DISCUSSION AND CONCLUSION

**7.1 Discussion and conclusions**

Optimization of organic solar cells is one of the greatest challenges in organic photovoltaics (OPV) technology. Several mathematical tools were introduced in order to simplify and understand the solar cell performance. In this work, one of our objectives was to find the optimum polymer solar cell performance using a statistical model. RSM is employed to find the optimum device structure of organic polymer solar cell. The central composite design for a second-order model was used with three independent variables, namely polymer concentration, polymer-fullerene ratio, and active layer spinning speed. Optimal device performance was achieved using 10.25 mg/ml polymer concentration, 0.42 polymer-fullerene ratio, and 1624 rpm of active layer spinning speed. The efficiency at the optimum stationary point was found to be 5.23% for the Poly(diketopyrrolopyrrole-terthiophene) (PDPP3T)/PC<sub>60</sub>BM solar cells. Moreover, 97% of the variation in the device performance was explained by quadratic model, which might help in approaching the optimum device performance efficiently. The solar cell experimental results are consistent with the CCD prediction, which proves that this is a promising and appropriate model for optimum device performance and fabrication conditions as well as the RSM was very useful in precisely optimizing solar device performance. We recommend RSM approach for future use to reduce cost and time. The ad-hoc technique used 60 experiments whereas CCD required only 24 experiments.



Canonical analysis was performed to explore the fitted second-order response surface. This method is useful to identify rising ridge behavior. Studying whether a ridge is rising ridge or stationary is useful to decide about how to continue for setting the process variables or explore in the response surface. To determine if the ridge is stationary or rising is by checking whether the stationary point of the fitted quadratic model falls inside the design space, if this stationary point is within the design region, then there is suggestion of stationary in a response surface (no rising ridge) because there is no direction of improvement out of the design region. Also, a ridge identification can be studied using the double linear regression (DLR) method for estimating the standard error of the eigenvalues. Then we construct the confidence intervals of the eigenvalues. The eigenvalues whose confidence intervals contain zero, suggest of rising ridge. For the organic solar cell, the confidence intervals for the first two the eigenvalues are clearly negative, and the surface show that the confidence interval of the eigenvalue  $\lambda_3$  contains zero which might be an indication of rising ridge with surface.

Simultaneous inference for the location of a stationary point in quadratic response surface model was addressed by constructing confidence regions and developing methods for construct rectangular simultaneous confidence intervals for the stationary point. Simulation is used to compare the coverage probabilities of the Bonferroni adjusted confidence intervals, the plug-in approach, and the bootstrap. The estimates of coverage probabilities for the three methods of constructing simultaneous confidence intervals for the location of the stationary point with various scenarios shown that the estimates of the coverage probabilities are the largest for the Bonferroni SCI followed by the plug-in

approach. For the Bonferroni and plug-in approaches, the estimates of the coverage probabilities as the sample size increases are pretty close to the nominal levels of 0.95.

Metaheuristic approach is employed in order to find an alternative order to the design point. Based on this technique, starting at the star point is an alternative better solution instead of starting at the corner point. This is reasonable because of CCDs provide high quality of predictions over the entire design space at the star points for the region of variables in factorial design.

## **7.2 Future research**

This research can be extended in a couple of ways. The first theoretical problem of interest relates to further simultaneous inferences on the stationary point of a quadratic response surface model. The second theoretical problem is the justification of the metaheuristic approach using simulation techniques or theoretical considerations.

## REFERENCES

- [1] T. Lundstedt, E. Seifert, L. Abramo, B. Thelin, Å. Nyström, J. Pettersen, R. Bergman, Experimental design and optimization, *Chemometrics and intelligent laboratory systems*, 42 (1998) 3-40.
- [2] G.E. Box, K. Wilson, On the experimental attainment of optimum conditions, *Journal of the Royal Statistical Society. Series B (Methodological)*, 13 (1951) 1-45.
- [3] R.H. Myers, D.C. Montgomery, and C.M. Anderson-Cook, *Response surface methodology: process and product optimization using designed experiments*, John Wiley & Sons., (2009).
- [4] D.C. Montgomery, *Design and analysis of experiments*, John Wiley & Sons, 2017.
- [5] M.A. Bezerra, R.E. Santelli, E.P. Oliveira, L.S. Villar, L.A. Escaleira, Response surface methodology (RSM) as a tool for optimization in analytical chemistry, *Talanta*, 76 (2008) 965-977.
- [6] R. Suliman, A.F. Mitul, L. Mohammad, G.D. Djira, Y. Pan, Q. Qiao, Modeling of organic solar cell using response surface methodology, *Results in Physics*, (2017).
- [7] A.I. Khuri, S. Mukhopadhyay, *Response surface methodology*, Wiley Interdisciplinary Reviews: Computational Statistics, 2 (2010) 128-149.
- [8] D.L. Massart, B.G. Vandeginste, L. Buydens, P. Lewi, J. Smeyers-Verbeke, *Handbook of chemometrics and qualimetrics: Part A*, Elsevier Science Inc., 1997.
- [9] G.E. Box, D.W. Behnken, Some new three level designs for the study of quantitative variables, *Technometrics*, 2 (1960) 455-475.
- [10] A.I. Khuri, J.A. Cornell, *Response surfaces: designs and analyses*, CRC press, 1996.
- [11] D.H. Doehlert, Uniform shell designs, *Applied statistics*, (1970) 231-239.

- [12] G.E. Box, J.S. Hunter, Multi-factor experimental designs for exploring response surfaces, *The Annals of Mathematical Statistics*, (1957) 195-241.
- [13] A. Khuri, A measure of rotatability for response-surface designs, *Technometrics*, 30 (1988) 95-104.
- [14] N.R. Draper, F. Pukelsheim, Another look at rotatability, *Technometrics*, 32 (1990) 195-202.
- [15] Y. Liang, Z. Xu, J. Xia, S.T. Tsai, Y. Wu, G. Li, C. Ray, L. Yu, For the bright future—bulk heterojunction polymer solar cells with power conversion efficiency of 7.4%, *Advanced Materials*, 22 (2010).
- [16] G. Li, R. Zhu, Y. Yang, Polymer solar cells, *Nat Photon*, 6 (2012) 153-161.
- [17] V. Gupta, A.K.K. Kyaw, D.H. Wang, S. Chand, G.C. Bazan, A.J. Heeger, Barium: An Efficient Cathode Layer for Bulk-heterojunction Solar Cells, *Sci. Rep.*, 3 (2013).
- [18] B.C. Thompson, J.M.J. Fréchet, Polymer–Fullerene Composite Solar Cells, *Angewandte Chemie International Edition*, 47 (2008) 58-77.
- [19] Q.K. Beg, V. Sahai, R. Gupta, Statistical media optimization and alkaline protease production from *Bacillus mojavensis* in a bioreactor, *Process Biochemistry*, 39 (2003) 203-209.
- [20] S.P.J. Namal Senanayake, F. Shahidi, Lipase-catalyzed incorporation of docosahexaenoic acid (DHA) into borage oil: optimization using response surface methodology, *Food Chemistry*, 77 (2002) 115-123.
- [21] G.S.N. Naidu, T. Panda, Performance of pectolytic enzymes during hydrolysis of pectic substances under assay conditions: a statistical approach, *Enzyme and Microbial Technology*, 25 (1999) 116-124.

- [22] O. Corzo, E.R. Gomez, Optimization of osmotic dehydration of cantaloupe using desired function methodology, *Journal of Food Engineering*, 64 (2004) 213-219.
- [23] D. Baş, İ.H. Boyacı, Modeling and optimization I: Usability of response surface methodology, *Journal of Food Engineering*, 78 (2007) 836-845.
- [24] D. De Faveri, P. Torre, P. Perego, A. Converti, Optimization of xylitol recovery by crystallization from synthetic solutions using response surface methodology, *Journal of Food Engineering*, 61 (2004) 407-412.
- [25] T. Stubhan, I. Litzov, N. Li, M. Salinas, M. Steidl, G. Sauer, K. Forberich, G.J. Matt, M. Halik, C.J. Brabec, Overcoming interface losses in organic solar cells by applying low temperature, solution processed aluminum-doped zinc oxide electron extraction layers, *Journal of Materials Chemistry A*, 1 (2013) 6004-6009.
- [26] R.V. Lenth, Response-Surface Methods in R, using rsm, *Journal of Statistical Software*, 32 (2009) 1-17.
- [27] R.V. Lenth, Surface Plots in the rsm Package, *Education*, 10 (2010) 30.
- [28] R.V. Lenth, Surface Plots in the rsm Package, *Education*, 20 (2010) 30.
- [29] H. Hoppe, N.S. Sariciftci, Morphology of polymer/fullerene bulk heterojunction solar cells, *Journal of Materials Chemistry*, 16 (2006) 45-61.
- [30] E. Del Castillo, *Process optimization: a statistical approach*, Springer Science & Business Media, 2007.
- [31] V. Sambucini, Confidence regions for the stationary point of a quadratic response surface based on the asymptotic distribution of its MLE, *Statistics and Computing*, 22 (2012) 739-751.
- [32] G. Casella, R.L. Berger, *Statistical inference*, Duxbury Pacific Grove, CA, 2002.

- [33] G.D. Djira, M. Hasler, D. Gerhard, F. Schaarschmidt, Inferences for ratios of coefficients in the general linear model, 2008.
- [34] D.R. Hare, J.D. Spurrier, Simultaneous inference for ratios of linear combinations of general linear model parameters, *Biometrical Journal*, 49 (2007) 854-862.
- [35] C.S. Locke, An exact confidence interval from untransformed data for the ratio of two formulation means, *Journal of Pharmacokinetics and Pharmacodynamics*, 12 (1984) 649-655.
- [36] G.O. Zerbe, On Fieller's theorem and the general linear model, *The American Statistician*, 32 (1978) 103-105.
- [37] M.H. Kutner, C. Nachtsheim, J. Neter, *Applied linear regression models*, McGraw-Hill/Irwin, 2004.
- [38] B.E. Ankenman, Identifying rising ridge behavior in quadratic response surfaces, *IIE Transactions*, 35 (2003) 493-502.
- [39] S. Bisgaard, B. Ankenman, Standard errors for the eigenvalues in second-order response surface models, *Technometrics*, 38 (1996) 238-246.
- [40] G.J.L. Frederick S. Hillier, *introduction to operation research 9th ed* McGraw-Hill, (2010 ).
- [41] C. Blum, A. Roli, Metaheuristics in combinatorial optimization: Overview and conceptual comparison, *ACM Computing Surveys (CSUR)*, 35 (2003) 268-308.
- [42] L. Bianchi, M. Dorigo, L.M. Gambardella, W.J. Gutjahr, A survey on metaheuristics for stochastic combinatorial optimization, *Natural Computing*, 8 (2009) 239-287.
- [43] F.A. Graybill, *Theory and application of the linear model*, Cengage Learning, (2000).

- [44] R.E. Bruns, I.S. Scarminio, B. de Barros Neto, Statistical design-chemometrics, Elsevier, 2006.
- [45] E. Sivertsen, F. Bjerke, T. Almøy, V. Segtnan, T. Næs, Multivariate optimization by visual inspection, Chemometrics and intelligent laboratory systems, 85 (2007) 110-118.
- [46] T.E. Murphy, K.-L. Tsui, J.K. Allen, A review of robust design methods for multiple responses, Research in Engineering Design, 15 (2005) 201-215.
- [47] R.N. Kacker, Off-line quality control, parameter design, and the Taguchi method, in: Quality Control, Robust Design, and the Taguchi Method, Springer, 1989, pp. 51-76.
- [48] G. Taguchi, Quality engineering in Japan, Communications in Statistics-Theory and Methods, 14 (1985) 2785-2801.
- [49] G. Taguchi, System of experimental design: engineering methods to optimize quality and minimize costs, UNIPUB/Kraus International Publications, 1987.
- [50] V.N. Nair, A.C. Shoemaker, The role of experimentation in quality engineering: a review of Taguchi's contributions, Statistical design and analysis of industrial experiments, (1990) 247-277.
- [51] G. Taguchi, Introduction to quality engineering. White Plains, NY: Unipub, (1986) 21-22.
- [52] M.S. Phadke, Quality Engineering Using Robust Design, PTR Prentice-Hall, Inc., Englewood Cliffs, NJ, (1989).
- [53] G.E. Box, Discussion of off-line quality control, parameter design and the Taguchi methods, Journal of Quality Technology, 17 (1985) 189-190.
- [54] G. Box, Signal-to-noise ratios, performance criteria, and transformations, Technometrics, 30 (1988) 1-17.

- [55] R. Easterling, Discussion of off-line quality control, parameter design, and the Taguchi method, *Journal of Quality Technology*, 17 (1985) 191-193.
- [56] J.J. Pignatiello, J.S. Ramberg, Discussion of off-line quality control, parameter design, and the Taguchi method, *Journal of Quality Technology*, 17 (1985) 198-206.
- [57] V.N. Nair, D. Pregibon, Analyzing dispersion effects from replicated factorial experiments, *Technometrics*, 30 (1988) 247-257.
- [58] V.N. Nair, B. Abraham, J. MacKay, G. Box, R.N. Kacker, T.J. Lorenzen, J.M. Lucas, R.H. Myers, G.G. Vining, J.A. Nelder, Taguchi's parameter design: a panel discussion, *Technometrics*, 34 (1992) 127-161.
- [59] J. Nelder, R. Wedderburn, Generalized linear models. *JR Statist. Soc. A* 135, 370-384. Nelder370135J. R, *Statist. Soc A*, 1972 (1972).
- [60] P. McCullagh, J.A. Nelder, *Generalized Linear Models*, no. 37 in *Monograph on Statistics and Applied Probability*, in, Chapman & Hall, 1989.
- [61] J.K. Lindsey, *Applying generalized linear models*, Springer Science & Business Media, 2000.
- [62] D. AJ, *An Introduction to Generalized Linear Models*, 2nd ed. Boca Raton: Chapman and Hall, (2001).
- [63] S.S. McCulloch CE, *Generalized, Linear, and Mixed Models*, New York: John Wiley & Sons, (2001).
- [64] A. Agresti, M. Kateri, Categorical data analysis, in: *International encyclopedia of statistical science*, Springer, 2011, pp. 206-208.



- [65] A.I. Khuri, S. Mukhopadhyay, GLM designs: the dependence on unknown parameters dilemma, *Response surface methodology and related topics*. World Scientific, Singapore, (2006) 203-240.
- [66] A.I. Khuri, B. Mukherjee, B.K. Sinha, M. Ghosh, Design issues for generalized linear models: A review, *Statistical Science*, (2006) 376-399.
- [67] T. Mathew, B.K. Sinha, Optimal designs for binary data under logistic regression, *Journal of Statistical Planning and Inference*, 93 (2001) 295-307.
- [68] C.J. Wu, Efficient sequential designs with binary data, *Journal of the American Statistical Association*, 80 (1985) 974-984.
- [69] R.R. Sitter, B. Forbes, Optimal two-stage designs for binary response experiments, *Statistica Sinica*, (1997) 941-955.
- [70] R. Sitter, C. Wu, Two-Stage Design of Quantal Response Studies, *Biometrics*, 55 (1999) 396-402.
- [71] R.R. Sitter, Robust designs for binary data, *Biometrics*, (1992) 1145-1155.
- [72] H.A. Dror, D.M. Steinberg, Robust experimental design for multivariate generalized linear models, *Technometrics*, 48 (2006) 520-529.
- [73] D. Woods, S. Lewis, J. Eccleston, K. Russell, Designs for generalized linear models with several variables and model uncertainty, *Technometrics*, 48 (2006) 284-292.
- [74] K.G. Russell, D.C. Woods, S. Lewis, J. Eccleston, D-optimal designs for Poisson regression models, *Statistica Sinica*, (2009) 721-730.
- [75] L. Fahrmeir, G. Tutz, Models for multicategorical responses: Multivariate extensions of generalized linear models, in: *Multivariate Statistical Modelling Based on Generalized Linear Models*, Springer, 2001, pp. 69-137.

- [76] M.A. Heise, R.H. Myers, Optimal designs for bivariate logistic regression, *Biometrics*, (1996) 613-624.
- [77] S.S. Zocchi, A.C. Atkinson, Optimum experimental designs for multinomial logistic models, *Biometrics*, 55 (1999) 437-444.
- [78] S. Mukhopadhyay, A. Khuri, Comparison of designs for multivariate generalized linear models, *Journal of Statistical Planning and Inference*, 138 (2008) 169-183.
- [79] A. Khuri, R.H. Myers, Modified ridge analysis, *Technometrics*, 21 (1979) 467-473.
- [80] S. Mukhopadhyay, A.I. Khuri, Optimization in a multivariate generalized linear model situation, *Computational Statistics & Data Analysis*, 52 (2008) 4625-4634.
- [81] J. Engel, A.F. Huele, A generalized linear modeling approach to robust design, *Technometrics*, 38 (1996) 365-373.
- [82] R.H. Myers, A.I. Khuri, G. Vining, Response surface alternatives to the Taguchi robust parameter design approach, *The American Statistician*, 46 (1992) 131-139.
- [83] G.E. Box, R.D. Meyer, Dispersion effects from fractional designs, *Technometrics*, 28 (1986) 19-27.
- [84] J.M. Grego, Generalized linear models and process variation, *Journal of Quality Technology*, 25 (1993) 288-288.
- [85] L. Chan, T. Mak, A regression approach for discovering small variation around a target, *Applied statistics*, (1995) 369-377.

## APPENDIX A

## Code for organic solar cell data

```
##### Organic polymer solar cell #####  
  
install.packages("rsm")  
  
library(rsm)  
  
set.seed(123)  
  
cube= cube(~ x1 + x2, x3 ~ x1 * x2, n0 = 4,  
  
coding = c(x1 ~ (concentration - 10)/3.5, x2 ~ (ratio - .5)/.085, x3 ~ (speed - 1600)/400))  
  
as.data.frame(cube)  
  
par(mfrow=c(1,2))  
  
varfcn(cube, ~ FO(x1,x2,x3))  
  
varfcn(cube, ~ FO(x1,x2,x3), contour = TRUE)  
  
cube$efficiency= c(5.59,5.13,3.08,5.25,3.18,3.4,5.10,2.43)  
  
anal1 = rsm(efficiency~ FO(x1,x2,x3), data=cube)  
  
summary(anal1)  
  
set.seed(123)  
  
foldover= foldover(cube, variable = "x1")
```

```

foldover$efficiency=c(3.17,4.54,5.14,2.2,4.69,4.7,3.11,3.45)

anal2 = rsm(efficiency~ Block + FO(x1,x2,x3), data = djoin(cube,foldover))

summary(anal2)

set.seed(123)

star= star(cube, n0 = 2, alpha = "orthogonal")

par(mfrow=c(1,2))

comb = djoin(cube, foldover, star)

varfcn(comb, ~ Block + SO(x1,x2,x3))

varfcn(comb, ~ Block + SO(x1,x2,x3), contour = TRUE)

star$efficiency=c(4.14,5.15,2.05,3.48,4.28,3.51,5.10,5.4)

anal5 = rsm(efficiency~ Block + SO(x1,x2,x3), data = djoin(cube, foldover, star))

summary(anal5)

##### Bootsrap for organic solar cell #####

fits = predict(anal5)

resids = resid(anal5)

boot.raw = replicate(1000, xs(update(anal5, fits + sample(resids, replace=TRUE) ~ .)))

boot = code2val(as.data.frame(t(boot.raw)), codings=codings(anal5))

```

```

par(mfrow = c(1,3))

plot(ratio ~ concentration, data = boot, col = "blue"); points( 10.3465404, 0.4171534, col
= "red", pch = 7 , xlim=c(0,12),ylim=c(-2,2))

plot(speed ~ concentration, data = boot, col = "blue"); points( 10.3465404,
1624.2459681, col = "red", pch = 7, xlim=c(0,12),ylim=c(1000,2000))

plot(speed ~ ratio, data = boot, col = "blue"); points(0.4171534, 1624.2459681, col =
"red", pch = 7, xlim=c(-2,2),ylim=c(1000,2000))

##### Contour plot for organic solar cell #####

png.hook <- list()

png.hook$pre.plot <- function(lab)

png(file = paste(lab[3], lab[4], ".png", sep = ""))

png.hook$post.plot = function(lab)

dev.off()

contour (anal5, ~x1+x2+x3, image = TRUE, at = xs, hook = png.hook)

par(mfrow = c(1,3))

persp (anal5, ~ x1+x2+x3, at = xs,

col = rainbow(50), contours = "colors")

##### Design space for solar cell data #####

par(mfrow=c(1,3))

```

```

contour(anal5, x1 ~ x2, bounds = list(x1=c(-8,8), x2=c(-10,10)),
      zlim=c(-100,100), col="gray", decode = FALSE);points( -0.97466554,0.09901154
, col = "blue", pch = 7, lwd=2)

lines(c(-1,1,1,-1,-1), c(-1,-1,1,1,-1), col="red") # design region

points(x1 ~ x2, data=canonical.path(anal5), col="gray", pch=1+7*(dist==0))

contour(anal5, x1 ~ x3, bounds = list(x1=c(-8,8), x3=c(-10,10)),
      zlim=c(-100,100), col="gray", decode = FALSE);points(0.06061492,0.09901154 ,
col = "blue", pch = 7,lwd=2)

lines(c(-1,1,1,-1,-1), c(-1,-1,1,1,-1), col="red") # design region

points(x1 ~ x3, data=canonical.path(anal5), col="gray", pch=1+7*(dist==0))

contour(anal5, x2 ~ x3, bounds = list(x2=c(-15,15), x3=c(-12,12)),
      zlim=c(-100,100), col="gray", decode = FALSE);points( 0.06061492 , -0.97466554
, col = "blue", pch = 7,lwd=2)

lines(c(-1,1,1,-1,-1), c(-1,-1,1,1,-1), col="red") # design region

points(x2 ~ x3, data=canonical.path(anal5), col="gray", pch=1+7*(dist==0))

#####

```

## APPENDIX B

## Code for simulation

```
##### Confidence regions for the stationary point with simulation #####
```

```
install.packages("mvtnorm")
```

```
library(mvtnorm)
```

```
install.packages("rsm")
```

```
library(rsm)
```

```
k=2
```

```
alpha = 0.05
```

```
XS=c(-0.1716,-0.1806)
```

```
x1=c(-1,1,-1,1,-1.414,1.414,0,0,0,0)
```

```
x2=c(-1,-1,1,1,0,0,-1.414,1.414,0,0)
```

```
x1x2 = x1*x2
```

```
x1sqr = x1^2
```

```
x2sqr = x2^2
```

```
Xsub1=x1-XS[1]
```

```
Xsub2=x2-XS[2]
```

```
A=matrix(c(-2.78112, -0.77500/2, -0.77500/2, -2.52355),nr=2)
```

```
y=c(88.55,85.80,86.29,80.44,85.50,85.39,86.22,85.70,90.21,90.85,91.31)
```

```
Combined=matrix(c(Xsub1,Xsub2),nr=2)
```

```
mod2=rsm(y ~ SO(x1,x2))
```

```
summary(mod2)
```

```
coef(mod2)
```

```
X1 = matrix(c((x1-0.1716275)^2,(x2-0.1806102)^2),nr=11)
```

```
X2 = matrix(c((x1-0.1716275)*(x2-0.1806102)),nr=11)
```

```
I = rep(1,11)
```

```
XZ=matrix(c(I,X1,X2),nr=11)
```

```
M5=2*A%%Combined # M matrix ###
```

```
Sigma = 3.1635
```

```
M6=M5%%t(M5)-M5%%XZ%%solve(t(XZ)%XZ)%t(XZ)%t(M5)
```

```
V= solve(solve(M6)*sigma)
```

```
B = coef(mod2)
```

```
vcov.b = vcov(mod2)
```

```
par(mfrow=c(1,1))
```



L = -1.8

U = 1.8

Grid =100

t1= seq(L,U, length=grid)

t2 = t1

Fcritical = 2\*qt(1-alpha,2,5)

plot(0,0, col="white", xlim=c(L,U), ylim=c(L,U), xlab="Xs1", ylab="Xs2", )

points( -0.17,-0.18 , col = "blue", pch = 7, lwd=2)

for (i in 1:grid) {

for(j in 1:grid) {

d1=-1.095 - 5.562\*t1[i]- 0.775\*t2[j]

d2=-1.045-0.775\*t1[i]-5.048\*t2[j]

d=c(d1,d2)

var1=3.1635\*(1/8 +4\*t1[i]\*t1[i]\*0.1772+t2[j]\*t2[j]/(4))

var2=3.1635\*(1/8+ t1[i]\*t1[i]/(4) + 4\*t2[j]\*t2[j]\*0.1772)

cov12=3.1635\*(4\*0.0521\*t1[i]\*t2[j] + t1[i]\*t2[j]/(4))

vard=matrix(c(var1,cov12,cov12,var2), nc=2)

```

if (t(d)%%solve(vard)%%d <= Fcritical){

points(t1[i], t2[j], pch=".", cex=3, col="blue")

}

}

}

lables=c("Bonf", "plug-in", "boot")

legend("bottomleft",lables, lwd=2, col=c("red","green", "purple"), lty=c(6,3,2))

##### Asymptotic confidence region #####

for (i in 1:grid) {

for(j in 1:grid) {

d1=t1[i]-XS[1]

d2=t2[j]-XS[2]

d=c(d1,d2)

if (t(d)%%V%%d <= Fcritical){

points(t1[i], t2[j], pch=".", cex=3, col="gray70")

}

}

}

```

```
}
```

```
##### SCI of Bon & ASY & Boot #####
```

```
##### Variance covariance matrix of stationary point #####
```

```
vcovf.statn <- function (n,b, vcov.b) {
```

```
  b0 = b[1]
```

```
  b1= b[2]
```

```
  b2 = b[3]
```

```
  b12 = b[4]
```

```
  b11 = b[5]
```

```
  b22 = b[6]
```

```
  bottom = 4*b11*b22-(b12^2)
```

```
  dx1s.b0 = 0
```

```
  dx1s.b1= -2*b22/(bottom)
```

```
  dx1s.b2 = b12/(bottom)
```

```
  u1= ((b12^2)*b2)
```

```
  u2=-4*b22*b1*b12
```

```
  u3=4*b22*b2*b11
```

$$u4=(bottom^2)$$

$$u5=u1+u2+u3$$

$$dx1s.b12=u5/u4$$

$$dx1s.b11=-4*b22*(-2*b22*b1+b12*b2)/u4$$

$$w1=(2*b1*(b12^2))$$

$$w2=-4*b12*b2*b11$$

$$w3=w1+w2$$

$$dx1s.b22=w3/u4$$

$$dx2s.b0=0$$

$$dx2s.b1=b12/bottom$$

$$dx2s.b2=-2*b11/bottom$$

$$v1=4*b1*b11*b22$$

$$v2=((b12^2)*b1)$$

$$v3=-4*b12*b11*b2$$

$$v4=v1+v2+v3$$

$$dx2s.b12=v4/u4$$

$$q1=2*(b12^2)*b2$$

$$q2 = -4 * b12 * b1 * b22$$

$$q3 = q1 + q2$$

$$dx2s.b11 = q3 / u4$$

$$t1 = -4 * b11 * (b12 * b1)$$

$$t2 = -4 * b11 * (-2 * b11 * b2)$$

$$t3 = t1 + t2$$

$$dx2s.b22 = t3 / u4$$

$$g1 = dx1s.b0$$

$$g2 = dx1s.b1$$

$$g3 = dx1s.b2$$

$$g4 = dx1s.b12$$

$$g5 = dx1s.b11$$

$$g6 = dx1s.b22$$

$$h1 = dx2s.b0$$

$$h2 = dx2s.b1$$

$$h3 = dx2s.b2$$

$$h4 = dx2s.b12$$

```

h5=dx2s.b11

h6=dx2s.b22

G=matrix(c(g1,h1,g2,h2,g3,h3,g4,h4,g5,h5,g6,h6),nr=2)

vcov.statn=G%*%vcov.b%*%t(G)

}

# end of function

##### Critical point qmvnorm #####

sigma2 = vcovf.statn(n, b,vcov.b )[]

Aysc95=qmvnorm(1- alpha ,corr = cor(sigma2), tail="both" )$quantile

##### Asymptotic with 95% #####

AsySCI1 = -0.1716+c(-1,1)*Aysc95*sqrt(sigma2[1,1])

AsySCI1

AsySCI2 = -0.1806+c(-1,1)*Aysc95*sqrt(sigma2[2,2])

AsySCI2

##### Bonferroni #####

Bonxs1= -0.1716+c(-1,1)*qnorm(1-alpha/(2*k))*sqrt(sigma2[1,1])

Bonxs1

```

```
Bonxs2= -0.1806 +c(-1,1)*qnorm(1-alpha/(2*k))*sqrt(sigma2[2,2])
```

```
Bonxs2
```

```
B = 2000
```

```
Boot.statnp = matrix(numeric(B),nrow=B,ncol=2,byrow = TRUE)
```

```
xs1.boot = rep(NA,B)
```

```
xs2.boot = rep(NA,B)
```

```
sqrt2 = sqrt(2)
```

```
x1= c(-1,1,-1,1,-sqrt2,sqrt2,0,0,0,0,0)
```

```
x2 = c(-1,-1,1,1,0,0,-sqrt2,sqrt2,0,0,0)
```

```
y=c(88.55,85.80,86.29,80.44,85.50,85.39,86.22,85.70,90.21,90.85,91.31)
```

```
fit.quad = lm(y ~ x1 + x2 + x1x2 + x1sqr + x2sqr )
```

```
resid.quad = fit.quad$resid
```

```
x1sqr = x1^2
```

```
x2sqr = x2^2
```

```
x1x2 = x1*x2
```

```
Beta.0 = 90.790
```

```
Beta.1 = -1.095
```

Beta.2 = -1.045

Beta.12 = -0.775

Beta.11 = -2.781

Beta.22 = -2.524

y.hat = Beta.0 + Beta.1\*x1 + Beta.2\*x2 + Beta.12\*x1x2 + Beta.11\*x1sqr +  
Beta.22\*x2sqr

resid.quad = fit.quad\$resid

##### Bootstrap sample #####

for(b in 1:B) {

resid.boot = sample(resid.quad, replace = TRUE)

y.boot= y.hat + resid.boot

fit.quad.boot= lm (y.boot ~ x1 + x2 + x1x2 + x1sqr + x2sqr)

##### Bootstrap for Estimating the stationary point #####

b.boot= fit.quad.boot\$coeff

Boot.vec = c( b.boot[2], b.boot[3])

Boot.mat = 0.5\*matrix (c(2\* b.boot[5], b.boot[4], b.boot[4], 2\* b.boot[6]), nc=2 )

Boot.statnp[b,] = -0.5\*solve(Boot.mat) %\*% Boot.vec



```

}

## End.Boot

xs1.boot = Boot.statnp[,1]

xs2.boot = Boot.statnp[,2]

alpha.adj = alpha/ (2*k)

points(-0.1716, -0.1806, col = "black", pch = 16)

q.boot1= quantile(xs1.boot , c( alpha.adj , 1- alpha.adj ))

q.boot2 = quantile(xs2.boot , c( alpha.adj , 1- alpha.adj ))

segments(q.boot1[1], q.boot2[1], q.boot1[2], q.boot2[1], col = "purple", lwd=2, lty=6)

segments(q.boot1[1], q.boot2[1], q.boot1[1], q.boot2[2], col = "purple",lwd=2, lty=6)

segments(q.boot1[2], q.boot2[1], q.boot1[2], q.boot2[2], col = "purple", lwd=2, lty=6)

segments(q.boot1[1], q.boot2[2], q.boot1[2], q.boot2[2], col = "purple", lwd=2, lty=6)

segments(AsySCI1[1], AsySCI2[1], AsySCI1[2], AsySCI2[1], col = "green", lwd=3, lty=3)

segments(AsySCI1[1], AsySCI2[1], AsySCI1[1], AsySCI2[2], col = "green", lwd=3, lty=3)

segments(AsySCI1[2], AsySCI2[1], AsySCI1[2], AsySCI2[2], col = "green", lwd=3, lty=3)

segments(AsySCI1[1], AsySCI2[2], AsySCI1[2], AsySCI2[2], col = "green", lwd=3, lty=3)

segments(Bonxs1[1], Bonxs2[1], Bonxs1[2], Bonxs2[1], col = "red", lwd=2, lty=2)

```

```
segments(Bonxs1[1], Bonxs2[1], Bonxs1[1], Bonxs2[2], col = "red", lwd=2, lty=2)
```

```
segments(Bonxs1[2], Bonxs2[1], Bonxs1[2], Bonxs2[2], col = "red", lwd=2, lty=2)
```

```
segments(Bonxs1[1], Bonxs2[2], Bonxs1[2], Bonxs2[2], col = "red", lwd=2, lty=2)
```

```
##### Probablity coverage of Bonferroni & plug-in & bootstrap #####
```

```
install.packages("mvtnorm")
```

```
library(mvtnorm)
```

```
install.packages("rsm")
```

```
library(rsm)
```

```
Nsim=10000
```

```
k= 2
```

```
statnp = matrix (rep(NA, 2*Nsim), nc=k)
```

```
eigen.sign = rep(NA,Nsim)
```

```
alpha=0.05
```

```
n=12
```

```
sqrt2 = sqrt(2)
```

```
x1=c(-1,1,-1,1,-sqrt2,sqrt2,0,0,0,0,0)
```

```
x2=c(-1,-1,1,1,0,0,-sqrt2,sqrt2,0,0,0)
```

$$x1sqr = x1^2$$

$$x2sqr = x2^2$$

$$x1x2 = x1*x2$$

$$\text{Beta.0} = 100$$

$$\text{Beta.1} = 0.4$$

$$\text{Beta.2} = 1.6$$

$$\text{Beta.12} = 1$$

$$\text{Beta.11} = -1$$

$$\text{Beta.22} = -2$$

$$\text{Sigma2} = 1$$

$$b.kwn = c(\text{Beta.1}, \text{Beta.2})$$

$$B.kwn = \text{matrix}(c(2*\text{Beta.11}, \text{Beta.12}, \text{Beta.12}, 2*\text{Beta.22}), \text{nc}=2)$$

$$Xs.kwn = -0.5*\text{solve}(B.kwn) \%*\%b.kwn$$

$$Xs.kwn$$

$$\text{eigen}(B.kwn)\$value$$

##### Variance covariance matrix of estimated stationary point #####

```
vcovf.statn <- function (n,b, vcov.b) {
```

$$b0=b[1]$$

$$b1=b[2]$$

$$b2=b[3]$$

$$b12=b[4]$$

$$b11=b[5]$$

$$b22=b[6]$$

$$\text{bottom}=4*b11*b22-(b12^2)$$

$$dx1s.b0=0$$

$$dx1s.b1=-2*b22/(\text{bottom})$$

$$dx1s.b2=b12/(\text{bottom})$$

$$u1=((b12^2)*b2)$$

$$u2=-4*b22*b1*b12$$

$$u3=4*b22*b2*b11$$

$$u4=(\text{bottom}^2)$$

$$u5=u1+u2+u3$$

$$dx1s.b12=u5/u4$$

$$dx1s.b11=-4*b22*(-2*b22*b1+b12*b2)/u4$$

$$w1=(2*b1*(b12^2))$$

$$w2=-4*b12*b2*b11$$

$$w3=w1+w2$$

$$dx1s.b22=w3/u4$$

$$dx2s.b0=0$$

$$dx2s.b1=b12/bottom$$

$$dx2s.b2=-2*b11/bottom$$

$$v1=4*b1*b11*b22$$

$$v2=((b12^2)*b1)$$

$$v3=-4*b12*b11*b2$$

$$v4=v1+v2+v3$$

$$dx2s.b12=v4/u4$$

$$q1=2*(b12^2)*b2$$

$$q2=-4*b12*b1*b22$$

$$q3=q1+q2$$

$$dx2s.b11=q3/u4$$

$$t1=-4*b11*(b12*b1)$$

$$t2 = -4 * b11 * (-2 * b11 * b2)$$

$$t3 = t1 + t2$$

$$dx2s.b22 = t3 / u4$$

$$g1 = dx1s.b0$$

$$g2 = dx1s.b1$$

$$g3 = dx1s.b2$$

$$g4 = dx1s.b12$$

$$g5 = dx1s.b11$$

$$g6 = dx1s.b22$$

$$h1 = dx2s.b0$$

$$h2 = dx2s.b1$$

$$h3 = dx2s.b2$$

$$h4 = dx2s.b12$$

$$h5 = dx2s.b11$$

$$h6 = dx2s.b22$$

$$G = \text{matrix}(c(g1, h1, g2, h2, g3, h3, g4, h4, g5, h5, g6, h6), nr = 2)$$

$$\text{vcov.statn} = G \% \% \text{vcov.b} \% \% t(G)$$

```

}

# end of function

##### Simulation loop start #####

plot(0.1,0.2,col= "white", xlim=c(-3,3), ylim=c(-3,3), xlab="x1.c", ylab="x2.c")

count.Bon = 0 # Counts the number of times the true stationary falls in the estimated
SCI

count.plug = 0

for(i in 1:Nsim)

{

##### Create b and vcovb #####

y=Beta.0 + Beta.1*x1 + Beta.2*x2 + Beta.12*x1x2 + Beta.11*x1sqr + Beta.22*x2sqr +
rnorm(n,0,sqrt(Sigma2))

SecoOrd.fit = lm(y~x1+x2+x1x2+x1sqr + x2sqr)

b = SecoOrd.fit$coeff

vcov.b = vcov(SecoOrd.fit)

b.vec = c(b[2], b[3])

B.mat = matrix (c(2*b[5], b[4], b[4], 2*b[6]), nc=2 )

```

```

eigen.sign [i] = prod(sign(eigen(B.mat)$value))

statnp[i,] = -0.5*solve(B.mat) %*%b.vec

vcov.statn = vcovf.statn(n,b,vcov.b)

var.xs1=vcov.statn[1,1]

var.xs2=vcov.statn[2,2]

Critical.Bon = qnorm(1-alpha/(2*k))

Bon.xs1 = statnp[i,1] + c(-1,1)*Critical.Bon*sqrt(var.xs1)

Bon.xs2 = statnp[i,2] + c(-1,1)*Critical.Bon*sqrt(var.xs2)

if ( ((Xs.kwn[1] >= Bon.xs1[1]) & (Xs.kwn[1] <= Bon.xs1[2])) &

      ((Xs.kwn[2] >= Bon.xs2[1]) & (Xs.kwn[2] <= Bon.xs2[2])) )

{

  count.Bon = count.Bon + 1

}

Critical.Equi = qmvnorm(1- alpha, mean = statnp[i,], corr = cor(vcov.statn), tail="both"
)$quantile

Asy.xs1 = statnp[i,1] + c(-1,1)*Critical.Equi*sqrt(var.xs1)

Asy.xs2 = statnp[i,2] + c(-1,1)*Critical.Equi*sqrt(var.xs2)

```



```

if ( ((Xs.kwn[1] >= Asy.xs1[1]) & (Xs.kwn[1]<=Asy.xs1[2])) &

      ((Xs.kwn[2] >= Asy.xs2[1]) & (Xs.kwn[2]<=Asy.xs2[2])) )

{

count.plug = count.plug + 1

}

points(statnp [i,][1], statnp [i,][2], col="gray70", pch = ".", cex=2)

}

# end of simulation loop

points(Xs.kwn[1],Xs.kwn[2], pch=16, col="red")

table(eigen.sign)

coverage.Bon = count.Bon /Nsim

coverage.Bon

coverage.plug = count.plug /Nsim

coverage.plug

points(statnp [,1][eigen.sign==-1],statnp [,2][eigen.sign==-1], pch = ".", cex=3, col=
"black")

##### A bivariate kernel density estimates #####

```

```
install.packages("MASS")
```

```
library(MASS)
```

```
plot(statnp[,1], statnp[,2], col="gray70", xlim=c(-2,2),ylim=c(-2,2), xlab="xs1",  
ylab="xs2", pch=".",cex=2)
```

```
par(new=TRUE)
```

```
f1 <- kde2d( n = 50, lims = c(-2,2,-2,2),h = rep(0.9,1))
```

```
contour(f1, levels = c(0.001,0.002, 0.02,0.01,0.02,0.07, 0.3, 0.5, 0.6 , 0.8, 0.1 ,0.4)  
,col="green" ,lwd=1)
```

## APPENDIX C

## Code of metaheuristic

```
install.packages("rsm")
```

```
library(rsm)
```

```
c = 0
```

```
c = as.numeric(c)
```

```
X1= matrix(0,1,6)
```

```
for(k in 1:23)
```

```
{
```

```
for(j in (1+k):24)
```

```
{
```

```
for(i in 1:6)
```

```
{
```

```
X1[1,i]=M1[k,i]
```

```
M1[k,i]=M1[j,i]
```

```
M1[j,i]=X1[1,i]
```

```
}
```

```
c=c+1

filename=paste("libALL", c ,".csv")

write.table(M1, filename , append = TRUE,sep = ",",
row.names=TRUE,col.names=TRUE)

}

}

for(i in 1:276)

{

filename=paste("libALL", i ,".csv")

#write.table(M1, filename , append = TRUE,sep = ",",
row.names=TRUE,col.names=TRUE)

dat1=read.csv(filename,header=TRUE)

beta1=matrix(0,10,14)

for (k in 19:24){

x3=dat1[1:k,]

fit=rsm(x3[,5]~SO(x3[,2],x3[,3],x3[,4]))

beta1[,k-10]=t(t(fit$coeff))
```

```
}  
  
beta1=beta1[,-1:-8]  
  
p1=0  
  
p1=as.list(p1)  
  
for (d in 1:6){  
  
p1[[d]]=sqrt(sum((beta1[,d]-beta1[,6])^2))/(sqrt(sum((0-beta1[,6])^2)))  
  
}  
  
p21=t(t(p1))  
  
filename1=paste("p", i ,".csv")  
  
write.csv(p21,filename1)  
  
}
```